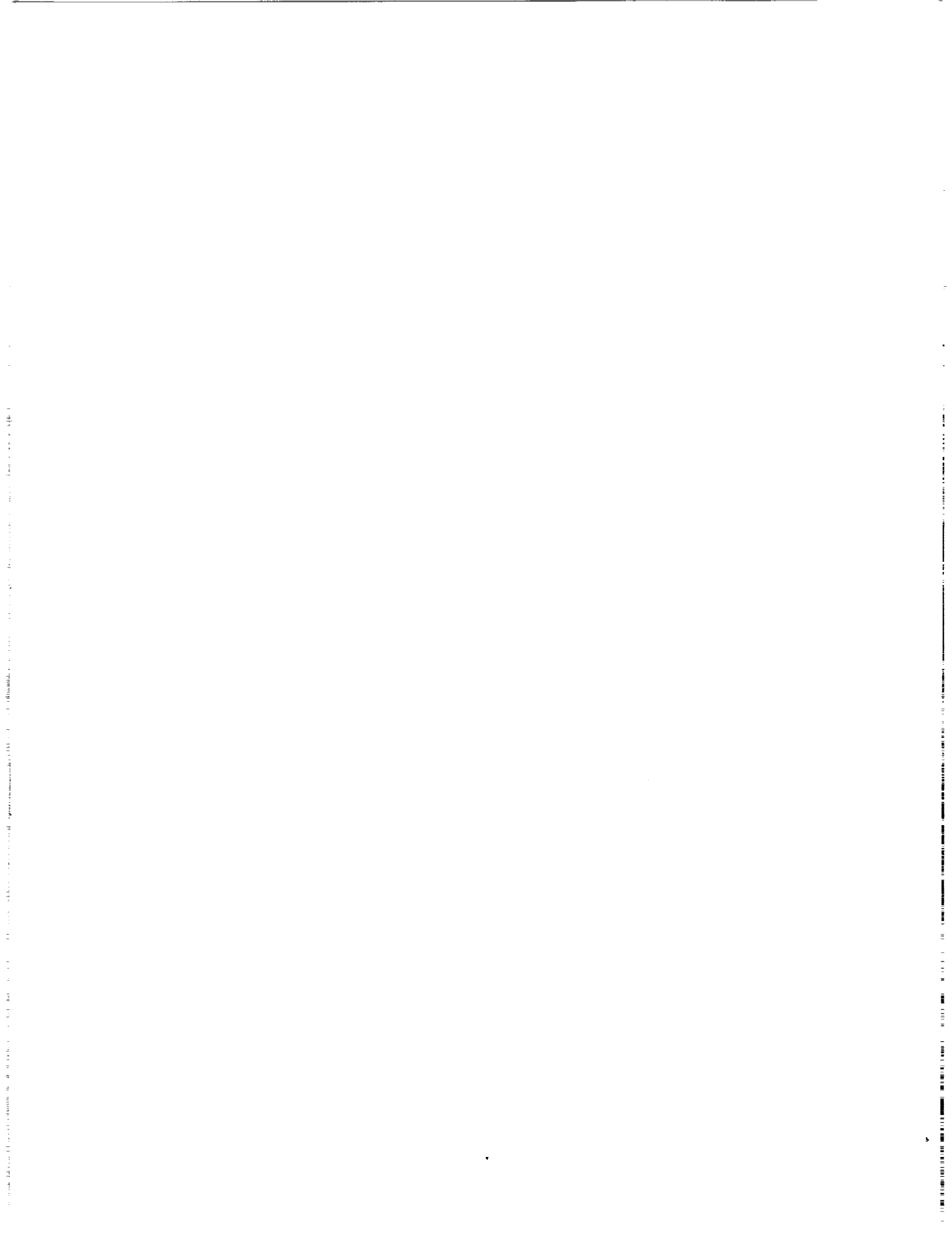


**Inter-Agency Consultative Group
for Space Science (IACG)**

**Handbook of Missions
and Payloads**

May 1994



Inter-Agency Consultative Group (IACG)

Handbook of IACG Missions and Payloads

May 1994

Table of Contents

	<u>Page</u>
Introduction	iii
Advanced Composition Explorer (ACE)	1
Akebono	6
APEX	11
Cluster	13
CORONAS	19
Fast.....	23
Galileo	25
Geotail	36
GOES	40
Interball	43
International Sun-Earth Explorer-3 (ISEE-3), now ICE	50
Interplanetary Monitoring Platform-8 (IMP-8).....	55
Mars-94	59
LANL Geosynchronous Spacecraft	63
Pioneer 10	65
Polar	69
Solar and Heliospheric Observatory (SOHO).....	75
Solar, Anomalous, and Magnetospheric Particle Explorer (SAMPEX)	80
Spartan	83
Ulysses	86
Upper Atmosphere Research Satellite (UARS)	91
Voyager	97
Wind.....	101
Yohkoh	106
 Appendices:	
Principal Investigators listed alphabetically	
Principal Investigators listed by mission	

Preface

The Interagency Consultative Group for Space Science (IACG) is an informal organization of space scientists from four major space organizations: ESA (Europe), IKI (Russia), ISAS (Japan) and NASA (USA). After its stunning success coordinating the Comet Halley encounters in 1986, the IACG selected Solar-Terrestrial Science as its next major space science discipline for coordinated attack. In 1993, the IACG specifically recommended that the membership and activities of the IACG science working group be expanded to include study of the three-dimensional heliosphere to recognize the unique opportunity presented by the operation of eleven solar observatories and heliospheric missions. The imminent and singular pole-to-pole pass of Ulysses over the Sun during solar activity minimum in 1994 and 1995 make this coordination particularly urgent.

The mission set of interest to IACG has expanded, and it has been some time since mission information was updated and compiled in one publication. Thus, this booklet brings together basic updated information about IACG missions expected to be involved in the IACG campaigns currently being planned. Older missions that are no longer active have been omitted, and some future missions for which we have inadequate information are also omitted. We request information on such future missions which are in the IACG Mission Set (See Table I), and we ask principal scientists to bring any errors to our attention so that we may correct them in subsequent printings.

*Elden Whipple, Chairman , IACG WG-1 (Science)
Space Physics Division, NASA Headquarters
Washington, DC
May 1994*

Table 1: The IACG Mission Set

<i>Mission</i>	<i>Number of Spacecraft</i>	<i>Agency</i>	<i>Launch</i>
Part I. Core Missions			
Geotail	1	ISAS/NASA	July 1992
Wind	1	NASA	1994
Polar	1	NASA	1995
Interball	4	Intercosmos	1994-95
Solar & Heliospheric Observatory (SOHO)	1	ESA/NASA	July 1995
Cluster	4	ESA/NASA	Dec 1995
Part II. Complementary Missions			
Interplanetary Monitoring Platform (IMP-8)	1	NASA	Oct 1973
Dynamics Explorer (DE)	1	NASA	Aug 1981
Geostationary Operational Environmental Satellite (GOES)	2 in orbit	NOAA	D-H: 1980-87 I-M: 1993-03
LANL Geosynchronous Spacecraft	3	LANL	1989-91
Akebono (formerly EXOS-D)	1	ISAS	Feb 1989
Active	2	Intercosmos	Sept 1989
APEX	2	Intercosmos	Dec 1991
Relict-2	1	Intercosmos	late 1995
Yohkoh	1	ISAS	Aug 1991
Upper Atmospheric Research Satellite (UARS)	1	NASA	Sept 1991
CORONAS-I	1	IZMIRAN	1992
SAMPEX	1	NASA	June 1992
SPARTAN	1	NASA	April 1993
Fast	1	NASA	Sept 1993
CORONAS-F	1	IZMIRAN	1994
ACE	1	NASA	1996
Part III. Spacecraft in Heliocentric Orbits			
Pioneer 10	1	NASA	March 1972
Voyagers	2	NASA	Aug/Sept 1978
International Cometary Explorer (ICE)	1	NASA	Aug 1978
Sakigake	1	ISAS	Jan 1985
SuiSei	1	ISAS	Aug 1985
Galileo	1	NASA/FRG	Oct 1989
Ulysses	1	ESA/NASA	Oct 1990
Mars-94	1	Intercosmos	1996

The Advanced Composition Explorer (ACE) Mission and Payload

The ACE spacecraft design is based on the Charge Composition Explorer (CCE) built by Johns Hopkins University (JHU) and the Applied Physics Lab (APL) for the AMPTE program. ACE is designed as a spinning spacecraft with its spin axis aligned to the Earth-Sun axis. The ACE launch weight will be ~633 kg, including 105 kg of scientific instruments and 184 kg of propellant. Using a Delta-class expendable launch vehicle, ACE will be launched into an L1 libration point ($240 R_e$) orbit. Telemetry will be 6.7 kbps average, using tape recorder storage with daily readout to DSN. The experiment power requirement is approximately 76 W nominal and 96 W peak.

The prime objective of the ACE mission is

- to determine accurate elemental and isotopic abundances including solar matter, local interstellar matter and local galactic matter
- to study the origin of elements and evolutionary processing in galactic nucleosynthesis, galactic evolution, origin and evolution of the solar system
- to study coronal formation and solar-wind acceleration processes
- to study particle acceleration and transport, including coronal shock acceleration, stochastic flare acceleration, interplanetary shock acceleration, and interstellar acceleration and propagation

To accomplish this objective, ACE will perform comprehensive and coordinated determinations of the elemental and isotopic composition of energetic nuclei accelerated on the Sun, in interplanetary space, and from galactic sources. These observations will span five decades in energy, from solar wind to galactic cosmic ray energies, and will cover the element range from ^1_1H to $^{40}_{22}\text{Zr}$. Comparison of these samples of matter will be used to study the origin and subsequent evolution of both solar system and galactic material by isolating the effects of fundamental processes that include nucleosynthesis, charged and neutral particle separation, bulk plasma acceleration, and the acceleration of suprathermal and high-energy particles.

Key ACE Mission Statistics

Mission Class:	Explorer
Launch Date:	June 1996
Launch Vehicle:	Delta II 7920
Launch Site:	CCAFS
Mission Duration:	5 years
Orbit:	Modified halo about the Earth-Sun L_1 point at $240 R_e$
A_Y :	300,000 km
A_Z :	300,000 km
Period:	178 days
S/C type:	Explorer. Irregular octagon, 1.2 m high, 2 m diameter
S/C mass:	633 kg
Propulsion ΔV :	1104 m/s (184 kg propellant)
Stabilization:	Spin, 5 rpm. Axis along Earth/Sun line
Pointing Accuracy:	10°
Pointing Knowledge:	1°

Power: 335 Watts
Science Telemetry: 6.7 kb/s
Data Storage: Tape recorder, 579 Mb, 72 kb/s

ACE Instruments

1) Cosmic Ray Isotope Spectrometer (CRIS)

The instrument mass is about 20.4 kg with a data rate of 0.46 kbps. It is designed to provide very good statistical measurements of all stable and long-lived isotopes of galactic cosmic ray nuclei from He to Zn ($Z = 2$ to 30) over the general energy range from 100 to 600 MeV/nuc. The CRIS instrument will also provide limited measurements of low energy H isotopes, and the first exploratory studies of the isotopes of ultra-heavy (UH) nuclei from Ga ($Z = 31$) through Zr ($Z = 40$). The detector system is of all solid-state design, and includes four identical telescopes composed of arrays of large-area lithium-drifted (LiD) silicon solid-state detectors. Each of the telescopes is composed of a horseshoe system made up of five position-sensitive detectors, followed by an energy-loss stack of six devices of graduated thickness. The instrument has an rms mass resolution of 0.25 amu or better, and a geometry factor of $200 \text{ cm}^2 \text{ sr}$.

2) Energetic Electron, Proton, and Alpha Monitoring (EPAM)

The EPAM instrument will measure solar and interplanetary particle fluxes with a wide dynamic range while covering nearly all directions of the full unit-sphere. It will use low-energy solar particle fluxes as probes of the morphological changes of coronal and large-scale interplanetary magnetic field structures, and investigate solar flare processes using non-relativistic and relativistic electrons. EPAM consists of five apertures in two telescope assemblies mounted by means of two stub arms. It measures ions ($E_i > 50 \text{ keV}$) and electrons ($E_e > 30 \text{ keV}$) with essentially complete pitch angle coverage from the spinning ACE spacecraft. It also has an ion elemental abundance aperture using the DE vs E technique in a three-element telescope. The detectors form three distinct silicon solid-state systems; the low energy magnetic spectrometers (LEMS), the low energy foil spectrometers (LEFS), and the composition aperture (CA). The LEMS/LEFS system provides pulse-height-analyzed single detector measurements with active anticoincidence. The CA provides elemental composition in an energy range similar to those of LEMS/LEFS, and it will provide $^3\text{He}/^4\text{He}$ isotope resolution for identifying ^3He -rich events. EPAM has a mass of 5 kg, consumes 5 W of power, and provides data at 160 bps.

3) Magnetometer (MAG)

The instrument has a total power requirement of 4 W, a total integrated mass of 4.7 kg, and requires a telemetry rate of 300 bps. The magnetometer system consists of two identical triaxial fluxgate magnetometers mounted at the ends of identical booms diametrically opposite each other. Under normal operation only one will be powered. They will take accurate measurements of the interplanetary magnetic field to provide essential supporting data for the composition studies carried out by the primary ACE instruments. It is estimated that absolute accuracies of 0.1 nT are achievable with this system.

4) Solar Energetic Particle Ionic Charge Analyzer (SEPICA)

The mass of the instrument is 16 kg and the power consumption is 6 W. The average science telemetry rate will be 604 bps. SEPICA is designed to measure the ionic charge state, Q ; the kinetic energy, E ; and the nuclear charge, Z , of energetic ions above 0.2 MeV/nuc. This includes ions accelerated in solar flares as well as ESP and CER events. During solar quiet times, SEPICA should also be able to directly measure the charge state of anomalous cosmic ray nuclei, including H, N, O, and Ne, which are presumed to be singly charged. The instrument will have the ability to resolve details of ionic charge states in the energy range 0.2 to 2.5 MeV/nuc and identify elements with energy up to 32 MeV/nuc. The instrument consists of six multi-slit collimators, each comprising a well adjusted stack of 12 thin (0.15 mm) stainless steel plates, separated by about 2.5 mm. The plates are covered with parallel narrow slits 10 mm long and 0.3 mm wide each for the moderate charge resolution section, and 0.1 mm wide for the high-resolution section. The back portion of the instrument is composed of three dE/dX thin-window proportional counters, each serving two instrument sections. A set of six position-sensitive silicon solid-state detectors (PSD's), one for each section, is placed within the counter gas volume terminating the proportional counter.

5) Solar Isotope Spectrometer (SIS)

The SIS instrument is designed to measure the elemental and isotopic composition of solar energetic particles, anomalous cosmic rays, and interplanetary particles, from He to Zn ($Z = 2$ to 30) over the general energy range from 8 to 150 MeV/nuc. It will also provide measurements of low-energy He isotopes, and exploratory studies of solar energetic nuclei from Ga through Zr ($Z = 31$ to 40). In addition, SIS will extend measurements of galactic cosmic ray nuclei to lower energies than is possible with CRIS. In order to resolve adjoining isotopes that differ in abundance by 100 to 1, SIS will have an rms mass resolution of 0.25 amu or better. The detector system, which is an all solid-state design, is a mosaic of four identical telescopes composed of arrays of large-area surface barrier and lithium drifted (LiD) silicon solid state detectors. Each telescope consists of a hodoscope system made up of a pair of two dimensional position sensitive "matrix detectors," followed by an "energy loss" stack of eight devices of graduated thickness. The final detector in each stack identifies particles which penetrate the entire telescope. SIS weighs 19.5 kg, requires 23.5 W, and transmits data at 2 kb/s.

6) Solar Wind Electron and Alpha Monitoring (SWEPAM)

The SWEPAM instrument provides high-quality measurements of electron and ion fluxes in the low-energy solar wind range of electrons from 1 to 900 eV, and ions from 0.26 to 35 keV. These measurements provide detailed knowledge of solar wind conditions required to interpret other ACE instrument data and study solar wind phenomena. Simultaneous independent electron and ion measurements are made with separate sensors, each using curved-plate electrostatic analyzers (ESA's). Biased channel electron multipliers are spaced along the exit apertures of the ESA's for ion and electron detection. The SWEPAM output data consists of ion and electron counts collected at each E/Q step, polar look direction, and azimuthal (spin) direction. Over a single spacecraft spin, the accumulated count matrix is sufficient to calculate fully the electron and ion distribution functions, $f(v)$, from which the first and second moments can be calculated on the ground. The instrument has a mass of 6.7 kg, requires 5.4 W of power, and transmits science data at 1 kb/s.

7) Solar Wind Ion Composition Spectrometer (SWICS)

The system will have an approximate mass of 5.5 kg and a data rate of 0.5 kbps, and will consume 4 W. The SWICS instrument weighs 5.5 kg, consumes 4.8 W, and provides science data at a rate of 0.5 kb/s. It will uniquely determine the elemental and ionic-charge composition, the temperature, and mean speeds of all major solar wind ions from H through Fe at solar wind speeds ranging from a minimum of 145 km/s (protons) to a maximum of 1532 km/s (Fe^{+8}). The instrument covers an energy per charge range from 0.11 keV/Q to 66.7 keV/Q in approximately 13 minutes, and combines an electrostatic analyzer with post-acceleration followed by a time-of-flight and energy measurement.

8) Solar Wind Ion Mass Spectrometer (SWIMS)

The SWIMS instrument will have a mass of 6.8 kg, consume 6 W, and provide data at 0.5 kbps. SWIMS is a versatile instrument with mass resolution $M/\Delta M > 100$ and excellent time resolution, which will provide unprecedented solar wind composition data over a wide range of solar wind bulk speeds for all conditions. The efficiency and geometry of the instrument will allow, for the first time, an accurate determination of the abundance of most of the elements and a wide range of isotopes in the mass range 4 to 60 amu every few minutes, and for the rarer isotopes as well as the ultraheavy elements (> 60 amu) every few hours. The velocity range of the sensor is mass dependent, extending from 200 to 1500 km/s for He and from 200 to 500 km/s for Fe. The sensor consists of a wide-angle variable energy/charge passband deflection system, a time of flight high-mass-resolution spectrometer, and associated high voltage supplies. Solar wind ions enter the wide-angle three-chamber deflection system which acts as a UV trap and an E/Q passband filter. The deflection analyzer accepts incident ions with energy/charge between $(E/Q)_{\min}$ and $(E/Q)_{\max}$. The E/Q passband can be adjusted by changing the deflection voltage: hence, protons can be excluded from the system. Solar wind ions passing the deflection analyzer enter the mass analyzer section of the sensor by passing through a thin (1 to 2 mg/cm²) carbon foil surface to a microchannel plate.

9) Ultra-Low Energy Isotope Spectrometer (ULEIS)

The ULEIS instrument weighs about 17 kg, has a data rate of 1 kbps, and consumes 15.1 W. The ULEIS instrument measures element and isotope fluxes over the charge range from He through Ni from 20 keV/nuc to 10 MeV/nuc, thus covering both suprathermal and energetic particle energy ranges. Exploratory measurements of ultra-heavy species (mass range above Ni) will also be performed in a more limited energy range near 0.5 MeV/nuc. The instrument is a time of flight mass spectrometer, which identifies incident ion mass and energy by simultaneously measuring the time of flight and residual kinetic energy of particles which enter the telescope cone and stop in one of the arrays of six silicon solid-state detectors. Low energy threshold is achieved by using the TOF technique with a thin (200 nm-thick parylene) entrance foil on the telescope; good mass resolution is obtained by combining TOF measurements of high accuracy with a long (50 cm) flight path; a large geometrical factor (1.0 cm² sr) is obtained by using large-area microchannel plates (8 cm x 10 cm) and an array of solid-state detectors with a total area of 75 cm².

ACE Instruments Summary

	<i>Investigation</i>	<i>Range</i>	<i>Type</i>
CRIS	Cosmic Ray Isotope Spectrometer	100–600 MeV/nuc	Hodoscope
EPAM	Energetic electron, Proton, and Alpha Monitoring	30 keV–5 MeV/nuc	5 Aperture telescope
MAG	Magnetometer	8.8–50000 nT	Fluxgate
SEPICA	Solar Energetic Particle Ionic Charge Analyzer	0.1–32 MeV/nuc	Multi-slit collimator
SIS	Solar Isotope Spectrometer	8–150 MeV/nuc	Hodoscope
SWEPAM	Solar Wind Electron and Alpha Monitoring	1 eV–35 keV	Curved plate ESA
SWICS	Solar Wind Ion Composition Spectrometer	0.1–66.7 keV/Q	Electrostatic
SWIMS	Solar Wind Ion Mass Spectrometer	4–6 amu	TOF
ULEIS	Ultra-Low-Energy Isotope Spectrometer	20 keV–10 MeV/nuc	TOF telescope

Program Scientist: Vernon Jones, NASA HQ, (202) 358-0885
 Project Scientist: Jonathan Ormes, GSFC, (301) 286-8801
 Principal Investigator: E. Stone (California Institute of Technology)

The Akebono (EXOS-D) Mission and Payload

As the first spacecraft associated with the Solar Terrestrial Energy Program (STEP), the Akebono (the dawn) satellite was launched on February 22, 1989 into a semi-polar orbit with an initial apogee, perigee and inclination of, respectively, 10,500 km, 274 km and 75° and with an evolution period of 212 minutes. The Akebono mission aims at the studies on the polar cap region and plasmasphere, and on the exploration of the auroral particles acceleration by an electric field parallel to the earth's magnetic field line connected to the polar ionosphere. It is known that the electric field generally exists in a range of altitude of 3,000 km to 20,000 km, centering around 6,000 km. Although some features of the acceleration processes have been identified based on previous satellite observations, there still are basic questions that remain unsolved about the physics of the acceleration region. By conducting direct observations of the particle acceleration regions above the auroral region with eight scientific instruments onboard, the Akebono mission was designed to seek solutions to the following questions:

- What is the initial causative agent for the formation of the acceleration region? Is it induced by fast plasma injection, high energetic electrons, or by magnetic field as original currents?
- Are the particles accelerated by an electrostatic shock, a double layer, or growing large amplitude waves?
- How is the development of the regions of acceleration related to the occurrence of magnetospheric disturbances, called substorms?

Key Akebono Statistics

Launch date	February 21, 1989
Launch vehicle	M-3SII-4
Orbit	10,500 km Apogee 274 km Perigee
Inclination	75°
Orbit period	212 minutes
Stabilization	Spin with nominal spin rate of 7.5 rpm
Data storage	67 Mbit with double data recorder
Data rate	65 kbps (S band)
Mass	296 kg
Power	250 W

Akebono Instruments

- 1) Electric Field Detector (EFD)
H. Hayakawa, PI

The EFD is designed for the measurement of the static and quasi-static ionospheric electric field. Specifically, the aims of EFD measurements are: electric field structure associated with the auroral particle precipitation and the global motion of the polar ionosphere; the role of the electric field in the acceleration and heating mechanisms of ions; propagation mechanism of the

electric field in the auroral ionosphere to the low latitude ionosphere; and the electric field structure in the equatorial ionosphere. The 2-D electric field measurements of EFD utilizes two different techniques: the double probe technique (EFD-P) and the ion beam technique (EFD-B). The EFD-P use the outer part of the wire antennae as probes, and the maximum range of the EFD-P is ± 120 V with a resolution of 3.66 mV/m. The EFD-B technique was newly developed for the Akebono mission. It measures the time of flight (TOF) of a Lithium ion beam ejected from the gun and which returns to the detectors on the satellite approximately on gyroperiod later when ejection directions are appropriate. Vector components perpendicular to the ambient magnetic field are obtained twice per spin by the EFD-B.

2) Magnetic Field Detector (MGF)

H. Fukunishi, PI

The MGF instrument consists of triaxial fluxgate magnetometer with ring core type sensors mounted on a 5-m long mast and a triaxial search coil magnetometer with three search coil sensors orthogonally mounted on a 3-m long mast. The fluxgate magnetometer has four automatically switchable ranges from ± 1024 to ± 65536 nT (full scale), and resolutions commensurate with a 16-bit A/D converter in each range (± 0.015 to ± 1 nT). The rate of sampling is 32 vectors per second. The triaxial search coil magnetometer has a frequency response up to 800 Hz. Signals in the frequency range higher than 100 Hz are used for VLF plasma wave experiments, while signals less than 100 Hz are used for magnetic field experiments. The three component measurement of magnetic field variations enables us to investigate detailed properties of wave phenomena, ion cyclotron and ion Bernstein modes in the magnetosphere and low frequency noises on the auroral field lines. The major scientific objectives of the MGF experiment are 1) to study the structures of large- and small-scale field-aligned currents and their relationships, and the closures and driving mechanisms of these currents; 2) to determine the charges carriers of the field-aligned currents; 3) to examine the contribution of field-aligned currents to the generation of various kind of plasma waves; and 4) to measure electromagnetic cyclotron waves of H^+ , He^+ , and O^+ in the equatorial magnetosphere and broad-band electromagnetic noises associated with auroral particle precipitation.

3) Very Low Frequency Plasma Wave Detector (VLF)

I. Kimura, PI

The VLF experiment is designed to investigate the behavior of plasma waves associated with energetic particle precipitations in the auroral zone, wave particle interaction mechanisms and propagation characteristics of whistler mode, ion cyclotron mode, and electrostatic mode waves in the magnetospheric plasma. The VLF is to measure the wave normal and Poynting flux directions of these wave phenomena in addition to their dynamic spectra. Vector electric as well as magnetic field components in the frequency range from 3.16 Hz to 17.8 kHz is covered by the VLF and higher frequency range is covered by the PWS, the other wave instrument of Akebono. The VLF wave instrument is composed of loop and dipole antennas, common preamplifiers directly connected with the sensors, and the following sub-systems: a wide band analyzer (WBA), multi-channel analyzers (MCA), Poynting flux analyzers (PEX), extra-low frequency analyzers (ELF) and a vector impedance probe (VIP).

4) Plasma Wave Detectors in High Frequency Range and Sounder (PWS)

H. Oya, PI

Because Akebono's orbit passes through the acceleration region of the auroral energetic particles, the PWS experiment is used to confirm the developing mechanism for the acceleration of the auroral particles, and to clarify the real mechanism of the generation of auroral kilometric radiation with relation to the particle accelerations. In addition to the polar region studies, the PWS is designed also to clarify the global feature of the plasma distribution including the equatorial region, for studies on the generation mechanism of the electromagnetic waves and electrostatic plasma waves in the plasmasphere, as well. The PWS is also intended to observe the feature of the conversion processes of the electrostatic plasma waves into electromagnetic waves in a wide variety of global plasma distribution features, such as the equatorial turbulent regions, the region of the auroral particle acceleration, and cusp region plasma. The PWS instrument consists of a sub-system for natural plasma wave observation (NPW), a sub-system for stimulated plasma wave experiments (SPW), and the instrumentation for measurement of the number density of electrons (NEI). The NPW sub-system consists of three components: a) dynamic spectra observation, b) polarization observation and c) Poynting vector observation. Five modes of operation can be carried out in the sub-system for the artificially stimulated plasma wave experiment (SPW). The measurement of the plasma density (NEI) is made by a swept frequency impedance probe. For accurate measurements of the electric field component, a fixed frequency impedance measurement is also possible. The PWS system is devoted to the phenomena in the frequency range from 20 kHz to 5.12 MHz in the NPW sub-system and from 20 kHz to 11.4 MHz in the SPW sub-system by considering the plasma condition of the media surrounding the spacecraft. The time resolution of PWS is from 62.5 msec to 32 sec, depending on the operation modes.

5) Low Energy Particle Spectra Analyzer (LEP)

T. Mukai, PI

The LEP instrument is designed to make three distinct types of charged particle observations in the auroral magnetosphere: 1) energy per charge (E/Q) and pitch angle distributions of electrons and ions, 2) a mass per charge (M/Q) analysis for positive ions, and 3) onboard detection of particle flux modulations in the HF and VLF ranges. In order to achieve these observations, LEP consists of four units: two identical three-dimensional energy/charge analyzers (LEP-S1 and LEP-S2), an energetic ion mass-spectrometer (MEP-M) and a data-processing electronics unit (LEP-E). The LEP-S are two nested sets of quadrispherical electrostatic analyzers for electrons and ions with an energy range of 10 eV–16 keV for electron measurement and 13 eV/Q–20 keV/Q for ion measurement. Their energy resolution is $\Delta E/E = 12\%$ and differential energy spectra at 64 steps. The LEP-M, composing of a 135° spectral electrostatic analyzer, a 40° magnetic analyzer and MCP, makes simultaneous measurements of mass and pitch-angle distributions with an energy range of 1 to 25 keV/Q.

6) Suprathermal Mass Spectrometer (SMS)

B. Whalen, PI

The SMS was developed to study the thermal (0–25 eV) and suprathermal (25 eV–several keV) ion distributions in the low altitude magnetosphere. The instrument has a dynamic range of mass (1–70 amu/e) and plasma density (10^{-3} to 10^5 cm⁻³) sufficient to measure, on a regular basis, the major and the minor distribution functions at apogee ($\sim 10^4$ km) as well as at perigee (~ 300 km). The instrument is a radio frequency type mass spectrometer and has a programmable mass resolution ($\Delta m/m$ from 0.06 to 0.20) which is independent of energy and mass selected. The

SMS instrument consists of an electrostatically selectrable entrance aperture and energy selector selection, a radio frequency (r.f.) analyzer, and an energy/mass analysis section which uses a microchannel plate (MCP) as the ion detector. The settings of (d.c.) voltages on the electrodes and r.f. frequency defines the energy per unit charge (E/Q) and ion velocity or equivalently the mass per unit charge (m/Q) of the ion. The electrodes potentials and the processing of MCP data is regulated by the SMS controller which is housed, along with the power and telemetry and command systems, in the bottom portion of the SMS instrument.

7) Temperature and Energy Distribution of Plasma (TED)

K. Oyama, PI

The TED instrument was designed to carry out direct measurements of the velocity distribution function and electron temperature of the thermal electrons in the energy range of 0 to a few eV. The main scientific objectives of the TED experiment are: 1) Detection of field-aligned current carriers responsible for the downward current (the thermal electron contribution) in the auroral region. 2) Confirmation of the anisotropy in either the auroral region or the ionospheric trough region. 3) Observation of thermal electrons in association with double layers or what are called V-shaped electric field. 4) Observation of a possible association of the thermal electrons with South Atlantic geomagnetic anomaly and/or with plasma bubbles. The TED sensors are mounted on the ends of the solar cell paddles in such a way that the two sensors are at right angle to each other. The TED system can be operated in the three modes: the electron temperature mode (TE), the probe characteristic mode (SH-DC) and the velocity distribution mode (SH-AC). The TE mode is for the measurement of electron temperature T_e and floating potential V_i with an energy range of $T_e = 0 \sim 1.0$ eV and -5 V $< V_i < 5$ V. The SH mode is for the velocity distribution and electron density measurements with energy range of 0~2.5 eV or 0~5.0 eV and density range of $10^2 \sim 10^6$ cm⁻³. The data acquisition rate is 2 samples/s (regardless of bit rate of telemetry) for TE mode and the data sampling rate is 1024 Hz for the SH mode.

8) Auroral Television Camera (ATV)

T. Oguti, PI

The ATV experiment is an auroral imager for studies of auroral dynamics and global monitoring of magnetospheric activities. It is equipped with a vacuum ultra-violet (UV) and visible (VIS) sensors. Target emissions are selected to be N₂ LBH bands and atomic oxygen lines, including the hydrogen Lyman-alpha emission in UVV imaging and the oxygen green line [OI] 5577Å in visible imaging. The UV sensor (with emission passband of 1150–1390Å) works mainly for investigations of dynamical developments of global aurora images with high shot rates with an 8 second interval maximum. The visible sensor (emission passband of 5457–5750Å) is expected to make liaisons with ground networks at low altitude perigee over the winter polar region. The VIS-sensor is equipped with an interference filter between a mechanical shutter (SHT) and optics (OPT) for extraction of the target emission, while the UV-sensor relies upon the quantum efficiency characteristics of the image intensifier (II)-photocathode material, KBr. The size of the sensitive area of the CCD, 4.88 mm (V) x 6.39 mm (H) provides an effective FOV for image data, that is 36° (H) x 36° (V) and 30° (V) x 40° (H) respectively for UV- and VIS-data.

Akebono Instrument Summary

	<i>Investigation</i>	<i>Range</i>
EFD	Measurements of static and quasi-static ionospheric electric field.	± 120 V with a resolution of 3.66 mV/m.
MGF	Study the magnetic field structure, field-aligned currents and their carriers, and the generation of various kind of plasma waves	from ± 1024 nT to ± 65536 nT. The sampling rate is 32 vectors per second.
VLF	Investigate behavior of various plasma waves, wave-particle interaction, and energetic particle precipitations in the auroral zone	frequency range from 3.16 Hz to 17.8 kHz.
PWS	Study the developing mechanism for the acceleration of the auroral particles and the generation of auroral kilometric radiation	frequency range from 20 kHz to 5.12 MHz–11.4 MHz
LEP	Make observations of energy/charge and pitch angle distribution for ions and electrons, and mass/charge analysis for positive ion,	10 eV–16 keV for electron and 13 eV/Q–20 keV/Q for ions
SMS	Study the thermal and suprathermal ion distributions in the low altitude magnetosphere.	E: 0 - several keV M: 1–70 amu/e n: 10^{-3} – 10^5 cm ⁻³
TED	Measure the velocity distribution function and electron temperature of the thermal electrons	E: 0–a few eV T: 0–1 eV u: –5V–5V
ATV	Take auroral images for studies of auroral dynamics and global monitoring of magnetospheric activities.	emission passbands: 1150Å–1390Å and 5457Å–5750Å

Hiroshi Oya, Geophysical Institute Tohoku University, Japan
 Koichiro Tsuruda, Institute for Space and Astronautical Science, Japan

The Active Plasma Experiments in the Earth's Magnetosphere (APEX) Mission and Payload

The APEX project, an international mission undertaken jointly by scientists from Russia, Hungary, Germany, Bulgaria, Poland, Rumania and Czechia, has the following primary objectives:

- Simulation and initiation of aurora and radio frequency radiation in an auroral area.
- Study of the dynamics of modulated beams and plasmoids in the near-earth plasma.
- Study of the nature of electrodynamic relationship of electromagnetic waves in magnetosphere and ionosphere.
- Determination of radio emission characteristics of modulated beams of charged particles and plasmoids.
- Search for non-linear wave structures of the electromagnetic solution type in disturbed environment.

The satellite and small subsatellite will be set into a polar orbits.

Key APEX Mission Statistics:

Launch Date:	18 December 1991
Orbits:	Apogee: 3080 km
	Perigee: 430 km
Inclination:	82°
Mission Duration:	nominal 2 years

APEX Instruments Summary

<i>Experiment</i>	<i>Code</i>	<i>Principal Investigator</i>
Electron accelerator	UEM-2	Dokukin, V.
Neutral plasma accelerator	UPM	Dokukin, V.
Electron and ion analyzers	PEAS	Gringauz, K., Shutte, N. M. Teltcov, M., and Fisher, S.
Electric field instrument	DEP-2E	Chmirev, V. and Stanev, G.
AC field analyzer	DEP-2R	Chmirev, V. and Stanev, G.
Potential and soft partical analyzer	DANI	Dachev, Tc. and Dokvicia, V
Cold plasma measurements	KM-10	Afonin, V. and Shmilauer, Ja.
VLF analyzer	NVK-ONCH	Milchailov, Yu.
Optical measurements	UF-3K	Ruzhin, Yu.
Optical measurements	FS	Petkov, N.
Fluxgate magnetometer	SGR-5	Chmirev, V.
Search-coil magnetometer	MNCH	Chmirev, V.
Mass-spectrometer	NAM-5	Istomin, V. and Shmilauer, Ja.
HF-field analyzer	VCH-VK	Pulinets, S. and Kloss, Z.
Fluxgate magnetometer	SGR-7	Chobanu, M
Magnetic and electric field analyzer	KEM-1	Triska, P.
Cold plasma analyzer	KM-12	Shmilauer, Ja.
Langmur probe	ZL-A-S	Sauer, K.
Radio wave spectrometer	PRS-2-C	Rothkachi, H.
Particle analyzer	DAN'-S	Dachev, Tc.
Particle analyzer	DOK-A-S	Kudela, K.
Particle analyzer	MPS	Fisher, S.
Particle analyzer	SEA	Fisher, S.
Photometer	FDS	Petkov, N.

Project Scientist: Prof. V. N. Oraevsky
 Project Managers: V. S. Dokukin and Yu. Ya. Ruzhin
 The Institute of Terrestrial Magnetism, Ionosphere and Radio-wave propagation
 of the Russia, Academy of Sciences, Moscow, Russia
 Tel. 007-095-334-0120
 Fax: 007-095-334-0124

The Cluster Mission and Payload

The Cluster mission is a joint venture between ESA and NASA within the framework of ESA's Solar Terrestrial Science Programme (STSP), and as part of NASA's International Solar-Terrestrial Physics (ISTP) program. The Cluster suite of spacecraft is currently scheduled for a December 1995 launch using an Ariane 5 expendable launch vehicle. The mission will consist of four spin-stabilized spacecraft carrying identical scientific experiment payloads. During launch the spacecraft are stacked.

The Cluster spacecraft will be spin stabilized at 15 rpm. The configuration is driven by the large amount of fuel needed to inject the spacecraft from an equatorial transfer orbit into the final near-polar orbit. Additional fuel is required for in-orbit separation maneuvers. The spacecraft are cylindrical in shape, with the platform on one side accommodating the instruments. Two rigid booms, each five meters long, will carry the magnetometers. Two pairs of wire booms, each with a tip-to-tip length of 100 meters, allow electric field measurements based on the wire boom technique. The EMC specifications aim at a background magnetic field of ~ 0.25 nT at the position of the fluxgate magnetometer sensor. Because the attitude reconstitution is important for the derivation of vectorial quantities, the designers are aiming at an accuracy of 0.25 degrees.

The Cluster mission comprises four satellites to perform three-dimensional studies of the microphysical properties of different plasma states in the Earth's magnetosphere and solar wind. The Cluster's primary scientific objectives include the:

- Exploration of the boundary regions of the Earth's magnetosphere as an example of the interface of two cosmic plasmas and investigate the detailed nature of the processes by which energy, mass and momentum are transferred across boundaries such as the magnetopause;
- Study of the magnetic reconnection process and the small-scale magneto-hydrodynamic (MHD) structures and plasma acceleration associated with the processes;
- Study of MHD turbulence, vortex formation, and eddy diffusion particularly in the polar cusp and boundary regions;
- Investigation of the structure and properties of collisionless shock waves, including the bow shock, and the associated particle acceleration and wave generation; and
- Determination of the small-scale structure of the solar wind flow around the Earth.

The four spacecraft will be placed into orbits that take them through key regions of the near-Earth space. These regions are the cusp, the magnetopause, the bow shock, and the solar wind and plasma sheet. The separation distances between the spacecraft will be varied in order to match the typical scale lengths of the plasma phenomenon to be studied. At particular regions along the orbit the four-spacecraft fleet will yield a tetrahedral spatial configuration.

Key Cluster Mission Statistics

Launch Date:	December 1995
Launch Vehicle:	Ariane 5
Launch Site:	Kourou
Mission Duration:	Two years
No. of Spacecraft:	Four
Operational Orbit:	4 R _e perigee, 19.8 R _e apogee, polar
Long Eclipses:	Up to 4 hours, 2 consecutive eclipses per year
Short Eclipses:	Up to 50 minutes, 12 consecutive eclipses per year
S/C Type:	Cylindrical, 2.9 m diameter/1.3 m height. Rigid radial booms (2 off), each approximately 4.5 m long; wire booms (4 off) each approximately 50 m long.
S/C Mass:	1200 kg (72 kg payload, 478 kg S/C bus, 650 kg propellant)
Propulsion ΔV :	3250 m/s, using restartable 400 N main engine and 10 N thrusters
Stabilization:	Spin stabilized at 15 rpm \pm 10%
Pointing Accuracy:	0.25° design goal
Pointing Knowledge:	\pm 0.1°
Power:	224W (total power at launch), 47 W (allocated to payload)
Science Telemetry:	220 kbps (realtime science data downlink), 4 kbps (telecommand rate), 2 kbps (realtime HK data downlink)
Data Storage:	2 tape recorders, 1 Gb each
Manufacturer:	ESA, Dornier Systems

Cluster Instruments

1) Active Spacecraft Potential Control (ASPOC) W. Riedler, PI

The ASPOC instrument is designed to keep the surface potential of the Cluster spacecraft near zero for the duration of their operational lives. ASPOC uses emitters to produce indium ions at approximately 6 keV. The ion current will be adjusted in a feedback loop with instruments measuring the spacecraft potential (EFW and PEACE). The ion emitter is a solid needle-type liquid metal ion source using indium as charge material. The ASPOC instrument consists of an electronics box and two cylindrical emitter modules with 4 needles each for redundancy. The ASPOC instrument has a mass of approximately 1.9 kg, consumes 2.7 W, and uses a data rate of 100 bps. The design life time is approximately 10,000 hours.

2) Cluster Ion Spectrometry (CIS) H. Reme, PI

The CIS experiment is a comprehensive ionic plasma spectrometry package capable of obtaining full 3-D ion distributions with high time resolution and mass per charge composition determination on board the four Cluster spacecraft. The CIS instrument complement consists of a Hot Ion Analyzer (HIA) and an ion composition and distribution function analyzer (CODIF). Both analyzers use symmetric optics resulting in continuous, uniform, and well characterized phase space coverage.

CODIF will measure the distributions of the major ions with energies from 0 to 40 keV/e with medium (22.5°) angular resolution, 1 spin time resolution, and two different sensitivities. CODIF will use a Retarding Potential Analyzer (RPA) assembly plus a time of flight spectrometer. The HIA sensor combines the selection of incoming ions according to their energy per charge by electrostatic deflection in a symmetrical hemispherical analyzer having a uniform angle-energy response, with a fast imaging particle deflection system based on microchannel plate electron multipliers. HIA will not provide mass resolution, but will provide $\frac{1}{2}$ spin time resolution, larger dynamic range, and an angular resolution capability ($2.8^\circ \times 5.6^\circ$) adequate for ion beam and solar wind measurements. The CIS instrument has a mass of approximately 11 kg, consumes 8.7 W, and uses a data rate of 5.5 kbps.

3) Digital Wave Processor (DWP)

L. J. C. Woolliscroft, PI

The Digital Wave Processor is included as part of the Wave Experiment Consortium (WEC), which comprises five coordinated experiments designed for measuring electric and magnetic fluctuations within critical layers in the Earth's magnetosphere. The WEC experiments will investigate waves with a frequency range from DC to over 100 kHz. The characteristic duration of these waves extends from a few milliseconds to minutes and a dynamic range of over 90 dB is desired. The DWP instrument will provide the processing system using a novel architecture with parallel processing and re-allocatable tasks for high reliability. The processing system will also perform particle and wave-particle correlations so as to study wave-particle interactions directly.

The heart of the DWP instrument is the bus to which all external data connections are made through interfaces protected by analog switches. Processing is done by any or all of the three processing modules connected to the bus. The onboard software will be coded as a series of three modules. The basic science module includes the software for the normal data processing unit capabilities (telecommand handling, etc.). The enhanced science module includes the software associated with the specific scientific capabilities (wave and particle correlations, etc.). The system module includes the software for the internal operation of the processor units (memory management, etc.). The DWP instrument has a mass of approximately 2 kg and consumes 1.56 W (3 processors operating).

4) Electron Drift Instrument (EDI)

G. Paschmann, PI

The Electron Drift Instrument is based on the electron drift technique. This method involves sensing the drift of a weak beam of test electrons emitted from small guns mounted on the spacecraft. For certain emission directions the electron beam returns to the spacecraft after one gyration, during which it probes the ambient electric field kilometers away from the spacecraft. The essential elements of the instrument are two electron guns, two detectors, digital controls, two correlators, and a controller unit.

The electron guns must be able to produce a beam 1° wide, steerable in any direction. Beam energies must be variable between 0.5 and 1.0 keV, and beam currents between less than 10^{-10} and 10^{-6} A. Electron time of flight measurements require that the beam can be switched on and off with a frequency of ~ 1 MHz. The EDI detector system is axially symmetric, covering more than 2π steradian. Guns and detectors are combined pairwise into a single unit, mounted on opposite sides of the spacecraft. The EDI experiment has a mass of approximately 9.9 kg, consumes 8.6 W, and uses a data rate of 1.5 kbps.

5) Electric Fields and Waves (EFW)

G. Gustafsson, PI

The EFW experiment is included as part of the Wave Experiment Consortium (WEC), which comprises five coordinated experiments designed for measuring electric and magnetic fluctuations within critical layers in the Earth's magnetosphere. The EFW experiment will measure the electric field and density fluctuations with sampling rates up to 40,000 samples per second in two channels. Langmuir sweeps will also be made to determine the electron density and temperature.

EFW will be capable of measuring the following: 1) instantaneous spin plane components of the electric field vector over a dynamic range of 0.1 to 700 mV/m, 2) low energy plasma density over a dynamic range of 1 to 100 cm⁻³, 3) electric fields in double layers of small amplitude from 0.1 to 50 mV/m, and 4) electric fields in electrostatic shocks or double layers of large amplitude from 0.1 to 700 mV/m. The EFW experiment has a mass of approximately 17.5 kg (includes electronics box and wire booms/4 units), consumes 3.1 W, and uses a data rate of 1.44 kbps.

6) Fluxgate Magnetometer (FGM)

A. Balogh, PI

The Fluxgate Magnetometer is a magnetic field investigation designed to provide inter-calibrated measurements of the magnetic field vector B at the four Cluster spacecraft. The instrumentation is identical on the four spacecraft: it consists of two triaxial fluxgate sensors and a failure-tolerant data processing unit. The combined analysis of the four-spacecraft data will yield such parameters as the current density vector, wave vectors, and the geometry and structure of discontinuities. The FGM consists of three elements: a sensor, the drive electronics, and the sense electronics. The magnetometers are eight-range instruments, providing a bipolar full-scale output voltage for field values from +/- 4 nT to +/- 65,536 nT, each range being four times the preceding range. The Fluxgate Magnetometer has a mass of approximately 3.4 kg, consumes 3.1 W, and uses a data rate of 1.2 kbps.

7) Plasma Electron and Current Analyzer (PEACE)

A. D. Johnstone, PI

PEACE consists of two sensors: the Low Energy Electron Analyzer (LEEA) and the High Energy Electron Analyzer (HEEA). The LEEA is designed to cover the lowest electron energies (0–10 eV) but is also capable of covering the energy range up to 1 keV. LEEA has a geometric factor appropriate for many of the high fluxes to be found at low energy. The HEEA has a geometric factor larger by a factor of five to extend the dynamic range and covers the energy range from 10 eV to 30 keV. Both sensors have a field of view of 180° and are of the same basic type consisting of hemispherical electrostatic analyzers of the so-called "Top Hat" type and an annular microchannel plate with a position sensitive readout as detector. The PEACE experiment has a mass of approximately 6.1 kg, consumes 4.7 W, and uses a data rate of 2.5 kbps.

8) Research & Adaptive Particle Imaging Detector (RAPID)

B. Wilken, PI

The RAPID instrument for the Cluster mission is an advanced particle detector for the analysis of suprathermal plasma distributions in the energy range from 20–400 keV and 2 keV/nuc–1500 keV for electrons and ions, respectively. The instrument consists of the Imaging Electron

Spectrometer (IES), the Imaging Ion Mass Spectrometer (IIMS), and the common Digital Processing Unit (DPU). The RAPID experiment has a mass of approximately 5.6 kg, consumes 4.5 W, and uses a data rate of 1 kbps.

Electrons with energies from 20 keV to 400 keV are measured with the IES. Advanced microstrip solid state detectors having a 0.5 cm x 1.5 cm planar format form the image plane for three acceptance "pinhole" systems. The IES provides electron measurements over a 180 degree fan of the polar range divided into 24 angular intervals. The IIMS is an energetic ion spectrometer which derives its particle identifier function from time of flight/energy measurement. The IIMS allows the identification of ions over an energy range of 5 keV/nuc to 1500 keV total energy with a mass resolution of about 4. The integrated sensor system of IIMS consists of three identical sensor units which cover a 180 degree fan in the polar plane with 12 contiguous angular intervals.

9) Spatial Temporal Analysis of Field Fluctuations (STAFF)
N. Cornilleau-Wehrin, PI

The STAFF experiment is included as part of the Wave Experiment Consortium (WEC), which comprises five coordinated experiments designed to measure electric and magnetic fluctuations within critical layers in the Earth's magnetosphere. The STAFF experiment consists of the following: 1) a three-axial, search coil magnetometer to measure the magnetic component of electromagnetic fluctuations (up to 4 kHz) and 2) a spectrum analyzer to perform onboard each satellite the auto and cross correlations between electric and magnetic components, also up to 4 kHz. Time resolution in the normal mode of operation is 1 second for the auto spectra and 4 seconds for the cross spectra. The STAFF experiment has a mass of approximately 3.85 kg, consumes 2.6 W, and uses a data rate of 3.25 kbps.

10) Wide Band Data (WBD)
D. A. Gurnett, PI

The WBD experiment is included as part of the Wave Experiment Consortium (WEC), which comprises five coordinated experiments designed to measure electric and magnetic fluctuations within critical layers in the Earth's magnetosphere. The WBD investigation will provide high-resolution spectral analysis of plasma waves. The wide-band receiver system provides wide-band waveform measurements of both electric and magnetic fields in selected frequency ranges from 10 Hz to 600 kHz. Continuous waveforms are digitized, formatted, and transferred to the spacecraft telemetry system using either a 250 kbps real-time mode or a 100 kbps burst-data mode.

The wide-band receiver processes signals from one of four sensors which can be chosen via an antenna selection switch located at the receiver input. The four selectable inputs consist of two electric field signals (from 2 EFW electric dipole antennas) and two magnetic field signals (from 2 STAFF search coil magnetometers). Input bandpass filters limit the incoming signal to one of four possible frequency bands ranging from baseband to 500 kHz.

11) Waves of High Frequency & Sounder for Probing of Electron Density by Relaxation (WHISPER), P. M. E. Decreau, PI

The WHISPER experiment is included as part of the Wave Experiment Consortium (WEC), which comprises five coordinated experiments designed to measure electric and magnetic

fluctuations within critical layers in the Earth's magnetosphere. The WHISPER experiment ensures two functions: 1) the measurement of the total density through the identification of the plasma frequency (from 0.2 to 80 cm⁻³), and 2) the continuous survey of the natural noise recorded by the electrical sensors in the high frequency range (from 4 to 80 kHz). The method chosen is the relaxation sounder, applicable to WHISPER and two other Cluster instruments, EFW and DWP. The WHISPER portion includes a transmitter and a receiver with a spectrum analyzer. The transmitter is connected to the shields of one electric wire boom pair through the EFW experiment module. The receiver is connected to the double sphere dipole probe, corresponding to the other wire boom pair, through the electric field module. The dynamic range of the signal is ~ 100 dB. The dynamic range of the spectrum analyzer itself is about 60 dB. The WHISPER experiment has a mass of approximately 2 kg, consumes 2.6 W, and uses a data rate of 1.2 kbps.

Cluster Instrument Summary

	<i>Investigation</i>	<i>Range</i>	<i>Type</i>
ASPOC	Active Spacecraft Potential Control	~ 20 μ A	Metal ion emitter
CIS	Cluster Ion Spectrometry	0-40 keV/q 3 eV/q-40 keV/q	Analyzer: RPA/TOF Analyzer: high resolution
DWP	Digital Wave Processor	DC to 100 kHz	Parallel processors
EDI	Electron Drift Instrument	0.1-10 mV/m	2 emitter/detector
EFW	Electric Fields and Waves	up to 10 Hz	2-pair wire booms
FGM	Fluxgate Magnetometer	up to 10 Hz	2 fluxgate sensors
PEACE	Plasma Electron and Current Analyzer	0-100 eV 0.1-30 keV	Electrostat. analyzer Electrostat. analyzer
RAPID	Research & Adaptive Particle Imaging Detector	2 keV/nuc-1500 keV 20400 keV	Time of flight, solid state detectors Microstrip solid state
STAFF	Spatial Temporal Analysis of Field Fluctuations	up to 10 Hz	Search coil sensor
WBD	Wide Band Data	up to 100 kHz	Sensors of EFW
WHISPER	Waves of High Frequency & Sounder for Probing of Electron Density by Relaxation	0.2- 80 cm ⁻³ 4 - 80 kHz	Relaxation sounder Filter banks

Project Scientist (ESA): R. Schmidt/C. Escoubet

Project Scientist (NASA): Melvyn Goldstein, GSFC, (301) 286-7828

Program Scientist (NASA): Elden Whipple, NASA/HQ, (202) 358-0888

The CORONAS Mission and Payload

The CORONAS mission will consist of three Earth orbiters, CORONAS-I launched on March 2, 1994, CORONAS-F to be launched in 1995-96 and a third, unnamed, spacecraft. The CORONAS mission is intended for the study of solar flare processes, including the following:

- Energy transfer from the solar interior to surface and subsequent release in solar flare events
- Explosive flare processes on the Sun
- Characteristics of solar cosmic rays, exit conditions, their propagation in the interplanetary magnetic field and effect of the Earth's magnetosphere
- Developing the theory of flares and techniques of forecasting their geophysical effects
- Investigation of solar global oscillation with the aim of studying the internal structure of the Sun

In addition, the following areas will also be investigated:

- The latitudinal and longitudinal distributions of galactic cosmic rays and albedo radiation
- The radiation belts and high-latitude structure of the Earth's magnetosphere

The satellites will be set into a polar orbit with altitude of about 500 km and an inclination of about 82.5°. The orbit will be quasi-synchronous to assure recurrence of the 20-day period outside the Earth's shadow.

CORONAS Instruments

- 1) Solar XUV Telescope (TEREK)
I. Sobelm and I. Zhitnik, PIs

The solar XUV telescope and optical coronagraph possesses both grazing and normal incidence mirrors. It registers images of the corona in the ranges of 5–25 Å, 52 Å (SiXII), 130Å(Fe XXIII, Fe XXIV), 170–180 Å, 304 Å (He II) and 4,000–6,000Å. It is intended for studies of the evolution of large and fine structures in the solar atmosphere, determination of hot solar plasma characteristics in active regions, and studies of coronal holes.

- 2) Solar X-Ray Spectrometer (RES-C)
I. SoBelman and I. Zhitnik, PIs

The solar x-ray spectrometer will provide images of the Sun in three spectral ranges: 180–205 Å (XUV channel), 8.41–8.43 Å (Mg XII channel) and 1.85–1.87 Å (Fe XXV channel). The XUV channel consists of the two subchannels. Each contains grazing incidence plane grating (2,400 line) with a multilayer coating spherical mirror working normal incidence. The spectral

resolution is 0.03 \AA ; the angular resolution $6'' \times 90''$. The Mg XII channel is observed with a bent quartz crystal spectrometer. The spectral resolution is $\sim 7 \times 10^{-3} \text{ \AA}$, the angular resolution is $7'' \times 7''$. The Fe XXV channel is also measured with a bent spherical quartz sensor. The spectral resolution is $2 \times 10^{-3} \text{ \AA}$, the angular resolution is $1'$.

3) Diagnostics of Energy Sources and Sinks in Flares (DIOGENES)

J. Sylwester, PI

The DIOGENES instrument comprises three independent units. These are a Bragg high-resolution spectrometer (BS), an x-ray spectrophotometer (BF), and a microcomputer that performs steering and control functions for BS and BF. DIOGENES is intended to provide the measurements that will enable the study of balance of the solar background spectrum.

4) HELIKON

E. Mazets, PI

The HELIKON instrument is an x-ray and gamma-ray scintillation spectrometer. It is sensitive to photons with energies between 10 keV and 750 keV and from 200 keV to 8.0 MeV. It has a time resolution from 2 ms to 0.25 ms.

5) Integral Radiation and Intensity Spectrometer (IRIS)

Yu. Charikov, PI

The IRIS instrument is a solar burst spectrometer for studies of integral intensity and spectra of solar x rays in the range 2–300 keV in 12 energy channels. It is also for studies of x-ray precursors of solar flares in the range of 2–20 keV with a sensitivity of $10^{-7} \text{ erg cm}^{-2} \text{ s}^{-1}$. IRIS also studies the dynamics of hard x-ray spectra in the range of 30–120 keV with a time resolution of $\sim 0.01 \text{ s}$.

6) Solar Ultraviolet Radiometer (SUVR)

T. Kazachevskaya, PI

The SUVR instrument is intended for patrol of solar radiation intensity in the extreme ultraviolet range $< 1300 \text{ \AA}$. The SUVR instrument registers solar EUV radiation using thermoluminescent phosphors (24 specimens arranged on a rotating wheel). Phosphor $\text{CaSO}_4(\text{Mn})$, which is practically insensitive to radiation at $\sim 1,130 \text{ \AA}$, is used. Under heating it re-radiates stored energy in the visible region ($\sim 5,000 \text{ \AA}$). A photomultiplier and electronic scheme transform visible light from phosphor into a signal which is transmitted to a telemetric system. The dynamic range of the measurements of solar EUV radiation is $0.1\text{--}30 \text{ erg cm}^{-2} \text{ s}^{-1}$. The instrument contains 24 screens: one without filters measuring the total EUV radiation flux, others with filters (MgF₂, Al foil, Mylar film). The filters isolate the following wavebands: soft x rays at 3–25 \AA ; soft x rays at 3–120 \AA , H-Lya line at 1,216 \AA ; total intensity at $< 1,300 \text{ \AA}$. The absolute error does not exceed 15%. Exposure time for the whole measurement cycle is 8 min.

7) Vacuum Ultraviolet Solar Spectrometer (VUSS)

A. Lomovsky, PI

The VUSS instrument performs absolute measurements of solar line intensities in the wave lengths region 200–580 \AA . Its operation is based on the new concept of collision photoionisation

spectroscopy. The use of a dual-channel scheme to measure differences makes this spectrometer insensitive to mechanical and electrical disturbances. The absence of optical elements and moving parts allow this instrument endure many years of exploitation. As a result, the VUSS instrument seems to be an appropriate choice when solving problems of long-time monitoring of the UV radiation of the Sun. The main part of the instrument is a cylindrical camera filled with a monoatomic gas (Ne) and provided at one end with a 16 x 20 mm window in the form of a microchannel plate. Two electron mirrors of original design are placed inside the camera. With such mirrors it is possible to minimize electron losses at the electrodes. Permanent magnets located in the camera produce a magnetic field of about 300 Oersteds oriented parallel to the plane of the electrodes. Cameras with gas and power supply systems are mounted on the metal frame. Its threshold sensitivity is 5×10^6 quanta $\text{cm}^2 \text{ s}$

8) Solar Optical Photometer (DIFOS)

Y. Zhugzhda, PI

The DIFOS instrument is a 3-channel solar white light photometer. This photometer is aimed to observe global solar oscillations. DIFOS will register the intensity of the continuum in the following optical spectral ranges: i) mean wavelength of 5,200 Å with a bandpass of 1,000 Å; ii) a mean wavelength of 7,100 Å with a bandpass of 1200 Å; and iii) a region of 4,000–10,000 Å. The DIFOS instrument has a relative light flow resolution of about one part per hundred thousand. Time resolution is 16 s. The thermostat supports a constant temperature of the photosensors during observations. Pointing accuracy is about 3–10 arc min, supported by the orientation system of the satellite.

The main scientific goal of DIFOS is to investigate the dynamics and structure of the solar interior by means of helioseismology. This goal subsumes the following subordinate goals: registration of the five-minute p modes of global oscillations; determination of their exact periods and relative amplitudes; investigation of the conditions in the near core areas with the aim of refining the standard solar model; determination of the differential rotation of the solar interior from observations of line splitting; an attempt to detect the modes of global oscillations with periods greater than one hour.

The DIFOS photometer will observe the Sun as a star. Consequently the selection of low degree oscillation mode with l up to 3 will only be possible using this instrument.

9) Solar Radio Spectrometer (SORS)

V. Fomichev and S. Pulinets, PIs

The SORS instrument will be used for investigations of solar radiobursts of types II, III, and IV. It will also be used for diagnostics of surrounding ionospheric plasma. SORS has two sweeping receivers in the frequency ranges 50 kHz–30 MHz and 25 MHz–300 MHz. On the CORONAS-F satellite, the multicomponent measurements will determine the direction of arrival and polarisation of the solar radio emission (3 magnetic components, 3 electric components). To study the detailed structure of radiobursts in the time scale of m~, the wide-band (~=4 MHz) channel will be used which could be tuned within the range 50 Hz–30 MHz. For plasma diagnostic purposes the impedance probe is provided in the range 50 kHz–30 Mhz. Within the same range the pulsed HF transmitter will be used in relaxation sounder regime.

The measurements mentioned above of solar radioemission in the range < 25 MHz will complement ground-based radioastronomical measurements with good time resolution. On the

same satellite, direct measurements of UV emission and local plasma density will improve ionospheric modeling and forecasting. The measurement of ionospheric parameters simultaneously with the investigation of solar activity will improve our knowledge of solar energy transfer to the near-Earth medium.

10) Solar Cosmic Rays Spectrometer (SCR)

V. Kuznetsov, PI

The SCR set of instruments will measure the intensity of photons with energies of 100 keV to 100 MeV, neutrons with energies greater than 30 MeV, and electrons and ions over a wide range of energies. The SCR instrument set consist of three instruments: SONG, SKI-3, and MKL. The SONG detects gamma rays in the energy of 0.1–100 MeV, neutrons with energies > 30 MeV, and protons with energies from 200–500 MeV. The SKI-3 instrument comprises four semiconductor energetic ion telescopes. It measures the flux of nuclei from $z=1$ to 10 with energies of 1.5–219 MeV/nucleon and Ne with the energy from 3.7–4.6/nucleon. The MKL particle detector is sensitive to electrons with energies from 0.5 to 12 MeV, protons with energies from 1–200 MeV, and alpha particles with energies from 30–60 MeV/nucleus.

CORONAS Instruments Summary

<i>No</i>	<i>Instrument</i>	<i>Code</i>
1.	Solar XUV telescope	TEREK
2.	x-ray spectrometer	RES-C
3.	x-ray spectrometer and photometer for diagnostics of energy sources and sinks in flares.	DIOGENES
4.	Scintillation X- and Y-ray spectrometer	HELIKON
5.	Solar burst spectrometer	IRIS
6.	Solar ultraviolet radiometer	SUVR
7.	Vacuum ultraviolet solar spectrometer	VUSS
8.	Solar optical photometer	DIFOS
9.	Solar radiospectrometer	SORS
10.	Solar cosmic rays spectrometer	SCR

Project Scientist (Russia - Coronas-I): V. Oraevsky, IZMIRAN*,

Fax 007-095-3340124; Telex: 421623 SCSTS SU

Project Scientist (Russia - Coronas-F): I. Sobelman, LPI**, Fax: 007-95-135-7880

Project Scientist (USA): None

Project Manager (Russia - Coronas-I): I. Kopayev, IZMIRAN, Telex: 421623 SCSTS SU

Project Manager (Russia - Coronas-F): V. Krutov, LPI, Fax: 007-95-135-7880

Program Scientist (USA): Bill Wagner, NASA/HQ, (202) 358-0911

* IZMIRAN is the Institute of Terrestrial Magnetism, Ionospheric and Radiowave Propagation of the Russian Academy of Sciences

** LPI is the Lebedev Physical Institute of the Russian Academy of Sciences

The FAST Mission and Payload

The Fast Auroral SnapshoT (FAST) is a small Explorer (SMEX) mission. SMEX missions can be developed at relatively low cost in a relatively short time and are launched on relatively inexpensive vehicles. The FAST satellite is to be launched on a Pegasus launch vehicle, a small, winged rocket designed to blast off from an airplane in flight, thus using less fuel and needing less weight than an Earth-based orbital launcher.

Scheduled for launch in 1994, FAST will investigate the plasma physics of auroral phenomena at extremely high time and spatial resolution—capturing auroral events "on the fly", and in great detail. The mission will utilize fast data sampling, a large burst memory and triggering on various event types to collect the specific data needed to address given problems. The FAST orbit baseline is 350 X 4200 km at 83° degrees inclination, and the principal science measurements will be taken when the spacecraft passes through the Earth's auroral zones.

The FAST mission is an innovative, high-time-resolution set of coordinated instruments designed for magnetospheric physics in the Earth auroral zone. The science objective of FAST will be to examine the electrodynamic causes of intricately complex auroral displays. Of special importance will be an attempt to reveal how electrical and magnetic forces guide and accelerate electrons, protons, and other ions in the auroral regions. The highest priority science involves studying the acceleration of electrons and ions by waves and quasi-static electric fields, the creation of parallel electric fields and double layers in the acceleration region, the production of waves, double layers, and solitons by electrons and ions, and nonlinear wave-wave interactions. Secondary scientific objectives of the FAST satellite involve lower-resolution global measurements which can be used in correlative studies with other space missions such as those of the International Solar Terrestrial Physics (ISTP) and rocket programs. The secondary objectives of FAST also include measurements of other magnetospheric and ionospheric phenomena as opportunity allows, such as equatorial spread-F, polar cap turbulence, and energetic radiation belt precipitation triggered by whistlers.

Key FAST Mission Statistics

Mission Class:	Small Explorer
Launch Date:	September 1994
Launch Vehicle:	Pegasus XL
Launch Site:	VAFB
Mission Duration:	One year nominal
No. of Spacecraft:	One
Operational Orbit:	Perigee radius of about 350 km and an apogee of about 4200 km, elliptical, not Sun synchronous
Orbital Inclination:	83 degrees
S/C type:	Circular aluminum deck with 8 aluminum struts
S/C mass:	181.4 kg
Stabilization:	Spin, 12 rpm
Pointing Accuracy:	$\pm 1^\circ$
Pointing Knowledge:	1° in the spin axis, $.1^\circ$ spin phase, and ± 3 km definitive orbit knowledge
Power:	60 watts (average)
Science Telemetry:	900 kbps, 1.5 Mbps, and 2.25 Mbps (downlink rates); 2 kbps (uplink rate)
Data Storage:	1 Gb

FAST Instruments

1) Electrostatic Electron Analyzer (EESA) - University of California at Berkeley

The Electrostatic Electron Analyzer will measure ion and electron particle species having an energy range of 3 eV to 30 KeV. The field of view of the EESA will be approximately 360x7 degrees with an angular resolution of 10x7 degrees. The instrument will require a maximum bit rate of 304 kbps, 1.33 watts of power, and 11.2 kg of weight.

2) Time-of-Flight Energy Mass Angle Spectrograph (TEAMS) - Lockheed Missile and Space Company and University of New Hampshire

The TEAMS will simultaneously determine the full three-dimensional distributions of O+ and H+ over the energy range of a few eV to 2 KeV. TEAMS' field of view will be approximately 360x8 degrees with an angular resolution of 11.2x22.5 degrees. The spectrograph will require a maximum bit rate of 200 kbps, 3.6 watts of power, and 6.4 kg of weight.

3) Electric Field Plasma Experiment (EFPE) - University of California at Berkeley

The Electric Field Langmuir Probe will continuously monitor (25 μ s resolution) the dominant frequency and amplitude of high frequency (up to 2 MHz) waves. The probe will require a maximum bit rate of 6400 kbps, 1.8 watts of power, and 12 kg of weight.

4) Magnetometer - University of California, Los Angeles

Two magnetometers will fly on FAST: a search coil magnetometer and a flux gate magnetometer. The magnetometers will measure vector (3-axis) magnetic fields from DC to ~2.5 KHz, with sensitivity of 1 nT for DC to ~100 Hz (fluxgate), and a sensitivity of better than 10^{-10} nT²/Hz at 1 KHz (search coil). These instrument will determine such quantities as the Poynting flux in EM waves. The search coil magnetometer will require a maximum bit rate of 240 kbps, 1.0 watts of power, and .8 kg of weight. The flux gate magnetometer will require a maximum bit rate of 48 kbps, 1.5 watts of power, and 1.05 kg of weight.

FAST Instruments Summary

	<i>Investigation</i>	<i>Range</i>	<i>Type</i>
EESA	Electrostatic Electron Analyzer	3 eV-30 keV	Ion /Electron Energy
TEAMS	Time-of-Flight Energy Mass Angle Spectrograph	10 eV-2 keV	H-NO Energy
EFPE	Electric Field Plasma Experiment	0.0001-1.0 v/m	Langmuir Probe
—	Magnetometer	0-50 Hz 10 Hz-2.5 kHz	Fluxgate Search Coil

Program Scientist: Elden Whipple, NASA HQ, (202) 358-0888
 Project Scientist: Robert Pfaff, GSFC, (301) 286-6328
 Principal Investigator: C. Carlson, University of California at Berkeley

The Galileo Mission and Payload

The Galileo mission consists of an entry Probe and a sophisticated Orbiter to study the planet, magnetosphere and satellites of Jupiter. Galileo will provide several unique additions to the space science program: the first in-situ sampling of the atmosphere of one of the outer planet; the first extended study of an outer planet system; and the first close up reconnaissance of an asteroid on the way to Jupiter. The Galileo spacecraft was launched by the Space Shuttle Atlantis on October 18, 1989, and a two-stage IUS propelled Galileo out of Earth parking orbit to begin its 6-year interplanetary transfer to Jupiter with gravity-assist flybys of Venus on February 10, 1990, and of Earth on December 8, 1990 and December 8, 1992. Galileo will arrive at Jupiter on December 1995, and the Orbiter will relay data back to Earth from an atmospheric Probe which is released five months earlier to descend on a parachute to a pressure depth of 20–30 bars in the Jovian atmosphere. Shortly after the end of Probe relay, the Orbiter will ignite its rocket motor to insert into orbit about Jupiter and make close encounters with the three outermost Galilean satellites—Europa, Ganymede, and Callisto. The nominal mission is scheduled to end in October 1997 when the Orbiter enters Jovian magnetotail.

The Galileo mission is an integrated project addressing multidisciplinary objectives concerning the entire Jovian system, combining in-situ atmospheric Probe measurements with an Orbiter which will provide a long-term magnetospheric survey, remote sensing of the atmosphere, and extremely close passes of the major satellites. The specific objectives are:

- Determine the chemical composition of the Jovian atmosphere
- Determine the atmospheric structure to a depth of at least 10 bars
- Determine the nature of the cloud particles and locations and structure of cloud layers in the Jovian atmosphere
- Determine the radiative heat balance and investigate the circulation and dynamics of the Jovian atmosphere
- Investigate the upper atmosphere and ionosphere of Jupiter
- Characterize the morphology, geology, and physical state of the satellite surfaces
- Investigate the surface mineralogy and surface distribution of minerals of the satellites
- Determine the gravitational and magnetic fields and dynamic properties of the satellites
- Study the satellites atmospheres, ionospheres, and extended gas clouds
- Study the interactions of the satellites and the Jovian magnetosphere

- Characterize the energy spectra, composition, and angular distribution of energetic particles and plasma throughout the Jovian magnetosphere, including plasma wave phenomena, to 150 R_J
- Characterize the vector magnetic fields throughout the Jovian magnetosphere to 150 R_J

Key Galileo Mission Statistics

Launch Date:	October 18 1989
Launch Vehicle:	Space Shuttle Atlantis/Two-stage Inertial Upper Stage (IUS)
Mission Duration:	nominal 8 years
Orbits:	the Venus-Earth-Earth Gravity Assist interplanetary trajectory to Jupiter; the Satellite Tour—10 highly elliptical orbits about Jupiter each contains a close flyby of one of the Galilean satellites; and finally the Tail Petal Orbit.
S/C Mass:	Orbiter: 2380 kg (includes 103 kg science payload) Probe: 335 kg (includes 28 kg science payload)
Stabilization:	Spin stabilized, 3.15 rpm
Power:	570 W (at launch; 480 W (after 6 years)
Telemetry rate:	Orbiter: 134 kbps (maximum) Probe: 128 bps
Data Storage:	A tape recorder with ~ 10 ⁹ bit capacity to buffer about 120 frames of imaging data or about 36 hours of low rate science

Galileo-Probe Instruments

1) Atmospheric Structure Experiment (ASI) A. Seiff, PI

The ASI will make in-situ measurements of the thermal structure of the Jovian atmosphere, i.e. the variation of temperature, pressure, and density with altitude, starting at about 10⁻¹⁰ bar level, when the Galileo Probe enters the atmosphere at a velocity of 48 km/s in December 1995, and continuing through its parachute descent to the 16 bar level. Other tasks are to define the temperature and pressure levels at which clouds form, the internal structure of the clouds (which may indicate phase changes or chemical processes), and depths and altitude separations of cloud layers and to help determine the radiative balance in the Jovian atmosphere by defining the temperature levels that govern infrared emission. Regions of adiabatic lapse rate and stable lapse rate will be sought to define regions in which convective overturning is occurring—important information relative to the circulation and dynamics of the atmosphere.

Three types of sensors are used to define the atmosphere's structure: temperature sensors, pressure sensors, and a three-axis accelerometer. Altitude resolution will be 0.2 to 0.06 km at descent velocities from 100 to 30 m/s. The temperature range is 0 to 500 K, while the temperature at the 16 bar level is expected to be 400 K, and the absolute uncertainty of the temperature measurement is expected to be about 1 K at the higher temperature and < 0.1 K near 100 K. The pressure sensor, covering from 0.1 to 16 bars by means of several sensors with three ranges of 0.5, 4, and 28 bars full scale, will be read to 10 bit resolution, giving least count values of 0.5, 4, and 28 mb, respectively. The accelerometers have 4 ranges in the probe axial

directions, with a dynamic range from 3 μg to 400g, and the measurement resolution is nominally 3 μg , 0.1mg, 3mg, and 0.1g, respectively.

2) Galileo Probe Mass Spectrometer (GPMS)

H. B. Niemann, PI

The GPMS is a Galileo Probe instrument designed to measure the chemical and isotopic composition including vertical variations of the constituents in the atmosphere of Jupiter to a high degree of accuracy. The measurement will be performed by in-situ sampling of the ambient atmosphere in the pressure range from about 150 mbar to 20 bar. In addition batch sampling will be performed for noble gas composition measurement and isotopic ratio determination and for sensitivity enhancement of non-reactive trace gases.

The instrument consists of a gas sampling system which is connected to a quadrupole mass analyzer for molecular weight analysis. To enhance the range of the measurements, the basic sample inlet system is supplemented by three selective subsystems: a noble gas purification cell and two enrichment cells for the more complex compounds. The mass range of the quadrupole analyzer is from 2 amu to 150 amu with maximum dynamic range of 10^8 . The detector threshold ranges from 10 ppmv for H_2O to 1 ppmv for Kr and Xe. The threshold values are lowered through sample enrichment by a factor of 100 to 500 for stable hydrocarbons and by a factor of 10 for noble gases. The instrument follows a sampling sequence of 8192 steps and a sampling rate of two steps per second. The measurement period lasts approximately 60 minutes through the nominal pressure and altitude range.

3) Helium Abundance Detector (HAD)

U. von Zahn, PI

The HAD experiment will accurately measure the relative abundance of helium in the Jovian atmosphere by a precision measurement of the refractive indices of the Jovian atmosphere over the pressure range from 2.5 to 12 bars. From these data the mole fraction of helium in the atmosphere of Jupiter is to be calculated with an estimated uncertainty of ± 0.0015 . Before measurements are made, the trace amounts of methane, ammonia, and water contained in the Jovian atmosphere are removed from the jovian gas sample by chemical absorbers.

The instrument uses a two-arm, double-path length interferometer or Jamin-Mascart interferometer. As a light source the instrument uses an infrared emitting diode which operates at a wavelength of 900 nm. An interference filter with a 15 nm passband aids in producing near-monochromatic light. A jamin plate produces two parallel and coherent light beams. Four chambers 100 mm in length each house the Jovian gas and the reference gas made up of 28% argon and 72% neon, which has approximately the same refractive index as one composed of 11% He and 89% H_2 . Additional optical elements are the collimator, the inversion prism, and the objective.

4) Galileo Probe Nephelometer Experiment (NEP)

B. Reagent, PI

The NEP is designed to make in-situ measurements of the vertical structure and microphysical properties of the clouds and hazes in the atmosphere of Jupiter along the descent trajectory of the Probe (nominally from 0.1 to 10 bars). The measurements, to be obtained at least every kilometer of the Probe descent, will provide the bases for inferences of mean particle sizes, particle number densities, and optical parameters such as the index of refraction. These quantities, especially the location of the cloud bases, together with other Probe measurements,

will yield strong evidence for the composition of the particles and species abundances, and are essential to an understanding of the energy balance of the planet. In addition the measurement in the upper troposphere will provide 'ground truth' data for correlation with remote sensing instruments aboard the Galileo Orbiter. The instrument consists of an optical unit and an electronics unit. The optical unit has a forward scatter unit immediately aft of a backward scatter unit. The forward scatter unit protrudes radially from the Probe's skin, while the edge of the backward scatter unit is flush with the skin. The instrument is carefully designed and calibrated to measure the light scattering properties of the particulate clouds and hazes at scattering angle of 5.8° , 16° , 40° , 70° , and 178° . The measurement sensitivity and accuracy is such that useful estimates of mean particle radii in the range from about 0.2 to 20 μ can be inferred. The instrument will detect the presence of typical cloud particles with radii of about 1.0 μ , or larger, at concentrations of less than 1 cm^3 .

5) Net Flux Radiometer (NFR)

L. A. Sromovsky, PI

The NFR experiment of the Galileo Probe mission is designed to measure the vertical profile of the difference between the upward and downward radiation (the net flux) in five spectral bands spanning the range from solar to far infrared wavelengths. These unique measurements within Jupiter's atmosphere, from which radiative heating and cooling profiles will be derived, will contribute to our understanding of the planet's radiation budget and thus to Jovian atmospheric dynamics, to detection of cloud layers in Jupiter's atmosphere and evaluation of their opacity in the visible and thermal regions of the spectrum, and to estimating the abundance of several molecular species which are felt to be important contributors to the atmospheric opacity. The NFR is the only probe instrument that has the potential for measuring the depth of penetration and the location of the deposition of solar radiation - the driving force for atmospheric dynamics.

The NFR consists of two major units, the optical head and the electronics module. The optical head contains optics, detectors and preamplifiers which rotate as a unit as they chop between upward and downward atmospheric views, or between ambient and internal heated black-bodies for on-board calibration measurements. The detector assembly consists of five spectral bandpass filters—3–500 μm , 0.3–3.5 μm , 3.5–5.8 μm , 14–35 μm , 0.6–3.5 μm , and a blind filter. The NFR integration period is seconds long; 5.5 seconds are used for measurement and 0.5 second for digitization and setting up for the next measurement. The 6-second integration period permits a vertical resolution of about 1.2 km at the beginning of the mission and about 0.25 km at the 10-bar level.

6) Energetic Particles Investigation (EPI)

H. M. Fischer, PI

The major science objective of EPI experiment, operating during the pre-entry phase of the Galileo Probe mission, is to study the energetic particle population in the innermost regions of the Jovian magnetosphere—within 4 radii of the cloud tops - and into the upper atmosphere. The EPI data obtained within 1.1–2 planetary radii will be used to test the validity of radial diffusion as a transport and acceleration mechanism in the deep inner magnetosphere; to infer the nature of field perturbations responsible for radial diffusion and the size distribution and radial structure of Jupiter's ring; and to identify possible additional inner magnetosphere source and loss mechanisms. The EPI data in the region about 5 to 1.1 planetary radii, together with previous mission observations, will provide information on any temporal variations of inner-zone particle fluxes.

To achieve these objectives the EPI instrument will make omnidirectional measurements of four different particle species - electrons, protons, alpha-particles, and heavy ions ($Z > 2$). Intensity profiles with a spatial resolution of about 0.02 Jupiter radii will be recorded. Three different energy range channels are allocated to both electrons ($>=3.2$, $>=8$ and > 8 MeV/nucl) and protons (42–131, 62–131, and 62–92 MeV/nucl) to provide a rough estimate of the spectral index of the energy spectra. In addition to the omnidirectional measurements, sectorized data will be obtained for certain energy range electrons, protons, and alpha-particles to determine directional anisotropies and particle pitch angle distributions. The detector assembly is a two-element telescope using totally depleted, circular silicon surface-barrier detectors surrounded by a cylindrical tungsten shielding with a wall thickness of 4.86 g cm^{-2} . The telescope axis is oriented normal to the spherical surface of the Probe's rear heat shield which is needed for heat protection of the scientific payload during the probe's entry into the Jovian atmosphere. The EPI instrument is combined with the Lightning and Radio Emission Detector (LRD) such that the EPI sensor is connected to the LRD/EPI electronic box. In this way, both instruments together only have one interface of the Probe's power, command, and data unit.

7) Lightning and Radio Emission Detector (LRD)

L. J. Lanzerotti, PI

The LRD instrument carried by the Galileo Probe will verify the existence of lightning in the atmosphere and will determine the details of many of its basic characteristics. The experiment will also measure the radio frequency (RF) noise spectrum in Jupiter's magnetosphere at about 5, 4, 3, and 2 planetary radii from Jupiter's center as the Probe approaches Jupiter. The RF data obtained in the magnetosphere will be analyzed jointly with the Probe EPI data to gain understanding of magnetospheric particle dynamics.

The LRD instrument consists of three basic sensors connected to one electronics box which is shared with the EPI instrument. One sensor is a ferrite-core radio frequency antenna (frequency range from about 10 Hz to 100 kHz), and two of the sensors are photodiodes behind individual fisheye lenses. The output of the RF antenna is analyzed both separately and in coincidence with the optical signals from the photodiodes. The RF antenna provides data both in the frequency domain (with three narrow-band channels, primarily for deducing the physical properties of distant lightning) and in the time domain with a priority scheme (primarily for determining from individual RF waveforms the physical properties of closeby-lightning).

Galileo-Orbiter instruments

1) Solid-State Imaging Experiment (SSI)

M. J. S. Belton, Team Leader

The SSI experiment utilizes a high-resolution (1500 mm focal length) television camera with an 800×800 pixel virtual-phase, charge-coupled detector. The F/8.5 camera system can reach point sources of $V(\text{mag}) \sim 11$ with $S/N \sim 10$ and extended sources with surface brightness as low as 20 kR in its highest gain state and longest exposure mode. The detector is 'pre flashed' before each exposure to ensure the photometric linearity. The dynamic range is spread over 3 gain states and an exposure range from 4.17 ms to 51.2 s. The objective of SSI is to study satellite science, Jupiter atmospheric science, magnetospheric interactions, Jovian rings, and other targets of opportunity such as asteroids 951-Gaspra and 243-Ida. SSI will return images of Jupiter and its satellites that are characterized by a combination of sensitivity levels, spatial resolution, geometric fidelity, and spectral range unmatched by imaging data obtained previously. The spectral range extends from approximately 375 to 1100 nm and only in the near ultra-violet

region (~350 nm) is the spectral coverage reduced from previously missions. The camera is approximately 100 times more sensitive than those used in the Voyager mission, and, because of the nature of the satellite encounters, will produce images with approximately 100 times the ground resolution (i.e. ~50 m lp⁻¹) on the Galilean satellites. The imaging system will also map the spatial variation in color and albedo at scale of 2 km or better and will monitor variations with time. It is expected to find the location of the spin axis, the rate of rotation, and the geometric figure to within 3 km for each Galilean satellites. For the Jupiter itself, SSI will determine the energetics, structures, mass and wind motions, and radiative properties of the Jovian atmosphere. Auroral phenomena in the atmosphere and on the satellites will be mapped and correlated with particle and field observations to determine the nature of interactions of the atmosphere with the magnetosphere. SSI will image the rings of Jupiter at the highest possible resolution to find any satellites that may be embedded in the rings. Also, photometric observations will determine color, albedo, column densities, and the size distribution of ring particles.

2) Near-Infrared Mapping Spectrometer (NIMS)

R. W. Carlson, PI

The NIMS is a remote sensing instrument with a combination of imaging and spectroscopic capabilities. The NIMS experiment objectives are to map and determine the mineral content of compositional units on the surfaces of the Jovian satellites and to investigate cloud properties and the temporal and spatial variability of minor constituents of the Jovian atmosphere. For geological studies of surfaces, NIMS can be used to map morphological features, while simultaneously determining their composition and mineralogy, providing data to investigate the evolution of surface geology. For atmospheres, many of the most interesting phenomena are transitory, with unpredictable locations. With concurrent mapping and spectroscopy, such features can be found and spectroscopically analyzed. In addition, the spatial/compositional aspects of known features can be fully investigated.

The instrument consists of a telescope, with one dimension of spatial scanning, and a diffraction grating spectrometer. Both are passively cooled to low temperatures in order to reduce background photon shot noise. The detectors consist of an array of indium antimonide and silicon photovoltaic diodes, contained within a focal-plane-assembly, and cooled to cryogenic temperatures using a radiative cooler. Spectral and spatial scanning is accomplished by electro-mechanical devices, with motions executed using commendable instrument modes. NIMS completes a spectral scan in 1/3, 4 1/3 and 8 2/3 seconds and covers the spectral range of 0.7 to 5.2 μ , which includes the reflected-sunlight and thermal-radiation regimes for many solar system objects, with spectral resolution of 0.025 μ . It has an angular field of 10 mrad x 0.5 mrad (20 pixels in cross-cone direction) with a resolution of 0.5 mrad x 0.5 mrad.

3) Ultraviolet Spectrometer (UVS)

C. W. Hord, PI

The primary objectives of the UVS investigation are to understand physical processes and characteristic properties of the upper atmosphere of Jupiter, the Io plasma torus and the surfaces of the Galilean satellites. Properties of the high atmosphere of Jupiter to be determined by the ultraviolet spectrometer include the molecular absorption features that may be characteristic of the colored clouds, auroral zone emissions arising from the bombardment of the high atmosphere by energetic particles, and airglow emissions from the atmosphere. For the satellites, UVS will determine the ultraviolet reflective properties of the surface that help to characterize surface materials and their physical state - ice, frost, and size of grains, it will also detect atomic

hydrogen, atomic oxygen, and nitrogen from the Galilean satellites to determine how these planet-sized bodies continue to evolve through the loss of volatile gases. Plasma torus of Io will be investigated by observing the emissions of multiply ionized oxygen and sulfur.

The UVS instrument consists of the Ultraviolet Spectrometer (UVS) mounted on the pointed orbiter scan platform and the Extreme Ultraviolet Spectrometer (EUVS) mounted on the spinning part of the orbiter with the field of view perpendicular to the spin axis. The UVS is a Ebert-Fastie design that covers the range 113–432 nm with a wavelength resolution of 0.7 nm below 190 and 1.3 nm at longer wavelength. The UVS spatial resolution is 0.4 deg x 0.1 deg for illuminated disc observations and 1 deg x 0.1 deg for limb geometries. The EUVS is a Voyager design objective grating spectrometer, modified to cover the wavelength range from 54 to 128 nm with wavelength resolution 3.5 nm for extended sources and 1.5 nm for point sources and spatial resolution 0.87 deg x 0.17 deg.

4) Photopolarimeter-Radiometer (PPR)

J. E. Hansen, PI

The PPR is a remote sensing instrument designed to measure the degree of linear polarization and the intensity of reflected sunlight in ten spectral channels between 410 and 945 nm to determine the physical properties of Jovian clouds and aerosols, including their size, shape, refractive index, and the vertical and horizontal distributions, and to characterize the texture and microstructure of satellite surface. The PPR also measure thermal radiation in five spectral bands between 15 and 100 μm to sense the upper tropospheric temperature structure. Two additional channels which measure spectrally integrated solar and solar plus thermal radiation are used to determine the planetary radiation budget components.

To accomplish the full complement of PPR polarimetric, photometric and radiometric measurements, the instrument utilizes a Cassegrainian Dall-Kirkham telescope with a 10 cm aperture scene-view and 50 cm effective focal length which gives excellent image quality for the 2.5 mrad instantaneous field view, with the image quality being dominated by diffraction at the longer wavelengths. Radiation from Jupiter or a satellite passes through a series of baffles, to be reflected by the primary and secondary mirrors through a radiometric stop and a hole in the primary mirror. The first set of optics is used to gather radiation from an object being surveyed; the other collects radiation from space. These two optical paths meet at a chopper which alternately admits radiation from planet or satellites and from space for radiometry measurements. When the instrument is being used for photometry and polarimetry, only radiation coming along the primary path is admitted to the detectors. The PPR has a high measurement accuracy with absolute resolution of $\pm 0.1\%$ for polarimetric measurement, $\pm 3\%$ for photometric measurement, $\pm 5\%$ for radiometric solar band, and ± 1 K (at 130 K) for radiometric thermal emission.

5) Magnetometer (MAG)

M. G. Kivelson, PI

The MAG experiment is designed to provide magnetic field data with which it will be possible to map the Jovian magnetosphere, monitor magnetospheric dynamics, study the large-scale structure and evolution of the solar wind, understand the structure of the bow shock and on upstream waves, and investigate magnetosphere-ionosphere coupling. In addition to providing data of direct importance for scientific investigations, the MAG performs a critical service function, providing the reference direction essential to the meaningful analysis of the plasma and energetic charged particle measurements. The magnetometer will provide highly accurate and stable measurements of field vectors over an exceptionally broad dynamic range from the low

values characteristic of the distant solar wind and the distant magnetotail (0.1 to 1 nT) to values larger than the largest anticipated ($\sim 6 \times 10^3$ nT) near closest approach to Jupiter. The MAG comprises two ring core fluxgate sensors. The outboard sensor, with dynamic ranges of ± 32 and ± 512 nT, is mounted at the end of a deployable boom about 11 m from the spacecraft spin axis. The inboard sensor covering the dynamic range from ± 512 and $\pm 16\,384$ nT is mounted on the same boom at a distance of 6.87 m from the spacecraft spin axis. The MAG instrument provides sensitive measurements with resolution of about 0.001 nT to 0.5 nT at the range of ± 32 nT to $\pm 16\,384$ nT.

6) Energetic Particle Detector (EPD)

D. J. Williams, PI

The EPD instrument is designed to measure the characteristics of particle populations important in determining the size, shape, and dynamics of the Jovian magnetosphere, and in understanding the interactions of satellites and magnetosphere, as well as the ionosphere-magnetosphere coupling. The EPD provides 4π angular coverage and spectral measurements for $Z \geq 1$ ions from 20 keV to 55 MeV, for electrons from 15 keV to > 11 MeV. The instrument has two separate bi-directional, solid-state telescopes mounted on a stepping platform to provide 64 rate channels and pulse height analysis of priority selected events by employing magnetic deflection, energy loss versus energy, and time-of-flight techniques. These telescopes form two subsystems: a Low-Energy Magnetospheric Measuring System (LEMMS) and a Composition Measuring System (CMS). The LEMMS is designed to measure low to medium energy ion and electron fluxes with wide dynamic range and high angular ($< 20^\circ$) and temporal (1/3 to 4/3 s) resolution. A full of coverage of the unit sphere is obtained by the use of a stepping platform in conjunction with satellite spin. The CMS is to measure the composition of ions in the Jovian environment from energies of ≥ 10 keV/nucl to > 10 MeV/nucl. The EPD data system provides a large number of possible operational modes from which a small number will be selected to optimize data collection during the many encounter and cruise phases of the mission. The EPD has demonstrated its operational flexibility throughout the long evolution of the Galileo program by readily accommodating a variety of secondary mission objectives occasioned by the changing mission profile, such as the Venus flyby and the Earth 1 and 2 encounters.

7) Plasma Instrumentation (PLS)

L. A. Frank, PI

The objective of the PLS instrument is to measure the physical properties of protons, heavy ions, and high energy electrons in and around the Jovian magnetosphere. The PLS comprises a nested set of four spherical-plate electrostatic analyzers and three miniature, magnetic mass spectrometers. The three-dimensional velocity distributions of positive ions and electrons, separately, are determined for the energy-per-unit charge (E/Q) range of 0.9 V to 52 kV that is divided into 64 passbands. A large fraction of the 4π -steradian solid angle for charged particle velocity vectors is sampled by means of the fan-shaped field-of-view of 160° , multiple sensors, and the rotation of the spacecraft spinning section. Thus such important plasma parameters as field-aligned currents, cross-field currents, plasma bulk flow velocities, heat fluxes, and free energy can be determined. The field-of-view of the three mass spectrometers are respectively directed perpendicular and nearly parallel and anti-parallel to the spin axis of the spacecraft. These mass spectrometers are used to identify the composition of the positive ion plasma, e.g., H^+ , O^+ , Na^+ , and S^+ , in the Jovian magnetosphere. The energy range of these three mass spectrometers is dependent upon the species. The maximum temporal resolutions of the instrument for determining the energy (E/Q) spectra of charged particles and mass (M/Q) composition of positive ion plasma are 0.5 s. Three-dimensional velocity distributions of electrons and positive ions require a minimum sampling time of 20s, which is slightly longer than the spacecraft rotation period. High temporal and angular resolutions of PLS instrument

will help to understand the formation and dynamics of plasma boundaries such as plasma sheet and current sheet, and the rate of mass loss from each satellite. The two instrument microprocessors provide the capability of inflight implementation of operational modes by ground-command that are tailored for specific plasma regimes, e.g., magnetosheath, plasma sheet, cold and hot tori, and satellite wakes, and that can be improved upon as acquired knowledge increases during the tour of the Jovian magnetosphere.

8) Plasma Wave Investigation (PWS)

D. A. Gurnett, PI

The basic objective of the PWS investigation is the study of plasma waves and radio emissions in the magnetosphere of Jupiter. The instrument uses an 6.6 m tip-to-tip electric dipole antenna, mounted at the end of the magnetometer boom approximately 10.6 m from the spacecraft, to detect electric fields, and two search coil magnetic antennas, mounted on the high gain antenna feed, to detect magnetic fields. The frequency range covered is 5 Hz to 5.6 MHz for electric fields and 5 Hz to 160 kHz for magnetic fields. The nearly simultaneous measurements of the electric and magnetic spectra allow PWS to distinguish electrostatic waves from electromagnetic waves, and the spinning of the spacecraft permits the use of a radio direction-finding technique to determine the locations of the radio sources. Onboard signal processing takes place within a main electronic package mounted near the base of the magnetometer boom. Signals from the antenna and the search coils are processed by four main elements: a low-frequency spectrum analyzer, a medium-frequency spectrum analyzer, a high-frequency spectrum analyzer, and a wideband waveform receiver. Low time-resolution survey spectrums are provided by the three spectrum analyzers. In the normal mode of operation the frequency resolution is about 10%, and the time resolution for a complete set of electric and magnetic field measurements is 37.33 s. High time-resolution spectrums are provided by the wideband receiver. The wideband receiver provides waveform measurements over bandwidths of 1, 10, and 80 kHz. These measurement can be either transmitted to the ground in real time, or stored on the spacecraft tape recorder.

9) Duster Detector (DDS)

Eberhard Grun, PI

The DDS is intended to provide direct observations of dust grains with masses between 10^{-19} and 10^{-9} kg in interplanetary space and in the Jovian system, to investigate their physical and dynamical properties as function of the distances to the Sun, to Jupiter and to its satellites, to study the interaction with the Galilean satellites and the Jovian magnetosphere. DDS will also studies the surface phenomena of the satellites (like albedo variations), the electric charges of particular matter in the magnetosphere and its consequences such as the effects of the magnetic field on the trajectories of dust particles and fragmentation of particles due to electrostatic disruption. The instrument comprises a set of grids, electron and ion collector for sensing the impact products of a dust particle, and a pulse rise-time circuits to determine the mass, electric charge, impact speed and direction of dust particles entering the wide field of view of 140° . The corresponding speed range of the dust detector is 1 to 70 km/s. The particles' electric charges are measured from 10^{-14} C to 10^{-10} C for negative charges and 10^{-14} C to 10^{-12} C for positive charges. DDS is a multicoincidence detector with a mass sensitivity 10^6 time higher than that of previous in-situ experiments which measured dust in the outer solar system.

10) Radio Science (RS)—Radio Propagation

H.T. Howard, Team Leader

The Radio Science investigations planned for Galileo's 6-year flight to and 2-year orbit of Jupiter use as their instrument the dual-frequency radio system (an S-band and an X-band) on the spacecraft operating in conjunction with various US and German tracking stations on Earth. The NASA Deep Space Network (DSN), operated by JPL, is responsible for tracking and commanding the spacecraft, receiving engineering and scientific telemetry, and for recording the basic measurements which become radio science data. The Radio Propagation Experiments are based on measurements of absolute and differential propagation time delay, differential phase delay, Doppler shift, signal strength, and polarization. These measurements will be used to study: the atmospheric and ionospheric structure, constituents, and dynamics of Jupiter; the magnetic field of Jupiter; the diameter of Io, its ionospheric structure, and the distribution of plasma in the Io torus; the diameters of the other Galilean satellites, certain properties of their surfaces, and possibly their atmospheres and ionospheres; and the plasma dynamics and magnetic field of the solar corona.

11) Radio Science (RS)—Celestial Mechanics

J. D. Anderson, Team Leader

The gravitation and celestial mechanics investigations during the cruise and Orbiter phases depend on Doppler and ranging measurements generated by the DSN at its three spacecraft tracking sites in California, Australia, and Spain. The investigation aims at the determination of the gravity fields of Jupiter and its four major satellites during the cruise phase, a search for gravitational radiation as evidenced by perturbations to the coherent Doppler link between the spacecraft and Earth, the mathematical modeling, and by implication tests, of general relativistic effects on the Doppler and ranging data during both cruise and orbiter phases, and an improvement in the ephemeris of Jupiter by means of spacecraft ranging during the orbiter phase. The gravity fields are accessible because of their effects on the spacecraft motion, determined primarily from the Doppler data. For the Galilean satellites the investigation will determine second degree and order gravity harmonic that will yield new information on the central condensation and likely composition of material within these giant satellites. The search for gravitational radiation is being conducted in cruise for periods of 40 days centered around solar opposition. During these times the radio link is least affected by scintillations introduced by solar plasma. Our sensitivity to the amplitude of sinusoidal signals approaches 10–15 in a band of gravitational frequencies between 10^{-4} and 10^{-3} Hz, by far the best sensitivity obtained in this band to date.

12) Heavy Ion Counter (HIC)

T. L. Garrard, Team Leader

The HIC experiment is designed to monitor the fluxes of energetic heavy ions trapped in the inner Jovian magnetosphere and high-energy solar particles in the outer magnetosphere in order to characterize the ionizing radiation to which electronic circuitry is most sensitive. With large geometry factors (e.g., the geometry factor for $E > 20$ MeV/nucl oxygen ions is ~ 4 cm² sr) and extended energy range the HIC will provide spectral information for ions from ${}^6\text{C}$ to ${}^{28}\text{Ni}$ with energies of ~ 6 to ≥ 200 MeV/nucl. Measurements with the HIC instrument will significantly reduce the uncertainty in the high-energy fluxes. The HIC consists of two solid-state detector telescopes called Low Energy Telescopes (LETs), an improved version of the Voyager Cosmic Ray Subsystem (CRS) LETs. LET E is optimized for the detection of nuclei with energies as

high as 200 MeV/nucl, requiring thicker detectors. Thick windows protect this system from low-energy proton pile-up, but also exclude lower energy oxygen and sulfur nuclei. The second telescope, LET B, has a substantially thinner window so that it can detect lower energy nuclei (down to ~ 6 MeV/nucl), especially in the outer magnetosphere. Telemetry of counting rates and pulse height analyzed events is rapid compared to the nominal 3 rpm spin rate of the spacecraft; thus pitch-angle distributions of the trapped radiation can be measured. Both telescopes have their axes oriented near the spin plane for this purpose. The time resolution of the HIC is in the range from 2/3 to 2 s, implying an angular resolution in the range from 12° to 36° , which is to be compared to the telescope opening angles of 25° in narrow geometry mode and 46° in wide geometry mode.

Galileo Instrument Summary

	<i>Investigation</i>	<i>Range</i>
<i>Probe—ASI</i>	Determine temperature, pressure, density, and molecular weight as a function of altitude	Temperature: 0–540 K Pressure: 0–28 bars
<i>Probe—GPMS</i>	Determine chemical composition of atmosphere	Cover 1–150 amu
<i>Probe—HAD</i>	Determine relative abundance of helium	Accuracy: 0.1%
<i>Probe—NEP</i>	Detect clouds and infer states of particles (liquid vs. solid)	0.2–20 μm particles, as few as 3 cm^{-3}
<i>Probe—NFR</i>	Determine ambient thermal and solar radiation as a function of altitude	6 infrared filters in 0.3–100 μm
<i>Probe—EPI/LRD</i>	Study the energetic particular population in the inner magnetosphere; verify the existence of lightning and measure energetic particles	e: ≥ 3.2 MeV p: 42–131 MeV 10 Hz–100 kHz
<i>Orbiter—SSI</i>	Map Galilean satellites at 1 km resolution, and monitor atmospheric circulation over 20 months	375–1100 nm 0.47° FOV,
<i>Orbiter—NIMS</i>	Observe Jupiter and its satellites in the infrared to study satellite surface composition, Jovian atmospheric composition and temperature	0.7–5.2 m range, 0.03 μm resolution 0.5m rad IFOV
<i>Orbiter—UVS</i>	Measure gases and aerosols in Jovian atmosphere, and S, O ion emissions of the Io torus, and H auroral and airglow emission of Jupiter	1150–4300 Å 54–128 nm
<i>Orbiter—PPR</i>	Determine distribution and character of atmospheric particles, compare flux of thermal and incoming solar emissions	visible and near-infrared bands, radiometry $> 42\ \mu\text{m}$
<i>Orbiter—MAG</i>	Monitor vector magnetic field and its changes	32–16384 γ
<i>Orbiter—EPD</i>	Measure high energy e, p, and heavy ions in and around Jovian magnetosphere	Ions: 0.02–55 MeV; e: 0.015–11 MeV
<i>Orbiter—PLS</i>	Assess composition, energy, and 3-D distribution of low-energy electrons and ions	0.9–52 keV in 64 bands
<i>Orbiter—PWS</i>	Detect electromagnetic waves and analyze wave-particle interactions	E: 5 Hz–5.6 MHz B: 5 Hz–160 kHz
<i>Orbiter—DDS</i>	Measure particles' mass, velocity, and charge	10^{-16} – 10^{-6} g, 2–50km/s
<i>Orbiter—RS</i>	Determine mass of Jupiter and its satellites, and measure atmospheric structure and size	S and X-band signals
<i>Orbiter—HIC</i>	Monitor the fluxes and composition of trapped heavy ions and solar particles in magnetosphere	ions from C to Ni, 6 to ≥ 200 MeV/nucl

Project Scientist: T. V. Johnson, JPL,
Program Scientist: Jay Bergstrahl, NASA HQ, (202) 358-0292

The Geotail Mission and Payload

Geotail is a collaborative project being undertaken by ISAS and NASA as part of the Collaborative Solar-Terrestrial Research (COSTR) program. The Geotail spacecraft was launched by a Delta II rocket from the Cape Canaveral Air Force Station on July 24, 1992. Geotail uses lunar gravitational assists to keep the spacecraft on the night side of the Earth in its initial distance orbit around the Earth. This orbit has an apogee up to 210 Earth radii and a perigee of approximately 8 Earth radii. Geotail will be repositioned later in a near-Earth elliptic orbit with an apogee of approximately 50 Earth radii and then 30 Earth radii; the perigee will be about 10 Earth radii. The solar wind draws the Earth's magnetic field into a long tail on the nightside of the Earth and stores energy in the stretched field lines of the magnetotail. During active periods, the tail couples with the Earth magnetosphere, sometimes releasing energy stored in the tail and activating auroras in the polar ionosphere. Geotail measures the flow of energy and its transformation in the magnetotail and will help clarify the mechanisms that control the input, transport, storage, release, and conversion of mass, momentum, and energy in the magnetotail.

The primary objective is to study the dynamics of the Earth's magnetotail over a wide range of distances extending from the near-Earth region (8 R_e) to the distant tail (210 R_e). Information gathered during the Geotail mission will allow scientists to model and more accurately predict Sun-Earth interactions and their effects on space exploration, communications, and ground technology systems.

The comprehensive Geotail instrument package will:

- Determine the overall plasma, electric, and magnetic field characteristics of both the distant and near geomagnetic tail
- Determine the role of the distant and near-Earth tail in substorm phenomena and in the overall magnetospheric energy balance, and relate these phenomena to external triggering mechanisms
- Determine the composition and charge state of plasma in the geomagnetic tail at various energies during quiet and dynamic periods, and distinguish between the ionosphere and solar-wind as sources for this plasma
- Study the processes that initiate magnetic field reconnection in the near-Earth tail, and observe the microscopic nature of the energy conversion mechanisms in the reconnection region
- Study plasma entry, energization, and transport processes in interaction regions such as the inner edge of the plasma sheet, the magnetopause, and the bow shock, and investigate associated boundary layer regions

Geotail will also provide data to support the Wind and Polar satellites of the Global Geospace Science (GGS) program, and perform simultaneous and closely coordinated measurements of key geospace regions.

Key Geotail Mission Statistics

Mission Class:	Intermediate
Launch Date:	24 July 1992
Launch Vehicle:	Delta-II
Launch Site:	CCAFS
Mission Duration:	4 Years
Orbit:	Double lunar swingby to an 8 x up to 210 R _e orbit, reduced to a 10 x 50 and then 10 x 30 R _e quasi equatorial orbit, 7.5° inclination.
S/C Type:	Drum shaped. 1.6 m long, 2.2 m diameter.
S/C Mass:	1009 kg
Propulsion ΔV :	~820 m/s (ΔV maneuvers every 1–2 months)
Stabilization:	Spin stabilized at 20 rpm
Pointing Accuracy:	0.2°
Pointing Knowledge:	1°
Power:	340 Watts
Science Telemetry:	64 and 16 kbps
Data Storage:	900 Mbits
Manufacturer:	Institute of Space and Astronautical Science (ISAS)

Geotail Instruments

1) Electric Fields Detector (EFD) K. Tsuruda, PI

Geotail's measurements of the electric fields in the tail is key to developing a theory about the formation of the magnetotail. Electric field in the near-Earth magnetosphere are closely coupled with the ionospheric electric field. EFD studies this coupling, especially during substorms, using electric field antennas and an electron beam technique. In addition, the merging of magnetic fields in the plasma sheet generates inductive electric fields that accelerate charged particles, which can be measured by other instruments onboard the spacecraft.

2) Magnetic Fields (MGF) S. Kokubun, PI

Information about the dynamics of the transport of mass, momentum, and energy between the magnetosphere and ionosphere can be inferred from changes in the magnetic field configuration in various regions. MGF measurements in the near-Earth tail plasma should provide more information about mechanisms (for example, field-line merging) that transfer energy and trigger substorms. MGF investigates magnetic merging in the magnetotail, which is thought to produce a bubble of plasma, called a plasmoid, that flows down the tail during active periods. Also, MGF observes the distant tail to determine its magnetic field structure--whether well ordered or filamentary, for example -- and its dynamic changes associated with substorms.

3) Low-Energy Particles (LEP) T. Mukai, PI

Low-energy electrons from 6 electronvolts (eV) to 36 kiloelectronvolts (keV) and ions from 7 eV to 42 keV per charge are observed in the magnetotail and in the interplanetary medium to study

the nature and dynamics of magnetotail plasmas, analyze the plasma conditions under which particle acceleration takes place, and study plasma circulation and its variability in response to fluctuations in the solar wind and in the interplanetary magnetic field. Particles from Earth's ionosphere are identified and the entry of plasmas into the magnetosphere from the magnetosheath is studied to improve our understanding of open versus closed magnetospheres.

4) Comprehensive Plasma Investigation (CPI)

L. Frank, PI

This investigation obtains complete three-dimensional plasma measurements in the Earth's magnetotail. Plasma parameters, including heat flux and field-aligned current density, are measured by a hot plasma and ion composition analyzer and a solar wind analyzer. The plasma data is correlated with the magnetic field, plasma waves, energetic particles, and auroral imaging to determine the magnetotail plasma dynamics. Studies are made to distinguish the source of plasma and the mechanism and efficiency of the coupling of the solar-wind energy (measured by instruments on the Wind satellite) into the magnetosphere as a function of solar-wind conditions upstream.

5) High-Energy Particles (HEP)

T. Doke, PI

Measurements of high-energy particles can indicate plasma boundary surfaces and reflect whether magnetic field lines are open or closed. The composition and charge state of energetic particles provide rich information on where particles originate, and different solar events produce different energetic particle signatures. Small, hot sites in the corona produce samples rich in Helium ions, for example. The origin and acceleration of galactic cosmic rays and their modulation in our galaxy are also investigated.

3) Energetic Particle and Ion Composition (EPIC)

D. Williams, PI

The EPIC investigation uses an ion composition spectrometer and a particle telescope to measure the charge state, mass, and energy of ions. These measurements are used to study the relative importance of ion sources and mechanisms for acceleration, transport and loss of particles, the formation and dynamics of magnetospheric boundary layers, and influence of these layers on magnetospheric behavior. Particularly important will be the determination of particle sources in large-scale structures such as plasmoids.

7) Plasma Wave Instrument (PWI)

H. Matsumoto, PI

During Geotail's excursions from the near-Earth to the far-tail regions, PWI measures plasma waves in frequency range up to 800 kilohertz (kHz) to sample wave phenomena related to plasma dynamics in the different regions on various scales within its range. These phenomena include magnetic-field-line merging, moving plasmoids, and particle acceleration via wave-particle interaction within the magnetotail.

Geotail Instruments Summary

<i>Investigation</i>	<i>Description</i>	<i>Range</i>
Electric Field (EFD)	Spherical probe and wire antenna	dc - 40Hz (2 comp)
	Electron boomerang	dc - 10Hz (3 comp)
	Ion emitter	
Magnetic Field (MGF)	Fluxgate	dc - 8 Hz (3 comp)
	Search Coil	0.5 - 50 Hz (3 comp)
Plasma (LEP)	Ion/electron 3-d velocity distribution	6 eV - 36 keV/q
	Solar wind ions	100 eV - 8 keV/q
	Ion mass/energy spectrum	5 eV - 25 keV/q
Plasma (CPI)	Ion/electron 3-d velocity distribution	1 eV - 50 keV/q
	Solar wind ions	150 eV - 7 keV/q
	Ion mass/energy spectrum	1 eV - 50 keV/q
Energetic Particles (HEP)	Low energy particles	0.002 - 1.5 MeV/n
	Ion/electron burst	0.7 - 3.5 MeV/n
	Medium energy ion isotope ratio	5 - 50 MeV/n
	High energy ion isotope ratio	20 - 100 MeV/n
Energetic Particles (EPIC)	Ion charge state/mass/energy	30 - 230 keV/q
	Ion mass and energy	> 50 keV - 5 MeV
	Electron energy	> 30 keV
Plasma Waves (PWI)	Frequency sweep	E: 25 Hz - 800 kHz
	Multichannel analyzer	H: 25 Hz - 12.5 kHz
	Waveform capture	10 Hz - 4 kHz

Geotail has a complement of seven instruments, the United States providing two and the Japanese providing three. The remaining two instruments are shared.

Program Scientist (NASA): E. Whipple, NASA/HQ, (202) 358-0888

Project Scientist (NASA): M. Acuna, GSFC, (301) 286-7528

Program Scientist (ISAS): A. Nishida

Project Scientist (ISAS): T. Mukai

The GOES Mission and Payload

The Geostationary Operational Environmental Satellite (GOES) program is a joint effort between the National Oceanic and Atmospheric Administration (NOAA) and the National Aeronautics and Space Administration (NASA) to provide continuous operational environmental observations of cloud cover, temperature profiles, sea surface temperatures, and severe and real-time storm warnings. The payload includes a Space Environment Monitor (SEM) instruments package from the Space Environment Laboratory (SEL), a component of the Environmental Research Laboratories of NOAA, in Boulder, Colorado. Data from the SEM are used by the Space Environment Services Center (SESC) to provide affected users with advisories and forecasts of conditions in the near-Earth space environment. The SEM instruments consist of two (redundant) magnetometers, an X-Ray Sensor (XRS), and an Energetic Particle Sensor (EPS). This description is focused on the SEM portion of the GOES mission. SEM systems have been flown on geostationary satellites since 1974, beginning with the first Synchronous Meteorological Satellite, SMS-1. SMS-1 and -2 were followed by the GOES series. Typically two satellites are maintained operational, one at about 135° geographic west longitude and one at about 75° geographic west longitude. The current operational satellites, GOES -6 launched in 1983 and GOES -7 launched in 1987, are in need of replacement. GOES -6 will be replaced by GOES-I, the first of a new series of five GOES satellites, launched on April 13, 1994 and GOES-7 will be replaced by GOES-J in April 1995. The GOES I-M, new series of satellites, will provide significant improvements in weather imagery and atmospheric sounding as well as some changes in the GOES SEM instruments. Some instrument modifications were necessary to accommodate the change from a spinning spacecraft to three-axis stabilized platforms in the new series. A new instrument, a Solar X-ray Imager (SXI), a joint effort of the USAF/NOAA/NASA, will be flown on one of the new series of GOES satellites around the turn of the century. The SXI will be capable of 1 image per minute of the sun in the spectral range from 6 to 60 angstroms and will have a resolution of 512 x 512 pixels with 5 arc second pixels.

Key GOES Mission Statistics

Launch Date:	GOES-I April 1994, GOES-J April 1995, followed by GOES-K,L,M
Launch Vehicle:	GOES I/J Atlas-Centaur (Atlas I); GOES K/L/M Atlas II or equivalent
Launch Site:	Eastern Test Range (ETR)
Mission Duration:	Design in-orbit lifetime duration is 5 years
Operational Orbit:	Geosynchronous (nominally, one spacecraft at 135° and one at 75° geographic west longitude)
Eclipse Duration:	maximum 73 min at equinox
S/C Mass:	2105 kg at launch, 977.2 kg dry
Stabilization:	3 axis-stabilized; two momentum wheels, a reaction wheel, two magnetic torquer coils and twelve 22-Newton thrusters
Pointing Accuracy:	1° or better for SEM instruments
Power:	Solar Array 1057-W capability at 5-year summer solstice, 2 nickel-cadmium batteries with 12 Ah each
Telemetry:	2000 bps (for data stream that includes SEM)
Data Storage:	Real-time telemetry link
Manufacturer:	Space Systems/Loral, Palo Alto, CA

GOES I-M Space Environment Monitor (SEM) Instruments

1) The Energetic Particle Sensor (EPS)

H. Sauer, Responsible Scientist

The EPS, built by Panametrics, Inc., comprises three detector assemblies: The EPS Telescope, the EPS Dome Detector Assembly, and the High Energy Proton and Alpha Detector (HEPAD). Together, these detectors monitor the energetic electron, proton, and alpha particle environment at geostationary orbit, from below 1 MeV to relativistic energies. The EPS telescope consists of two surface-barrier detectors and their shields and collimator which define their angular field of view. The channel particle and energy responses are established by electronic thresholds and their associated logic. The Dome Detector Assembly contains three units, each consisting of a solid-state detector shielded by a hemispheric dome moderator which primarily determines its particle and energy response. Finally, the HEPAD is a solid-state/Cerenkov telescope which observes relativistic particles with a large (60 deg) acceptance aperture. The in-flight gain of the HEPAD photomultiplier is monitored by a built in-light pulser using a radioactive isotope source. Regular in-flight calibration is performed on all the EPS electronics.

The particle environment at geostationary orbit observable by the EPS consists, generally, of three components: first, a geomagnetically trapped and highly variable population of electrons of up to some tens of MeV, and protons up to several MeV in energy; second, sporadic, sometimes large, fluxes of electrons, protons and alpha particles (usually a few percent of the proton flux) of solar origin, with both trapped and solar fluxes superposed on a background resulting from ever-present Galactic Cosmic Rays ranging from several MeV to highly relativistic energies. Knowledge of the near-earth energetic particle environment is important in establishing the natural radiation hazard to humans at aircraft altitudes and in space, as well as risk assessment and warning of episodes of surface charging, deep dielectric charging, and single event upset of satellite systems. Further, the state of the ionosphere is strongly modified by varying energetic particle precipitation into the earth's atmosphere. These modifications result in disturbance and occasional disruption of radio communications and navigation systems, in addition to their being associated with geomagnetic disturbance phenomena.

2) The Magnetometer

H. Singer, Responsible Scientist

The magnitude and direction of the ambient magnetic field are measured by two (redundant) Schonstedt magnetometers. The three-axis orthogonal sensors are located in a sensor assembly and attached to a boom that places the sensors 3 m and 2.7 m away from the body of the spacecraft. The electronics for the sensors are mounted separately on the spacecraft equipment platform. The three analog signals representing the x, y, and z components of the surrounding magnetic field are digitized by a 16-bit analog to digital converter. The sampling rate is 0.512 s. The magnetometer provides a sensitivity of about 0.1 nT while accommodating fields within the range of +/- 1000 nT. The measurement accuracy is 4 nT uncorrected, and 1 nT with temperature correction. An on-board calibrating system, under ground command, provides a calibration of basic instrument scale factor and verifies operation by superimposing a calibration field to the ambient field. Spacecraft interference fields, such as those generated by torquer coils, will need to be subtracted from the data. Prior, spin-stabilized GOES spacecraft, used two-sensor magnetometers with one in the spin plane and one along the spin axis. Spacecraft spin made it possible to make a 3-component vector measurement. The magnetometer data can be

used to characterize the general level of geomagnetic activity; to monitor currents systems in space; to detect magnetopause crossings, storm sudden commencements, and substorms; and for general use by the scientific community.

3) The Solar X-ray Sensor (XRS)
 H. Garcia, Responsible Scientist

The function of the solar X-ray Sensor (XRS), built by Panametrics, Inc., is to provide whole-sun measurements of the X-ray spectrum in two, broad energy bands: 1-8 and 0.5-4 angstroms. Comparing data from these energy ranges allows an estimate of the hardness of the solar spectrum. On the new GOES series, the overall dynamic range of the XRS is the same as on previous missions, but has been shifted to higher intensities to be able to encompass larger solar flares. The XRS sensor has two ion chambers with window transmission and gas filling characteristics chosen to provide a response in the desired spectral bands. However, special precautions are necessary to shield the sensor from the energetic electron environment at geosynchronous altitudes. Specifically, the ion chambers are mounted behind a common collimator which serves to reduce the access of electrons directly into the ion chamber window, and, by means of a transverse magnetic field provided by a permanent magnet assembly. Electrons stopped by the collimator, ion chamber, and spacecraft structure produce a background of bremsstrahlung radiation. The overall background after collimation, is expected to be just comparable with the minimum detectable X-ray flux. This can be checked if necessary by temporarily offsetting the sensor from the sun.

The GOES I-M X-ray sensor is continuously staring at the sun. The collimator and ion chamber assembly are mounted on a single axis positioner which in turn is mounted on the spacecraft solar array yoke. The single axis positioner moves the X-ray sensor along the north/south direction to track the sun declination of +/- 23.5°. The north/south positioner tracks the sun in closed loop through a sun sensor on the positioner. The east/west motion of the X-ray sensor is provided by the solar array drive. Prior GOES XRS used the satellite spin to perform an on-board subtraction of on and off sun measurements. They were therefore likely to be less sensitive to steady background contributions by charged particles, but could be disturbed by strong particle anisotropies.

GOES Instrument Summary

	<i>Investigation</i>	<i>Range</i>
SEM-EPS	Monitor the energetic electron, proton, and alpha particle environment at geostationary orbit.	e: 0.6->4.0 MeV p: 0.8-> 700 MeV α: 4->3400 MeV
SEM-MAG	Measure the magnitude and direction of the ambient magnetic field	0.1 nT ± 1000 nT with accuracy up to 1 nT.
SEM-XRS	Provide whole-sun measurements of the X-ray spectrum	energy band: 1-8Å and 0.5-4 Å.

Goes Project Scientist: Ron Zwickl, SEL, NOAA (303-497-3029)
 SEL SEM Project Engineer (NOAA): Richard Grubb (303-497-3284)
 SEL SEM Instrument Manager (NOAA): Lorne Matheson (303-497-3164)

The INTERBALL Mission and Payload

To study the details of the energy, momentum and mass transfer in the critical regions of the solar wind/magnetosphere system, scientist from Russia, Austria, Bulgaria, Canada, Cuba, Czechoslovakia, Finland, France, Germany, Greece, Hungary, Italy, Poland, Romania, Slovak, Sweden, UK, Ukraine, and ESA have developed the INTERBALL project. This project consists of four satellites: two Russia-made Prognoz satellites (TAIL probe and AURORAL probe), each supplied with one Czechoslovakia-made subsatellite (Tail C2-X and Auroral C2-A).

The Tail probe with its subsatellite will be launched in 1994 into an elongated elliptical orbit with an inclination of 65 degrees, apogee and perigee height of 200,000 km and 500 km, respectively. The separation between this pair will change from less than 100 km, allowing the study of small-scale wave and plasma structures at the boundaries, to about 1–2 Earth radii to study large plasma structures in the tail. The Auroral probe with its subsatellite will be launched soon after the Tail probe, also to a 65 degree inclination orbit, but with an apogee of 20,000 km and perigee of 500 km above the northern auroral zone and polar cap. The separation between the Auroral probe-subsatellite pair at apogee is planned to be between 10 and 1000 km, i.e. comparable to the size of thin auroral sheet currents and related auroral discrete forms.

The main objectives of INTERBALL is to study the physical mechanisms responsible for the transmission of solar wind energy to the magnetosphere, its storage there and subsequent dissipation in the tail and auroral regions of the magnetosphere, ionosphere and atmosphere during magnetospheric substorms. Two specific main cause-and-effect physical relationships will be addressed:

- Solar wind/magnetosheath plasma characteristics and their interactions with the magnetopause, cusp, and other outer regions of the magnetosphere at the dayside and at the flanks, and the resulting energy, mass, and momentum inputs to the magnetosphere and ionosphere from the solar wind
- Active plasma processes in the polar and auroral magnetic flux tubes being induced, and fed, by the currents and fields generated in the tail plasma sheet. These active processes in particular include adiabatic and non-adiabatic plasma heating and acceleration, substorm-type phenomena of various scales, strong current generation and related plasma instabilities, magnetosphere-ionosphere interactions, involving plasma convection and auroral phenomena, thermospheric heating, drag forcing of the upper atmosphere and the respective auroral and airglow manifestations, etc.

Key INTERBALL Mission Statistics

Launch Date:	INTERBALL-Tail: May, 1994
	INTERBALL-Auroral: Mid-August, 1994
Launch Vehicle:	-
Launch site:	Baikonur
Mission Duration:	nominally two years
Apogee:	200,000 km (Tail probe)
	20,000 km (Auroral probe)
Perigee:	500 km (Tail and Auroral probes)

Inclination:	65 degree (Tail and Auroral probes)
Stabilization:	Spin stabilized, 0.5 rpm
Separation distance:	1,000 to 10,000 km (Tail probe and C2-X) 10 to 1,000 km (Auroral and C2-A)
S/C Mass:	1050 to 1100 kg (Tail and Auroral probes) less than 50 kg (subsatellites)
Science Telemetry:	up to 32 to 40 kbit/s
Data Storage:	140–180 Mbytes/day

INTERBALL-Tail Instruments

1) 3D Ion Distribution (SKA-1)

O. Vaisberg and V. Smirnov (Russia), Co-PI's

This instrument will measure angular and energetic distributions of ions (0.1–5 keV/q) at all directions, and measure energy spectra of ions with M/q selection (M=1, 2, 4, 16) in the energy range of 5–100 keV at the sun direction. (Mass: 26.1 kg; Time resolution: 3.7 and 8 second; Data rate: 2 and 0.03 kbit/s).

2) 3D Spectral Ion Faraday Cup (VDP)

G. Zastenker and A. Fedorov (Russia), Co-PI's

This instrument will take omnidirectional fast measurements of integral fluxes of ion or electron with $E > 0$ eV and their directions. (Mass: 4.9 kg; Time resolution: 0.1 second; Data rate: 1 kbit/s).

3) 3D Electron Distribution Function (ELECTRON)

J. A. Sauvaud (France) and O. Vaisberg (Russia), Co-PI's

This instrument is for the measurements of energy spectra of electrons at all directions in the energy range of 0.01–26 keV. (Mass: 6.9 kg; Time resolution: 3, 7, and 120 seconds; Data rate: 1 kbit/s).

4) Wide-range 3D Ion Spectrometer (CORALL)

R. Jimenez (Cuba) and Yu. Yermolaev (Russia), Co-PI's

This spectrometer will measure angular and energy distributions of ions at all directions in the energy of 0.05–30 keV/q. (Mass: 5 kg; Time resolution: 120 seconds; Data rate: 1 kbit/s).

5) Energy-Mass Analyzer (AMEI-2)

R. Koleva (Bulgaria) and V. Smirnov (Russia), Co-PI's

This is an energy and mass analyzer will measure the energy spectra of ions (H+, He+, He++, and O+, and more heavier ones) at all directions in the energy range of 0.1–10 keV/q. (Mass: 9 kg; Time resolution: 120 seconds; Data rate: 0.2 kbit/s).

6) Solar Wind Analyzer (MONITOR-3)

A. Fedorov (Russia) and Ya. Shafrankova (Czechoslovakia), Co-PI's

This analyzer will take the measurements of the solar wind ion fluxes in the range of 0.4–15 keV/q and energy/angular distributions of H⁺ and He⁺⁺ around the Sun direction with high time resolution. (Mass: 7.8 kg; Time resolution: 1 second; Data rate: 8 kbit/s).

7) Ion Composition 3D Spectrometer (PROMICS-3)

I Sandahl (Sweden) and N. Pissarenko (Russia), Co-PI's

This instrument will make the ion composition (M=1-50) and 3-D energy distribution (10 eV–30 keV/q) measurements. (Mass: 12.9 kg; Time resolution: 1.2 and 2.6 seconds; Data rate: 2 kbit/s).

8) Ion Trap (ALFA-3)

V. Bezrukikh (Russia), PI

This instrument is for the thermal plasma ion flux measurements in energy range of $E \leq 25$ eV/q. (Mass: 3.5 kg; Time resolution: 16 seconds; Data rate: 1 kbit/s).

9) Low and Energetic Charged Particle Composition and Anisotropy (SKA-2)

E. Morozova (Russia) and S. Fisher (Czechoslovakia), Co-PI's

This experiment will make the measurements of charged energetic particles ($E = 40$ – 200 keV for electrons and $E = 0.05$ – 150 MeV for ions) composition and anisotropy. (Mass: 22.4 kg; Time resolution: 120 seconds; Data rate: 0.25 kbit/s).

10) Electron and Proton Fluxes and Anisotropy (DOK-2X)

K. Kudela (Czechoslovakia) and V. Lutsenko (Russia), Co-PI's

This instrument will measure spectra, flux and anisotropy of electrons ($E = 15$ – 400 keV) and ions ($E = 15$ – 1000 keV). (Mass: 5.5 kg; Time resolution: 120 seconds; Data rate: 2 kbit/s).

11) Solar X-rays (RF-15-I)

O. Likin (Russia), F. Farnik (Czechoslovakia), and J. Silvester (Poland), Co-PI's

This instrument is for the solar X-ray burst spectra and time profile measurements in the range of 2–200 keV, and for the position estimation. (Mass: 10 kg; Time resolution: 0.1 seconds; Data rate: 0.01 kbit/s).

12) Measurements of Electric Field (OPERA)

E. Amata (Italy), S. Savon (Russia), and M. Nozdrachev (Russia), Co-PI's

This experiment will measure three-component electric field fluctuations in the frequency range of 0–250 kHz, including onboard spectra calculations. (Mass: 3.7 kg; Time resolution: 1/64 seconds; Data rate: 3 kbit/s).

13) Measurements of Magnetic Field (MIF-M)
S. Romanov and M. Nozdrachev (Russia), Co-PI's

This experiment will measure three-component directly two-component alternatively magnetic field fluctuations in the frequency range of 0–40 kHz. (Mass: 7.5 kg; Time resolution: 1/64 seconds; Data rate: 2.5 kbit/s).

14) Measurements of Ion Flux and Electron Flux Functions (IFPE)
J. Buchner (Germany), A. Skalsky and A. Belikova (Russia), Co-PI's

This instrument will take measurements of ion (at two directions) and electron flux fluctuations in frequency range from 0.1 to 1000 Hz. (Mass: 4.9 kg; Time resolution: 1/64 seconds; Data rate: 2.5 kbit/s).

15) Multi-channel Spectrum Analyzer (ADS)
J. Juchnievicz (Poland), A. Skalsky and A. Belikova (Russia), Co-PI's

This is a nine-channel spectra-analyzer and cross-correlator for two-component measurements of current fluctuations in frequency range from 0.25 Hz to 40 kHz. (Mass: 6.7 kg; Time resolution: 2 seconds; Data rate: 2 kbit/s).

16) Magnetic Field (IMAP-2)
I. Arshinkov (Bulgaria) and V. Stiazhkin (Russia), Co-PI's

This is a three-component magnetometer in frequency range from DC to 10 Hz with two dynamic ranges: 700 nT with 0.1 nT resolution, and 70,000 nT with 1 nT resolution. (Mass: 4.9 kg; Time resolution: 0.12 seconds; Data rate: 0.5 kbit/s).

17) Kilometric Radioemission (AKR-X)
L. Fisher (Czechoslovakia) and V. Grigorjeva (Russia), Co-PI's

This detector is to measure radioemission in the frequency range from 100 kHz to 1.5 MHz. (Mass: 2.1 kg; Time resolution: 0.06 seconds; Data rate: 1.8 kbit/s).

18) Subsatellite for Measurements of Electric and Magnetic Fields, Waves, Plasma and Energetic Particles (C2-X)
P. Triska and Ya. Voita (Czechoslovakia), Co-PI's

The instruments onboard the subsatellite C2-X will make multi-measurements of plasma, energetic particles, electric and magnetic fields and waves. (Mass: 50 kg; Time resolution: ---; Data rate: 20 kbit/s).

19) Adaptive Processing of Wave Information (PRAM)
S. Romanov and N. Rybyevea (Russia), Co-PI's

20) Wave Complex (ASPI)
S. Klimov and S. Romanov (Russia), Co-PI's

INTERBALL-Auroral Instruments

1) Electron and Proton Distribution and Ion Anisotropy (SKA-3)

A. Kuzmin and R. Kovrazhkin (Russia), Co-PI's

This instrument will measure electron and proton distributions ($E = 0.13\text{--}15\text{ keV}$), ion ($M = 1, 4, 16$) anisotropy ($E = 30\text{--}500\text{ keV/q}$). (Mass: 32 kg; Time resolution: 1.5 and 0.2 seconds; Data rate: 3 kbit/s).

2) Ion Spectra and Anisotropy (ION)

J. A. Sauvaud (France) and R. A. Kovrazhkin (Russia), Co-PI's

This detector will make the measurements of ion ($M = 1, 2, 4, 16$) and electron energy spectra and anisotropy in the energy range from 5 eV to 20 keV/q. (Mass: 17 kg; Time resolution: 3.2 seconds; Data rate: 3 kbit/s).

3) Ion composition 3D Spectrometer (PROMICS-3)

I Sandahl (Sweden) and N. Pissarenko (Russia), Co-PI's

This experiment is for the ion composition ($M = 1\text{--}50$) and three-dimensional energy distribution ($E = 10\text{ eV--}30\text{ keV/q}$) measurements. (Mass: 12.9 kg; Time resolution: 1.2 and 2.6 seconds; Data rate: 2 kbit/s).

4) Magnetic Field (IMAP-3)

I Arshinkov (Bulgaria) and V. Stiazhkin (Russia), Co-PI's

This is a three-component magnetometer similar to instrument IMAP-2 onboard the Tail probe. It can measure magnetic field from 1 to 60,000 nT with frequency range from DC to 10 Hz. (Mass: 4.8 kg; Time resolution: 0.12 seconds; Data rate: 1 kbit/s).

5) Electric Field (IESP-2)

V. Chmyrev (Russia) and G. Stanev (Bulgaria), Co-PI's

This detector can measure electric field fluctuation in frequency range of 0–50 Hz with very high time resolution. (Mass: 6.7 kg; Time resolution: 0.03 seconds; Data rate: 7.2 kbit/s).

6) VLF Electromagnetic Waves (NVK-ONCH)

O. Molchanov and A. Goljavin (Russia), Co-PI's

This experiment is aim to measure VLF electromagnetic waves from 20 Hz to 20 kHz. (Mass: 17 kg; Time resolution: 2 X 12 kHz).

7) Electromagnetic Waves in Wide Band (MEMO)

F. Lefeuvre (France) and M. Mogilevsky (Russia), Co-PI's

This is a magnetic wave analyzer that can measure electromagnetic waves in very wide frequency range from 10 Hz to 2 MHz. (Mass: 14.5 kg; Time resolution: 0.25 to 120 seconds; Data rate: 20 kbit/s).

8) Auroral Kilometric Radiation (POLRAD)

J. Hanash (Poland), I. Lishin and M. Mogilevsky (Russia), Co-PI's

This experiment will make an auroral kilometric radioemission measurements in the frequency range from 20 kHz to 3 MHz. (Mass: 22.5 kg; Data rate: 2.3 kbit/s).

9) Ion Mass Analyzer (HYPER-BOLOID)

J. J. Berthelier (France) and T. Muliarchik (Russia), Co-PI's

This is an ion mass analyzer with energy range of $E = 0-100$ eV, velocity range of 0.1-20 km/s for H⁺, He⁺, O⁺, O⁺⁺, N⁺, N²⁺, NO⁺, and O²⁺. (Mass: 15 kg; Time resolution: 1 seconds; Data rate: 8 kbit/s).

10) Temperature of Cold Plasma Electrons (KM-7)

J. Smilauer (Czechoslovakia) and V. Afonin (Russia), Co-PI's

This instrument is for cold plasma electron temperature up to 10 eV. (Mass: 2.7 kg; Time resolution: 0.1 seconds; Data rate: 0.3 kbit/s).

11) Ion Trap (ALPHA-3)

V. Bezrukikh (Russia), PI

This experiment can make thermal plasma ion ($E < 25$ eV/q) flux measurements. (Mass: 3.5 kg; Time resolution: 1 seconds; Data rate: 0.16 kbit/s).

12) Ion Emitter (RON)

W. Riedler (Austria), R. Schmidt (Netherlands), and Yu. I. Galperin (Russia), Co-PI's

This is an ion (N²⁺, and In⁺) emitter for spacecraft neutralization with current range from 1 to 10 mA. (Mass: 7.5 kg; Data rate: 0.2 kbit/s).

13) Electron and Proton Anisotropy (DOK-2A)

K. Kudela (Czechoslovakia) and V. Lutsenko (Russia), Co-PI's

This experiment will make the measurements of fluxes, spectra and anisotropy of electrons ($E = 10-400$ keV) and ions ($E = 15-1000$ keV). (Mass: 5.5 kg; Time resolution: 1 seconds; Data rate: 0.8 kbit/s).

14) Intensities of the Lines (UFSIPS)

K. Palazov (Bulgaria), and A. Kuzmin (Russia), Co-PI's

This instrument can measure the UV-emission in the lines of 130.4, 135.6, and 149.3 nm. (Mass: 25 kg; Data rate: 0.2 kbit/s).

15) UV Auroral Imager (UVAI)

L.L. Cogger (Canada) and Yu. I. Galperin (Russia), Co-PI's

This UV auroral imager can measure UV emissions between 140 to 160 nm. (Mass: 20 kg; Data rate: 3 kbit/s).

16) Subsatellite for Measurements of Electric and Magnetic Field, VLF Waves, Plasma and Energetic Particles (C2-A) P. Triska and Ya. Voita (Czechoslovakia), Co-PI's

The instruments onboard subsatellite C2-A are for measurements of electric and magnetic field, VLF waves, plasma and energetic particles. (Mass: 50 kg; Data rate: 40 kbit/s).

For more information, contact
A. A. Galeev, Yu. I. Galperin, and L. M. Zelenyi
Space Research Institute, Russian Academy of Sciences,
117810, Moscow, Russia

The International Sun-Earth Explorer-3 (ISEE-3) Mission and Payloads (now renamed ICE)

The prime objective of the original International Sun-Earth Explorer-3 (ISEE-3) mission was to provide continuous data on the interplanetary environment and solar wind upstream from the Earth. On August 12, 1978, the spacecraft was launched into a 100-day transfer trajectory towards the Sun-Earth L1 libration point. It was subsequently inserted into a large-amplitude halo orbit around the L1 point on November 20, 1978, after three orbit maneuvers with a total ΔV of 57 m/s, and thus became the first libration-point satellite.

ISEE-3 was maintained in its 6-month-period halo orbit until June 1982, when it was retargeted to the Earth's magnetotail to begin a new phase called the "extended mission." The extended mission phase was a double lunar-swingby trajectory with outer loops designed to traverse the deep geomagnetic tail. ISEE-3 became the first spacecraft to explore the geomagnetic tail between 80 and 237 Earth radii. The extended mission phase lasted until December 22, 1983, when a lunar flyby at an altitude of only 120 km hurled ISEE-3 into a heliocentric trajectory designed to intercept comet Giacobini-Zinner as the comet made its descending-node passage of the ecliptic plane on September 11, 1985. While in its L1 halo orbit ISEE-3 made important contributions to solar wind physics, the study of solar-terrestrial relationships, cosmic-ray physics, and astrophysics. In addition, ISEE-3 served as an early warning station for interplanetary disturbances, which reach the Earth's magnetosphere about an hour after detection at the L1 point.

During the deep geomagnetic tail phase of its mission ISEE-3 yielded a number of new scientific discoveries, one of the most remarkable being the observation of large plasmoids moving very rapidly down the tail in association with magnetospheric substorms. The lengthy coverage near apogee was particularly important because a dramatic increase in plasma disturbance was found beyond 180 Earth radii.

Although ISEE-3 was renamed International Cometary Explorer (ICE), the science payload is not ideal for cometary investigations. It does not have any imaging devices or dust detectors but is heavily oriented towards cosmic-ray studies. However, at least six ICE experiments provided useful data on the interaction of the solar wind with a comet during the Giacobini-Zinner encounter phase of the mission.

To date, the ICE spacecraft remains operational. Its main mission in 1994 is to provide in-ecliptic measurements at the same heliographic longitude as Ulysses during a critical period of the Ulysses polar pass. Eventually, in August 2014, ICE's trajectory will bring it back to the Earth-Moon system. When this occurs, the spacecraft will be retargeted for an energy-robbing leading-edge swingby of the Moon that will place it into a high-energy geocentric orbit.

Key ICE Mission Statistics

Mission Class:	Large Explorer
Launch Date:	12 August 1978
Launch Vehicle:	Delta 2914
Launch Site:	CCAFS
Mission Duration:	Ongoing
Orbit:	Heliocentric, circular, radius 1 AU
Inclination:	0.06°
Period:	355 days
S/C Mass:	479 kg
Stabilization:	Spin stabilized at 20 rpm
Pointing Accuracy:	1°
Pointing Knowledge:	0.1°
Power:	140 watts
Science Telemetry:	256 bps

ICE Instruments

1) Solar Wind Plasma J. Gosling, PI

Two 135-degree spherical section electrostatic analyzers furnish electron and ion measurements of solar wind on ISEE-3. Each of these instruments utilizes a divided secondary emitter system to intercept the analyzed particles. Secondary electrons selected from all of the emitters simultaneously provide fast two-dimensional measurements of the particle fluxes integrated over polar angle. At a slower rate, secondary electrons are successively selected from individual emitters to provide three-dimensional measurements. The speed of the ion measurements is increased by a factor of two by using an active proton peak tracking system to reduce the total range of energy per charge which has to be covered. At these words are being printed, the ion element has failed.

2) Gamma Ray Bursts B. Teegarden, PI

This instrument consists of one germanium crystal and two CsI crystals to measure the intensity time histories and energy spectras of gamma ray burst. The instrument is sensitive to gamma rays in the energy range of 50 keV to 6.5 MeV, and has an energy resolution of 120 keV at 6.5 MeV and 3.5 keV at energies less than 1 MeV.

3) Low Energy Cosmic Ray D. Hovestadt, PI

This instrument is designed to measure the elemental abundances, charge state composition, energy spectra, and angular distributions of energetic ions in the energy range 2 keV/charge to 80 MeV/nucleon and of electrons between 75 and 1300 keV. The instrument consists of three different sensor systems: ULECA (Ultra Low Energy Charge Analyzer) is an electrostatic deflection analyzer system with rectangular solid-state detectors as energy-determining devices. ULECA's energy range is ~3 to 560 keV/charge. The ULEWAT (Ultra Low Energy Wide Angle

Telescope) is a double dE/dX versus E thin-window flow-through proportional counter/solid-state detector telescope covering the energy range from 0.2 to 8– MeV/nucleon (Fe). The ULEZEQ (Ultra Low Energy Z, E, and Q) sensor consists of a combination of an electrostatic deflection analyzer and a thin-window dE/dX versus E system with a thin-window proportional counter and a position-sensitive solid-state detector. The energy range is 0.4 MeV/nucleon to 6 MeV/nucleon. While the ULECA and ULEWAT sensors are designed mainly for interplanetary and outer magnetospheric studies, the ULEZEQ sensor also obtains composition data in the trapped radiation zone. Sixty-five rates and pulse-height data can be obtained with sectoring in up to 16 sectors.

4) Energetic Protons
R. Hynds, PI

This experiment is designed to investigate the problems of low energy proton behavior in the energy range 35 to 1600 keV. The Energetic Protons experiment provides three-dimensional proton flux distribution measurements with good energy resolution at a time resolution of 16 seconds; thus, it provides 180 independent points on the proton phase space distribution function every 16 seconds. The three-dimensional distribution of fluxes is measured by means of three identical particle telescopes inclined at 30°, 60°, and 135° with respect to the spacecraft spin axis. Each telescope unit incorporates 1) a light rejection collimator, 2) an electron rejection magnet with antiscatter baffles, 3) a detector stack, 4) an inflight calibration source, 5) an amplifier chain for each detector, and 6) detector current monitoring circuits.

5) Cosmic Ray Electrons and Nuclei
P. Meyer, PI

This experiment measures the energy spectrum of cosmic electrons in the range 5–400 MeV. In addition, the energy spectra and relative abundances of nuclei from protons to the iron group, with energies ranging from 30 MeV/n to 15 GeV/n, are analyzed. Primary scientific objectives involve the study of the long- and short-term variability of these components as a probe of the structure of the heliosphere. Particles are identified by multiparameter analysis using the pulse height analyzed signals from eight active detectors, including three lithium drifted silicon solid-state detectors, one CsI scintillator viewed simultaneously by photodiodes and a photomultiplier, two plastic scintillators, one gas Cerenkov counter, and one quartz/sapphire Cerenkov counter. Overall instrument weight is 8.9 kg, and operating power is 3.2 W.

6) Plasma Composition
K. Ogilvie, PI

The Ion Composition experiment uses an ion mass spectrometer to measure the ionic composition of the solar wind from the ISEE-3 spacecraft. The resolution and dynamic range of the instrument are sufficient to be able to resolve up to twelve individual ions or groups of ions. The spectrometer is composed of a stigmatic Wien filter and hemispherical electrostatic energy analyzer. The spectrometer is controlled by a microprocessor based on a special purpose computer which has three modes of operations: full and partial survey modes and a search mode. In the search mode, the instrument locks on to the solar wind. This allows four times the time resolution of the full survey mode and yields a full mass spectrum every 12.6 minutes.

7) Plasma Waves

G. Greenstadt, PI

The Plasma Wave Investigation is designed to provide comprehensive information on interplanetary wave-particle interactions. Three spectrum analyzers with a total of 19 bypass channels cover the frequency range from 0.3 Hz to 100 kHz. The main analyzer, which uses 16 continuously active amplifiers, gives two complete spectral scans per second in each of 16 filter channels. The instrument sensors include a high-sensitivity magnetic search coil, and electric antennas with effective lengths of 0.6 and 45 m. Overall instrument weight is 3.55 kg, and operating power is 3.8 W.

8) Radio Mapping

J. Steinberg, PI

The Radio Mapping Experiment is designed to provide maps of the large scale structure of the interplanetary magnetic field from ten solar radii in altitude to the Earth orbit, in and out of the ecliptic. This instrument tracks type III solar radio bursts at 24 frequencies in the range 30 kHz–2 MHz thus providing the positions of 24 points along the line of force which guides the electrons producing the radio radiation. The antennas are two dipoles: one (90 m long) in the spin plane, the other (15 m long) along the spin axis. The receiver was designed for high sensitivity (0.3 μ V in 3 kHz BW), high intermodulation rejection (80 dB/1 μ V input for order 2 products), large dynamic range (70 dB), high selectivity (-30 dB response 6.5 kHz away from the center frequency of 10.7 MHz for the 3 kHz BW channels), and high reliability.

9) Helium Vector Magnetometer

E. Smith, PI

The Vector Helium Magnetometer is a slightly modified instrument that originally served as the spare unit for the Pioneer 10 and 11 missions to Jupiter. This magnetometer is designed to perform continuous observations of the interplanetary magnetic field near 1 AU. The magnetometer sensor is mounted at the end of a 3-meter spacecraft boom to remove it from on-board sources of interference. The absorption of circularly polarized light from the He lamp by the He cell is modulated by the vector sum of the ambient field H and a rotating field generated by three Helmholtz coils. The resulting variations are monitored by an infrared detector. The sensor measures the three steady-state components of the ambient magnetic field and their variations with frequencies up to 3 Hz. Overall instrument weight is 3.4 kg, and operating power is 4.42 W.

10) Medium Energy Cosmic Ray

T. von Roseninge, PI

The experiment is designed to measure the charge composition of nuclear energetic particles over wide ranges in energy (\sim 1–500 MeV/nucleon) and in charge ($Z=1-28$). Individual isotopes are resolvable for $Z=1-7$ over a restricted energy range. Electrons of \sim 2–10 MeV are also measured. These measurements are accomplished using two all solid state detector telescopes, both the surface barrier and the lithium-drifted types, with detectors ranging in thickness from 153000 μ m. The Very Low-Energy Telescope System is designed to measure the charge composition of low-energy nuclei from hydrogen to iron. The High-Energy Telescope System is designed to measure the energy spectra of electrons and all elements from hydrogen to iron over a broad range of energies. Heliospheric gradients and other characteristics of solar modulation

are measured in conjunction with identical telescopes flown on the Voyager 1 and 2 spacecraft and similar telescopes on Pioneer 10 and 11.

ICE Instruments Summary

<i>Experiment</i>	<i>Range</i>	<i>Type</i>
Gamma Ray Bursts	50 keV-6.5 MeV	germanium and CsI crystals
Solar Wind Plasma	150 eV-7 keV 5 eV-2.5 keV	Spherical electrostatic analyzers
Low Energy Cosmic Ray	0.2-80 MeV/n 0.4-6 MeV/n 3-560 keV/charge	ULEWAT ULEZEQ ULECA
Energetic Protons	35 keV to 1.6 MeV	Particle telescopes
Cosmic Ray Electrons and Nuclei	5-400 MeV 30 MeV/n-15 GeV/n	Eight active detectors
Plasma Composition	470 eV/z-10.5 eV/z	Ion mass spectrometer
Plasma Waves	17 Hz-100 kHz 17 Hz-1 kHz 0.316 Hz-8.8 Hz	16-ch spectrum analz. 8-ch spectrum analyzer 3-ch spectrum analyzer
Radio Mapping	30 kHz-2 MHz	3-D tracing
Helium Vector Magnetometer	0-3 Hz	Magnetometer sensor
Medium Energy Cosmic Ray	1-500 MeV/n 2-10 MeV	Solid-state detectors

Project Scientist: Keith Ogilvie GSFC, (301) 286-5904
 Program Scientist: Vernon Jones, NASA/HQ, (202) 358-0885

The Interplanetary Monitoring Platform-8 (IMP-8) Mission and Payload

IMP-8 was launched in October 1973 into a 12-day geocentric orbit with apogee and perigee near $40 R_e$ and $30 R_e$ respectively. The spacecraft has exceeded its planned mission life, and is now operating in an open-ended extended mission in its original orbit. The orbit has been stable over the past 20 years, but the inclination varies from -55° to $+55^\circ$ with a period of many years. Now, in support of the Global Geospace Science (GGS) program and of such deep space missions as Voyager and Ulysses, the primary mission objective of IMP-8 is to perform detailed and near-continuous observations of the near-Earth interplanetary environment.

Key IMP-8 Mission Statistics

Mission Class:	Large Explorer
Launch Date:	25 October 1973
Launch Vehicle:	Delta 1604
Launch Site:	CCAFS
Mission Duration:	On-going
Initial Orbit Apogee:	288,672 km
Initial Perigee:	141,050 km
Initial Inclination:	28.64°
Initial Period:	11 days, 23 hrs, 40.5 mins
S/C Mass:	401 kg
Stabilization:	Spin stabilized at 22.3 rpm
Pointing Accuracy:	1°
Power:	150 watts
Science Telemetry:	1.6 kb/s
Data Storage:	15 kb

IMP-8 Instruments

1) Magnetic Fields R. Lepping, PI

This experiment measures vector magnetic fields in the dynamic range ± 36 gammas. Three mutually orthogonal fluxgate sensors are located at the ends of a 3 m instrument boom to study the interplanetary magnetic field, the Earth's magnetic field, and the interaction of the solar wind with the geomagnetic field.

2) Cosmic Rays R. McGuire, PI

This experiment measures electrons from 2 to 12 MeV, and isotopes of hydrogen and helium in the range of 4 to 80 MeV. Data from this experiment are used to study solar modulation, quiet-time and flare-associated anisotropies, solar and magnetospheric particle acceleration processes, and solar composition. The experiment consists of four separate telescopes made up of various combinations of de/dx and E detectors including scintillators, surface barrier, and lithium-drifted silicon detectors.

3) Cosmic Rays and Solar Flare Isotopes
J. A. Simpson, PI

This experiment was designed to study solar flare particle acceleration and particle containment in the vicinity of the solar wind. It also measures energy spectra, nuclear composition, and electrons over a wide range of energies and fluxes using a solid-state telescope. Nucleons are measured in the range 0.5 to 1200 MeV, with a flux dynamic range of at least 10⁵. Electrons are measured in the range of 0.3 to 10 MeV.

4) Energetic Particles
D. J. Williams, PI

This experiment studies the propagation characteristics of solar cosmic rays through the interplanetary medium, electron and proton patches throughout the geomagnetic tail and the flanks of the magnetopause, and the entry of solar cosmic rays into the geomagnetic field. The instrumentation consists of a three-element telescope employing solid-state detectors and a magnetic field to deflect electrons. Two side-mounted detectors are used to detect the electrons deflected by the magnet. 50 keV–4.5 MeV protons and 30 keV–200 keV electrons are measured.

5) Charged Particles
S. M. Krimigis, PI

The objective of this experiment is to measure concentrations of protons, alpha particles, heavier nuclei, and X-rays over a wide energy range. The data is used to study angular distributions, energy spectra, and the propagation of particles emitted by the Sun as well as those streaming along the magnetospheric tail away from the Earth. The experiment consists of three solid-state detectors placed inside a scintillator cup, and thin-window Geiger-Müller tubes inside an anti-coincidence scintillator.

6) Electrons and Isotopes
E. C. Stone, PI

This experiment studies the local acceleration of particles, solar particle acceleration processes, particle storage in the interplanetary medium, and the interstellar propagation and solar modulation of particles. This is accomplished by measuring the differential energy spectra of electrons and hydrogen and helium isotopes. The instrument consists of a multi-element, totally depleted solid-state telescope with anti-coincidence shielding. 1–40 MeV/n nuclei and .16–5 MeV electrons are measured.

7) Ions and Electrons
F. Ipevich, PI

This experiment determines the composition and energy spectra of low-energy particles observed during solar flares and 27-day solar events. An electrostatic analyzer separates the particles depending on their energy/charge ratio, then a combination of solid state detectors measures their energy.

8) Low Energy Particles

L. A. Frank, PI

This experiment studies the differential energy spectra of low-energy electrons and protons measured over the geocentric radial distance of 40 Earth radii. The aim is to improve our understanding of geomagnetic storms, aurora, tail and neutral shield, and other magnetospheric phenomena. The instrument consists of a dual-channel, curved-plate electrostatic analyzer employing continuous channel multiplier systems in conjunction with an Anton-type 213 Geiger-Müller tube. Electrons and protons are measured over the energy range of 5 eV to 50 eV.

9) Solar Plasma Electrostatic Analyzer

J. Gosling, PI

The objective of this experiment is to make a comprehensive study of electrons and positive ions in the IMP-8 orbital path, and to coordinate this data with the magnetometer and other data. The instrument is capable of detecting ions at least as heavy as oxygen, and separately identifying them in the energy-per-charge spectrum when the solar wind ion temperatures are low. The basic instrument is a plasma analyzer consisting of a set of hemispherical analyzer plates and an electron multiplier, together with associated detector electronics. The analyzer measures electrons in the energy range 4 eV to 20 keV, and protons in the energy range 70 eV to 20 keV.

10) Solar Plasma Faraday Cup

Alan Lazarus, PI

This experiment measures plasma properties in the interplanetary region and the Earth's magnetosheath. Parameters measured include energy distributions and the angular distributions of electrons in the equatorial plane of the spacecraft. The basic instrumentation consists of a split collector Faraday cup (split about the plane of the spacecraft) with a modulation potential applied to one of the grids.

IMP-8 Instruments Summary

<i>Investigation</i>	<i>Range</i>	<i>Type</i>
Magnetic Fields	± 36 g	Fluxgate
Cosmic Ray	2–80 MeV	Scintillators
Cosmic Ray and Solar Flare Isotopes	0.3–1200 MeV	Solid state
Energetic Particles	30 keV–4.5 MeV	Solid state telescope
Charged Particles	0.3–500 MeV	Solid state/GM
Electron and Isotopes	0.2–40 MeV	Solid state telescope
Ions and Electrons	100 keV–2 MeV	Solid state
Low Energy Particles	5–50 eV	Electrostatic Analyzer
Solar Plasma Electrostatic Analyzer	4 eV–20 keV	Plasma analyzer
Solar Plasma Faraday Cup	200 eV–8 keV	Faraday cup

Project Scientist: Joe King: (301) 286-7355
 Program Scientist: Vernon Jones, NASA/HQ, (202) 358-0885

Mars-94 Mission and Plasma and Field Payload

After nearly 20 years, Russia will launch in October 1994 two identical spacecraft, Mars-94 to study Martian atmosphere, surface, and interior, as well as the magnetic field of Mars and plasma processes in the Martian environment. Along the Earth-Mars trajectory some measurements of interplanetary space parameters, and astrophysical observations will also be made by Mars-94. Each spacecraft includes an orbiter, a balloon station in the atmosphere of Mars, two small stations on the surface of Mars, two penetrators in underlying surface layers, and an optional small Martian rover on the surface of Mars. Scientists from 20 countries are involved in the Mars-94 mission.

The main scientific objectives of Mars-94 are:

- to investigate the surface of Mars, including topography of the surface with high-resolution studies of the terrain, mineralogical mapping, investigation of the elemental composition and organics of the soil, and the studies of the cryolithozone and its deep structure.
- to monitor the climate of the planet and to investigate its atmosphere, such as the minor component abundances and variation of the atmosphere, the distributions and variations of atmospheric temperature and pressure, typical features of the atmosphere near the volcanic mountains, characteristics of the atmospheric aerosol, and neutral and ion composition of the upper atmosphere.
- to study the inner structures of the planet, in particular the crust thickness, magnetic field, interior heat flow, and active volcanism.
- to determine the Martian magnetic field, the structure of the magnetosphere and its boundaries, and to measure the 3-D distribution functions of ion and energetic particles and plasma wave characteristics near Mars and on the Earth-Mars trajectory.
- to study the localization of cosmic g-bursts and solar and star occultations.

Mars-94 Mission Statistics

Launch Date:	October 22 1994	
Launch Vehicle:	Proton carrier-rocket	
Mission Duration:	nominal 2 years	Earth-to-Mars flight: 315 days
		Active lifetime: one year
Preliminary Mass:	Launch mass of the S/C	6580 kg
	Orbiter (without fuel)	1611 kg
	Autonomous engine (with no fuel)	470 kg
	Fuel (autonomous engine and thrusters)	3200 kg
	Descender (balloons and rovers)	600 kg
	Scientific payload	240 kg
	Small stations (2)	90 kg
	Penetrators (2)	40 kg
	Platforms for point optical instruments	70 kg

Stabilization: Three axis orientation
Telemetry rate: 65 kbps (Martian orbit)
Data volume: ~ 1 Gbt/day

Mars-94 Orbiter Plasma and Field Instruments

1) Energy-mass analyzer of ions and neutral-particle imager (ASPERA-S) R. Lundin, PI

The main scientific objectives of ASPERA-S are to study in-situ neutrals and remote processes associated with the interaction between the plasma and neutrals near the Mars. The ASPERA-S consists of an Ion-Mass Imaging Spectrometer (IMIS), a neutral Particle Imager (NPI), and a scanner platform ($\pm 90^\circ$) providing a full coverage of the unit sphere by spectrometer. The IMIS, with an energy range of 0.5–50000 eV, and mass range of 1–100 a.m.u., is an electrostatic "top hat" analyzer followed by cylindrical sector magnet momentum analyzer with the lateral magnetic field. Ions are detected by an "imaging" sensor using a microchannel plate assembly with position sensitive anodes, 32x32 (angle x mass) matrix. The NPI includes two sensors, NPI-1 is to determine the energy of incident neutral atoms with energies greater than 5 keV/nucleon and mass less than 100 a.m.u., and NPI-2 is for the detection of secondary ions and electrons (with energy range of > 10 eV and mass range of 1– 10^{12} a.m.u.) generated by impinging neutral particles. In front of NPI, there is an electrostatic filter designed to remove all charged particles with energies less than 300 keV/g. The ASPERA-S has energy resolution of 0.07 to < 1.0 and angular resolution of 5° . This experiment is cooperated by scientists from Sweden, Russia, Finland, Poland, Germany, USA, Norway.

2) Fast omnidirectional non-scanning energy-mass analyzer (FONEMA) A. Johnstone, PI

The FONEMA is designed for the investigations of the structure, dynamics and origin of the plasma population in the near-Mars space by measurements of three-dimensional distribution functions of hot ions and flux parameters with high time resolution of 0.1 s (maximum). The instrument consists of 48 Thomson parabola energy-mass analyzers for measurements within their own solid angle determined by the collimator system and by the double-curved mirror. Multisensor energy-mass analyzer will measure three dimensional distribution functions for several ions (with mass of 1–30 amu) in a wide energy range of 20 eV–7 keV. The FONEMA has a full 4π angular coverage with $30^\circ \times 45^\circ$ angular resolution. The energy resolution and mass resolution are 0.2 and 6 respectively. This experiment is cooperated by scientists from Czechoslovakia, England, Ireland, France, and Russia.

3) Omnidirectional ionospheric energy-mass spectrometer (DIMIO) J. J. Berthelier, PI

The DIMIO is for the investigation of the dynamics of the Martian ionosphere and of magnetospheric population of ionospheric origin. It will measure parameters of the ionosphere such as ion number densities and ion composition, ion temperature and convective velocity, and parameters of ions escaping from the ionosphere and their contribution to the ion composition of the magnetosphere. It will also study the dynamics of the ionosphere and magnetosphere and their relationship with the solar wind interaction with Mars. DIMIO is an omnidirectional ion mass-spectrometer with energy and angular distribution analysis capabilities. It will cover ions with mass range from 1 to 44 amu and temperature range of 200–10000°K. The number density range of the instrument is 10^{-1} – 10^5 cm⁻³ with 10% accuracy. The ion velocity determination

accuracy is 100 m/s and 10% for V_i greater and less than 1000 °K, respectively. This experiment is cooperated by scientists from Germany, France, USA, and Russia.

4) Ionospheric plasma spectrometers (MARIPROB)

V. Afonin, PI

The MARIPROB is an experiment aims at studies of the Martian ionosphere and convection of cold plasma in the Martian magnetosphere by using retarding potential method. It will measure some important parameters of the ionosphere such as electron and ion number density (in a range of $0.1-5 \times 10^5 \text{ cm}^{-3}$), electron and ion temperature up to 15000 °K, mass composition of major components (H^+ , O^+ , and O_2^+), and full vector of plasma drift (10 m/s to 35 km/s). The MARIPROB experiment consists of two identical ion energy spectrometers (two sets of 28 retarding potential analyzers each with microchannel plate) combined with the electron probe, and a spherical retarding potential analyzer operating also in a floating mode with periodic measurements of integral cold ion energy spectrum. This experiment is cooperated by scientists from Austria, Belgium, Bulgaria, Czechoslovakia, Hungary, Ireland and Russia.

5) Electron Analyzer and Magnetometer (MAREMF)

W. Reidler, PI

The main scientific objectives of the MAREMF experiment are to measure in situ with high accuracy and time resolution the three-dimensional velocity distribution of electrons and the magnetic field vector in the plasma environment of Mars and in the solar wind. It is designed to determine the characteristics of the Martian magnetic field and the magnetic field topology by monitoring the electron "Strahl", to study feature of the solar wind interaction with Mars, to explore characteristics of Martian bow shock, and to study physical processes in the magnetosheath and magnetotail. The instrument combines dual fluxgate magnetometers and a three-dimensional electron analyzer used also for aboard control of magnetic field measurements. The magnetometer has a dynamic range of $\pm 32 \text{ nT}$ to $\pm 128 \text{ nT}$ with a resolution of 4 nT, and its maximum sampling rate is 100 vectors/s. The measurement range (in E/q) of the electron analyzer is 0.5 eV to 2 keV. This experiment is cooperated by scientists from Austria, Belgium, England, Hungary,, Germany, France, Ireland, USA, and Russia.

6) Electromagnetic Plasma Wave Complex (ELISMA)

S. Klimov, PI

The ELISMA is designed to study the Martian planetosphere oblateness by the solar wind and the energy transfer through the shock and planetopause, to identify instabilities in the ionosphere and magnetosphere, to study waves of atmospheric origin generated by sandstorms and lightnings, to make global mapping of the plasma convection, to study temperature and density distributions of the thermal plasma down to an altitude of 300 km, and study the dynamic relationship between the upper atmosphere and the lower ionosphere. The ELISMA complex consists of electric field sensors (three double Langmuir probes consisting of four non coplanar identical spheres mounted on booms), magnetic field sensors (three orthogonal search coil sensors), one Langmuir probe, high frequency (HF) and mutual impedance (MI) probe, a frequency spectrum analyzer, and a microprocessor system. The frequency range for electric field is up to $2 \times 10^6 \text{ Hz}$, and magnetic field to $2 \times 10^3 \text{ Hz}$. The temperature and number density range for electrons are $10-10^5 \text{ cm}^{-3}$ and 10-1 to 10 eV, respectively. This experiment is cooperated by scientists from Bulgaria, ESA, France, Poland, UK, USA, and Russia.

7) Low Energy Charged Particle Spectrometer (SLED-2) S. MacKenna-Lawlor, PI

The SLED-2 experiment is for detailed studies of the energetic particle radiation in the Martian environment and monitoring of low energetic cosmic rays during the cruise phase. The SLED-2 instrument consists of one electron telescope protected by a foil and four ion telescopes with electron broom magnets. The energy range of SLED-2 is 10 keV–30 MeV in 12 channels, and the field-of-view (FOV) for each telescopes is 30°. This experiment is cooperated by scientists from Czechoslovakia, Germany, Ireland, Hungary, and Russia.

Mars-94 Plasma and Field Instruments Summary

	<i>Investigation</i>	<i>Range</i>
ASPERA-S	Study processes associated with the interaction between the plasma and neutrals near the Mars	E: 0.5 eV–300 keV M: 1–10 ¹² amu
FONEMA	Investigate the structure, dynamics and origin of the plasma in the near-Mars space	E: 20 eV–7 keV M: 1–30 amu
DIMIO	Study the dynamics of the Martian ionosphere and magnetospheric population of ionospheric origin	M: 1–44 amu T: 200–10000°K
MARIPROB	Study the Martian ionosphere and convection of cold plasma in the Martian magnetosphere	N: 0.1–5 x 10 ⁵ cm ⁻³ T: < 15000°K V: 0.01–35 km/s
MAREMF	Measure 3-D electrons velocity distributions and the magnetic field near Mars and in the solar wind	B: ±32–±128 nT E/q: 0.5 eV–2 keV
ELISMA	Study the plasma distribution and convection, plasma waves and instabilities, and the Martian planetosphere oblateness.	E frequency: 0–10 ⁶ Hz B frequency: 0–10 ³ Hz N _e : 10–10 ⁵ cm ⁻³ T _e : 0.1–10 eV
SLED-2	Study the energetic particle radiation in the Martian environment and monitor low energy cosmic rays during the cruise phase	Energy range: 10 keV–30 MeV in 12 channels

Project Scientist: A. A. Galeev, Space Research Institute
Russia Academy of Sciences, Moscow, Russia

LANL Geosynchronous Spacecraft Mission and Plasma Payload

The Los Alamos National Laboratory fields instruments that measure the plasma and energetic particle environments at several locations simultaneously around geosynchronous orbit. These instruments, mounted one each per satellite, are the Magnetospheric Plasma Analyzer (MPA) and the Synchronous Orbit Particle Analyzer (SOPA). Simultaneous sampling at multiple locations of a combination of low-energy plasma and energetic particles using instruments deployed on these spacecraft provides a unique opportunity for characterization of the inner magnetosphere for collaborative studies with other investigators.

Three sets of those instruments are presently in space at GEO, carried on three spinning spacecraft with International Designators of 1989-046, 1990-095, and 1991-080. Multiple satellites are used to make simultaneous measurements of points along the respective satellite paths. The current plan is to deploy more spacecraft from time to time and maintain a constellation of three to five.

Key LANL Geosynchronous Spacecraft Mission Statistics

Orbit:	Geosynchronous Earth
Period:	24 hours
Altitude:	40,000 km
Stabilization:	Spin, 6 rpm
Period Accuracy:	Better than 1°
Science Telemetry:	5 kb/s

LANL Geosynchronous Spacecraft Mission Instruments

- 1) Magnetospheric plasma Analyzer (MPA)
D. McComas, PI

The purpose of the MPA is to measure spacecraft plasma environment, including full 3-D velocity distributions of electrons and ions.

The low weight and power MPA (3.6 kg and 3.5 watts) is designed for spacecraft with limited resources. The instrument, composed of a single electrostatic analyzer coupled to an array of channel electron multipliers, measures three-dimensional (3D) E/q distributions of both ions and electrons in a range of ~ 1 eV/q to ~ 40 keV/q.

The electrostatic analyzer is composed of a set of curved plates with spherical section geometry such that the bending angle from center of the entrance aperture is a constant of 60° , independent of the polar angle of entry. Electrons and ions are analyzed with the same set of plates using two identical analyzer voltage supplies which provide sets of positive-polarity sweep voltages on opposite analyzer plates. After analysis, the particles are directed and post accelerated into an array of six CEMS for detection. Each CEM covers a separate 15° polar angle field-of-view (FOV), together covering $> 90\%$ of 4π sr. Upon striking the appropriate CEM, the analyzed particle is counted and its polar angle of entry is identified in the spacecraft coordinate system.

2) Synchronous orbit particle Analyzer (SOPA)

R. Bellan, PI

The SOPA instrument detects energetic particles (e.g. electrons, protons, and other ions) in various energy ranges depending on the species. Protons are detected from 50 keV to ~ 50 MeV and electrons from 50 keV to > 1.6 MeV. Alphas and heavy ions in certain energy ranges are also detected. SOPA can also be used to calculate parameters such as temperature and density of protons and electrons.

The SOPA consists of three solid state telescopes that accept particles from three different directions relative to the spacecraft spin axis. This arrangement provides nearly complete pitch angle distribution coverage. Each telescope consists of a thin front solid-state detector and a thick rear detector surrounded by high and low Z shielding to reduce the incidence of side-penetrating particles to an acceptable level. The solid state detector pair is fronted by a collimator-baffle system.

Energetic electrons pass through the thin front detector and deposit < 10 keV of energy therein. Particle detection thresholds on the thin/thick detectors are ~ 45 keV, therefore the thin detector does not register electrons. Electrons are monitored in the thick back detector. Ions are monitored in the front detector until reaching their penetration energy. Measurement of ion energies above penetration levels requires coincidence between the front and rear detectors.

A unique feature of the thin detector is that for ions of a given mass number and for energies above the penetration energy, a characteristic energy is deposited. That energy is a weak function of the particle energy. This characteristic allows use of the thin-thick pair as a $dE/dx-E$ detector and as such would, in principal, allow for the identification of ions of any mass. The SOPA makes use of this characteristic to uniquely monitor helium, carbon, nitrogen, oxygen, and heavy ions.

LANL Geosynchronous Spacecraft Instrument Summary

	<i>Investigation</i>	<i>Range</i>	<i>Type</i>
MPA	Measurement of spacecraft plasma environment, including full 3-D velocity distribution of electrons and ions	Energy range: electrons: 1 eV-40 keV; ions: 1 eV/q-40 keV/q	Curved plate ESA
SOPA	Measure of energetic particles and determine their parameters such as temperature and density	Energy range: electrons: 50 keV-1.6 MeV; Ions: 50 keV-1.5 MeV to 80 MeV	Solid state telescope

MPA/SOPA Project Coordinator: Phil Barker, LANL, (505) 667-0944

The Pioneer 10 Mission and Payload

The planetary phases of the Pioneer 10 and 11 missions to Jupiter and Saturn were completed in September 1979. Since then both spacecraft have been on an extended mission of outer heliospheric exploration. Pioneer 10 is at a heliocentric radius of 56 AU (March 93), and is traveling towards the tail region of the heliosphere (in a direction opposite to that of the Sun's motion through the galaxy) at about 2.7 AU per year. Pioneer 11 is 37 AU from the Sun (March 93), and traveling toward the bow-shock region of the heliosphere about 2.5 AU per year.

The projected amount of electrical power from the RTG's—supplemented by radioisotope heating units—will be adequate to maintain the temperatures of spacecraft subsystems and the instrument bay at a comfortable level and to supply the necessary electronic power for the spacecraft and instruments until the mid-1990's (1994 for Pioneer 11, 1997 for Pioneer 10). Instruments are on time-sharing operations in order to continue at reduced power levels. The supply of fuel for the attitude control system is more than adequate for this time period. The RTG power supply to Pioneer 11 is diminishing more quickly than that for Pioneer 10, and only Pioneer 10 is expected to be available for the Solar-Heliospheric IACG campaign.

The scientific objectives of the Pioneer Extended Missions are as follows:

- To search for the heliospheric boundary with interstellar space and study the large-scale electrodynamic structure of the solar plasma and magnetic field
- To measure the intensity and composition of the galactic cosmic radiation, and study the radial gradient of cosmic ray intensity and its dependence on solar activity
- To search for gravitational radiation

Key Pioneer 10 Statistics

Basic Data

Launch Date:	2 March 1972
Launch Vehicle:	Atlas/Centaur
Launch Site:	CCAFS
Mission Duration:	To RTG expiration

Asymptotic Trajectory Parameters for Pioneer 10 and the Direction and Speed of the Solar System Relative to the Local Interstellar Medium in Heliocentric Ecliptic Coordinates with an Equinox of 1950.

Asymptotic Trajectory	Pioneer 10	Solar System
Longitude	83°	252± 3°
Latitude	+3°	3° ± 3°
Speed (AU/yr)	2.39	26 ± 1 km/s

Mission Statistics

Mass: 258 kg
 Stabilization: Spin stabilized at 4.4 rpm
 Pointing Accuracy: ±1°
 Pointing Knowledge: ±0.3°
 Power: 4 RTGs, 155W (total power at launch)
 Science Telemetry: 16 b/s
 Data Storage: 49.152 kb

1) Helium Vector Magnetometer (HVM)
E.J. Smith, PI

The JPL/HVM measures the vector magnetic field in the heliosphere, with selectable operating ranges from ± 4.0 gamma to 1.41 gauss. The Pioneer 10 instrument has failed, but the Pioneer 11 instrument is operational.

2) Solar Wind Plasma Analyzer (PA)
A. Barnes, PI

The ARC/PA is an electrostatic energy per unit charge (e/q) spectrometer capable of measuring the flux as a function of E/q and incident direction of positive ions and electrons. This instrument is capable of determining incident plasma distribution parameters over the energy range of 100–18,000 eV for protons and approximately 1–500 eV for electrons. It covers the dynamic range for charged particle fluxes from 1×10^2 to $3 \times 10^8 \text{ cm}^{-2} \text{ s}^{-1}$ and is capable of resolving proton temperature down to at least the $2 \times 10^3 \text{ K}$ level.

3) Charged Particle Instrument (CPI)
J.A. Simpson, PI

The UC/CPI separately identifies individual nuclei, including protons and helium nuclei, through to the higher mass nuclei up to oxygen and measures the energy and differential flux of these particles over the range from 0.5 to 500 MeV/nucleon. Integral fluxes of nuclei with energies greater than 500 MeV/nucleon from protons through iron are also measured. Electron spectra are measured from 3 to 30 MeV.

4) Cosmic Ray Telescope (CRT)
F.B. McDonald, PI

The instrument comprises three solid state telescopes. The high-energy telescope is a three-element linear array operating in two modes, penetrating and stopping. For penetrating particles, differential energy spectra are obtained for He and H₂ from 50–800 MeV/nucleon. The stopping particle mode covers the range from 22–50 MeV. The low-energy telescope I responds to protons and heavier nuclei from 3 to 22 MeV/nucleon, providing both energy spectra and angular distribution over this range. Low-energy telescope II is designed primarily to study solar radiation. It will stop electrons in the 50–150 keV range and protons in the 50 keV–3 MeV range, and will respond to electrons in the interval 150 keV–1 MeV and protons from 3 to 20 MeV.

5) Geiger Tube Telescope (GTT)
J.A. Van Allen, PI

This instrument utilizes seven Geiger Mueller tubes as elementary detectors. Three tubes are arranged in an array parallel to the X-Y plane of the spacecraft to form a telescope for penetrating particles ($E_p > 70$ MeV) moving in the +Z or -Z (spacecraft rotational) axis direction. The useful dynamic range extends from 0.2 to 1×10^6 counts per second for individual tubes. Three other detectors are arranged in a triangular array and fully enclosed in a 7.2 g/cm² shield of lead to form a shower detector. A final detector is configured as a scatter detector, admitting large-energy electrons $E_e > 0.06$ MeV but discriminating against protons ($E_p > 20$ MeV).

6) Trapped Radiation Detector (TRF)
R.W. Fillus, PI

This is a Cerenkov detector which measures the gradient and transport properties of very high-energy cosmic rays. It counts galactic cosmic rays in the range above 500 MeV/nucleon, and measures anisotropies perpendicular to the spacecraft spin axis. Thus the radial gradient of the galactic cosmic rays and their modulations caused by the solar radiation are observed.

7) Ultraviolet Photometer (UV)
D.L. Judge, PI

The USC/UV is a two channel UV photometer operating in the 200–1400 Å range, with a field of views (FWHM) of 1.15° x 9.3°. An aluminum filter in conjunction with a channeltron sensor provides hydrogen Lyman-alpha data at 1216 Å, and a lithium fluoride target cathode with a second channeltron sensor provides helium data at 584 Å.

Pioneer Instruments Summary

	<i>Experiment</i>	<i>Range</i>	<i>Type</i>
HVM	Magnetometer	0.01 pT–140 μ T	Helium Vector
PA	Solar Wind Plasma Analyzer	100 eV–18 keV	26 CCM's
CPI	Charged Particle Instrument	0.4 Mev–500 MeV	Solid State
CRT	Cosmic Ray Telescope	0.05 MeV–800 MeV	3 Telescopes
GTT	Geiger Tube Telescope	40 keV–5 MeV	7 GM Tubes
TRD	Trapped Radiation Detector	0.5 MeV–12 MeV	Cerenkov
UV	Ultraviolet Photometer	200–1400 \AA	2 Channeltrons

Project Scientist: Palmer Dyal, ARC, (415) 604-1165
Program Scientist: Vernon Jones, NASA/HQ, (202) 358-0885

The Polar Mission and Payload

The Polar mission is a key to the Global Geospace Science (GGS) inventory of plasma and energy sources and sinks in the solar-terrestrial system. It will initially provide measurements of plasma entry and transport in both the north dayside cusp regions at high altitudes and over the southern polar cap at low altitudes as well as global imaging of the northern auroral zone. The Polar spacecraft, sharing a design and hardware heritage from the Dynamics Explorers, will use hydrazine propellant, with four thrusters (2.2 N) for spin up and spin down and four thrusters (4.4 N) for spin axis precession. The early-stage orbit will incline 90 degrees from the Equator with a apogee of 9 Earth radii and a perigee of 1.8 Earth radii. The orbit will precess with time so that measurements can be taken at low altitudes in the northern polar cusp and at high altitudes in the southern polar cap with global imaging of the southern auroral zone from high altitudes. Polar is scheduled for launch in 1994.

To fulfill Polar's science objectives, the payload will contain instruments dedicated to ionospheric and polar magnetospheric physics. In particular, the Polar satellite will measure complete plasmas, energetic particles, and fields in the high-latitude polar regions. The objectives of the Polar mission include the:

- Investigation of energy input to the ionospheric region through the dayside cusp,
- The determination of the mechanisms of ionospheric plasma outflow,
- The study of the characteristics of the auroral plasma acceleration regions,
- The provision of global, multi-spectral auroral images of the footprint of magnetospheric energy disposition into the ionosphere and upper atmosphere,
- Assisting in the determination of the role of the ionosphere in substorm phenomena and the overall magnetospheric energy balance, and
- The documentation of ions leaving the atmosphere and subsequently appearing in the solar wind, or electrons of solar wind origin precipitating to auroral altitudes.

Key Polar Mission Statistics

Mission Class:	Medium
Launch Date:	Summer 1994
Launch Vehicle:	Delta II 7925
Launch Site:	Vandenburg
Mission Duration:	Three years nominal
Operational Orbit:	Eccentric polar orbit with a perigee radius of 1.8 R_e and an apogee of 9 R_e
Orbital Period:	Maximum of 18 hours; minimum of 9.78 hours
Eclipse Duration:	Maximum of 90 minutes
S/C Type:	Cylindrical, 2.4 m diameter, 2.1 m height
S/C Mass:	1230 kg
Propulsion ΔV :	45 m/s, 269 kg Hydrazine

Stabilization:	Spin stabilized open loop control
Pointing Accuracy:	Antenna pointing to within 1°
Pointing Knowledge:	0.05° to 0.25° (despun platform ±0.02° to ±0.06°)
Power:	394 W (maximum load)
Science Telemetry:	55.5 kbps (tracking mode, real-time), 512 kbps (playback)
Data Storage:	Two tape recorders for 1.2 x 10 ⁹ bit/unit
Manufacturer:	Martin Marietta

Polar Instruments

1) Charge and Mass Magnetospheric Ion Composition Experiment (CAMMICE)

T. Fritz, PI

The CAMMICE will determine the composition of major energetic particle populations in the near-Earth plasma sheet and in the ring current over the range of 6 keV/Q to 60 MeV per ion. For full angular distribution, CAMMICE will measure at a rate of 10 samples per minute, or once per spin of Polar. Measurements of the following ion flux ratios: ²H/¹H, ³He/⁴He, ¹²C/¹⁶O, ¹⁴N/¹⁶O, ⁴He/²⁰Ne, ²⁰Ne/³⁶Ar, and ²⁴Mg/¹⁶O, and the following charge state density ratios: He⁺⁺/H⁺, He⁺/H⁺, O⁺/H⁺, and O⁺⁺/O⁺ at different locations and over a wide energy range, will serve as the principal tracers of plasma origin.

The CAMMICE consists of two types of sensor systems: the Magnetospheric Ion Composition Sensor (MICS) and the Heavy Ion Telescope (HIT). The MICS sensor uses a conically-shaped electrostatic analyzer, a secondary electron generation/detection system, and a solid state detector to measure the energy, time of flight, and the energy per charge of the incident ion flux. These three parameters permit a unique determination of the ion charge state, mass, and incident energy over the energy range from ~ 6 keV/Q to 400 keV/Q. The HIT sensor uses a three-element, solid-state detector telescope to measure the rate of energy loss and the ion incident energy. These parameters permit determination of the ion mass, elemental identification, and determination of incident energy over the energy range from 100 keV per ion to 60 MeV per ion. The CAMMICE has a mass of approximately 13 kg and uses a data rate of 1.28 Kbps.

2) Comprehensive Energetic Particle Pitch Angle Distribution (CEPPAD)

B. Blake, PI

The CEPPAD consists of three packages. The first package consists of the Imaging Proton Sensor (IPS) and the Digital Processing Unit (DPU). The second consists of the Imaging Electron Sensor (IES) and the High Sensitivity Telescope (HIST). The single despun platform package is the Source/Loss-Cone Energetic Particle Spectrometer (SEPS). The IPS measures protons over the energy range from ≈ 10 keV to 1 MeV using a spectrometer which incorporates a Microstrip Solid State Detector (MSSD). The IES measures electrons over the energy range from ≈ 25 to 400 keV using a spectrometer which incorporates a MSSD. The complete IES system has a nominal geometric factor of 6 x 10⁻³ cm². The nominal angular resolution of a detector element is 12° x 12° and its elemental geometric factor is approximately 3.8 x 10⁻⁴ cm. Three of these detector segments provide the desired electron measurements over a FOV of ± 12° x 180°. The satellite spin is used to obtain measurements over the full 4π steradians. The CEPPAD has a mass of approximately 14.4 kg and uses a data rate of 4.38 Kbps.

3) Electric Fields Investigation (EFI)

F. Mozer, PI

The EFI, a dual probe instrument, will sample the three components of the electric field vector and the thermal electron density over a frequency range of DC to above 20 kHz. The dynamic range of the electric field measurement is 0.02 to 1000 mV/m, while the plasma density will be measured at least over the range of 0.1 to 100 particles per cm³. It will also measure the floating potential of the spacecraft over the range of about +1 to +90 volts. The EFI will sense electric field strengths at a rate of 40 samples per second in the normal mode and more than 1000 per second in the burst mode.

The EFI consists of sensors and electric field preamplifiers. The EFI sensors are arranged as three orthogonal sphere pairs. Two of these sphere pairs are in the satellite spin plane on the ends of wire booms that provide tip to tip sphere separations of 100 and 130 meters respectively, while the third pair is aligned along the spacecraft spin axis with a 14 meter tip to tip separation provided by rigid stacer booms. The electric field preamplifiers have frequency responses to above 1 MHz to accommodate their use by the Plasma Wave Instrument. The EFI has a mass of approximately 32 kg, consumes 12.4 W, and uses a data rate of 2.5 kbps.

4) Fast Plasma Analyzer (HYDRA)

J. Scudder, PI

The Hydra instrument will make model-independent determinations of the probability distribution function for arrival of electrons throughout 4π steradians between 1 eV and 30 keV with $\sim 1^\circ$ resolution within $\pm 30^\circ$ of magnetic field vector. The main portion of the HYDRA instrumentation is a deployment of cylindrical electrostatic analyzers (ESA's) providing a dense coverage of the 3-D velocity space. The HYDRA investigation includes a sensor for flight called a "loss cone sensor," a version of a parallel plate electrostatic analyzer (PPA). The PPA sensor has a laboratory proven optical section and a previously flight proven 2-D position sensitive microchannel plate (MCP) detector that allows a $1.5^\circ \times 1.5^\circ$ pixel resolution, an electronically despun image of both the loss and the anti-loss cone directions can be simultaneously sampled. The HYDRA has a mass of approximately 17.5 kg, consumes 14 W, and uses a data rate of 4.9 kbps.

5) Magnetic Fields Experiment (MFE)

C. Russell, PI

The Magnetic Field Experiment will investigate the coupling of the solar wind and the magnetosphere through currents driven in the polar cusp, in particular, the experiment will study the behavior of field-aligned current systems and the role they play in the acceleration of particles and the dynamics of the fields in the polar cusp, magnetosphere, and magnetosheath. The MFE consists of two triads of orthogonal fluxgate magnetometer sensors mounted on a 6 meter boom with associated analog and data processing circuits mounted inside the spacecraft. The instrument will sample the magnetic field in the frequency range from 0 to 50 Hz. The dynamic range of the magnetic field measurement will be from 10^{-6} to 0.6 gauss. The raw measurements will be processed onboard at more than 100 vector samples per second for broadcast to other instruments, thus allowing an economical compression of plasma data. Typically, 10 samples per second are transmitted; however, a burst mode allows 100 vector samples per second to be telemetered to the ground. The MFE has a mass of approximately 5 kg, consumes 5.2 W, and uses a data rate of 500 bps.

6) Polar Ionospheric X-Ray Imaging Experiment (PIXIE)
W. Imhof, PI

The PIXIE will provide global measurements of the spatial distribution and temporal variation of bremsstrahlung x-ray emissions from Earth's atmosphere. The PIXIE instrument is a multiple pinhole x-ray camera using a multiwire position-sensing gas proportional counter for the focal plane detector. Images of atmospheric bremsstrahlung emission will be obtained over an energy range from 3 to 60 keV with a $\pm 21^\circ$ field of view, good spatial and energy resolution (up to a full 64-channel energy resolution), and with sufficient time resolution (a few minutes) to generate movies of the dynamical variations of auroral luminosities and associated atmospheric effects. For imaging the aurora at a distance of 8 Earth radii, about 10 counts/pixel/minute will be registered when viewing a typical diffuse aurora. The PIXIE has a mass of approximately 24.5 kg and uses a data rate of 3.5 kbps.

7) Plasma Wave Instrument (PWI)
D. Gurnett, PI

The PWI will measure the power spectral and wave vector characteristics electromagnetic and electrostatic plasma waves generate by both space plasma processes and ground-based experiments over the frequency range from 0.1 Hz to 800 kHz for wave electric and magnetic fields. The PWI employs seven distinct sensors for detecting the electric and magnetic fields of plasma waves, and consists of five main receiver systems: a high-time-resolution multichannel analyzer (MCA); a narrow-band sweep frequency receiver (SFR); a waveform receiver (WFR); a low frequency AC receiver (LFAC); and a wideband receiver (WBR). The PWI has a mass of approximately 18.4 kg and uses a data rate of 2.52 Kbps.

8) Thermal Ion Dynamics Experiment (TIDE)
T. Moore, PI

The TIDE will provide three dimensional low-energy (focus on ≤ 100 eV per charge) measurements with range and resolution adequate for the full characterization of features known to exist in the low-energy plasma population. TIDE's seven angular sectors/ channels will monitor all mass species simultaneously which eliminates the need for any sweeps except energy and delivers a 7-kbps image of the distribution function for each of five ion species once each 6 second spin. TIDE will compress these images appropriately so as to obtain single spin resolution when the available telemetry rate of 4 kbps permits. The TIDE has a mass of approximately 33.3 kg, consumes 10 W, and uses a data rate of 4 kbps.

9) Toroidal Ion Mass Spectrograph (TIMAS)
E. Shelley, PI

The TIMAS instrument will measure the full 3-D velocity distribution functions of all major magnetospheric ion species within half of a satellite spin period (10 times per minute). The TIMAS is a "spectrographic" imaging instrument that simultaneously measures all mass/charge (M/Q) components from 1 AMU/e to greater than 32 AMU/e over a nearly $360^\circ \times 10^\circ$ field-of-view in 20 milliseconds. With the rotation of the spacecraft, the TIMAS sweeps out a 4π solid angle image in a half spin period. The 3-D ion distributions are measured with approximately 11° angular resolution over the energy per charge range of 15 eV/e to 32 keV/e. The TIMAS has a mass of approximately 16.5 kg, consumes 14 W, and uses a data rate of 3.6 kbps.

10) Ultraviolet Imager (UVI)
G. Parker, PI

The UVI instrument will provide 2-D images of the dayside and nightside auroras. The UVI is an intensified charge-coupled device used in conjunction with a fast reflective optical system which has a nominal frame rate of 37 seconds and a noise equivalent signal within one frame of ~ 10 R. The instrument has an 8° field of view and is located on a despun platform which permits simultaneous imaging of the entire aurora oval for at least 9 hours of every 18 hour orbit. The dynamic range is > 1000 and can be positioned within an overall gain range of 10^4 , thus allowing measurement of both the very weak polar cap emissions and the very bright aurora. The UVI has a mass of approximately 21 kg, consumes 20 W, and uses a data rate of 12 kbps.

11) Visible Imaging System (VIS)
L. Frank, PI

The VIS will provide images of the nighttime auroral oval as viewed from Polar's eccentric polar orbit. The VIS is a set of three low-light-level cameras. Two of these cameras are low- and moderate-resolution auroral cameras that share primary and some secondary optics and produce auroral images with 12 narrow passband (~ 1 nm) filters at visible wavelengths at a frame rate of 12 seconds. The emissions of interest include those from N_2^+ at 391.4 nm, OI at 557.7 nm and 630.0 nm, HI at 656.3 nm, and OII at 732.0 nm. A third camera (i.e. the Earth camera) is used to monitor the directions of the fields of view of the auroral cameras with respect to the sunlit Earth and therefore to allow onboard verification that the visible cameras are sighted in the proper direction and protected from extremely bright sources, such as the Sun and sunlit Earth. The VIS has a mass of approximately 28.6 kg, consumes 30 W, and uses a data rate of 11 kbps.

Polar Instrument Summary

		<i>Range</i>	<i>Type</i>
CAMMICE	Charge and Mass Magnetospheric Ion Composition Experiment	6–400 keV/Q 0.1–60 MeV/ion	Solid state detector Solid state/telescope
CEPPAD	Comprehensive Energetic Particle Pitch Angle Distribution	10 keV–1 MeV 25–400 keV	Solid state detector Solid state detector
EFI	Electric Fields Investigation	0–1.25 mHz 0–3.5 kHz	Preamplifier/voltage Preamplifier current
HYDRA	Fast Plasma Analyzer	1 eV–30 keV	Electrostatic analyzer
MFE	Magnetic Fields Experiment	0–50 Hz	Sensors/electrons
PIXIE	Polar Ionospheric X-Ray Imaging Experiment	3–60 keV	Pinhole x-ray camera
PWI	Plasma Wave Instrument	5.6 Hz–311 kHz 0.2–800 kHz 20 Hz–16 kHz 0.1–25 Hz 11, 22, or 90 kHz	MCA SFR WFR LFAC WBR
TIDE	Thermal Ion Dynamics Experiment	0–300 eV	Electrostatic ion optic
TIMAS	Toroidal Ion Mass Spectrograph	0.015–32 keV/e	Spectrograph imager
UVI	Ultraviolet Imager	1300–1900 Å	Charge-coupled device
VIS	Visible Imaging System	308–732 nm 125–150 nm	Auroral camera Earth camera

Project Scientist: Mario Acuna, GSFC, (301) 286-7258
 Program Scientist: Elden Whipple, NASA/HQ, (202) 358-0888

The Solar and Heliospheric Observatory (SOHO) Mission and Payload

The primary science objectives of the SOHO mission are as follows:

- The study and understanding of the solar coronal phenomenon; in particular, its heating mechanism and its expansion into the solar wind. This study will be accomplished both by remote sensing of the solar atmosphere with high-resolution spectrometers and by *in situ* measurements of the composition of the resulting particles in the solar wind
- The study of the Sun's structure and interior dynamics from its core to the photosphere by helioseismological methods, and the measurement of the solar irradiance variations

The SOHO spacecraft will be provided by the European Space Agency (ESA). The size and configuration of the spacecraft are dominated by the size of the large coronal instruments and the requirements of the liquid propulsion system. The spacecraft consist of two modules, a Payload Module (PM) to house the Sun-pointing instruments and a Service Module (SM) to house the remainder of the instruments and the spacecraft subsystems. The SM will be accommodate the propulsion system and the service module bus. The SOHO spacecraft will be 3-axis-stabilized in all mission phases including transfer orbit and final orbit at the L1 libration point.

Key SOHO Mission Statistics:

Planned Launch Date:	July 1995
Launch Vehicle:	ATLAS IIAS
Launch Site:	Eastern Test Range
Mission Duration:	Two years nominal; six years possible
Operational Orbit:	Heliocentric, halo orbit around the Sun-Earth L1 Lagrangian point
Orbital Period:	Six months
S/C Mass:	1850 kg (640 kg of payload)
Power:	1150 W (total power at launch), 450 W (allocated to payload)
Stabilization:	Permanently pointed to Sun center within 10 arc sec (absolute error); roll stability of 1.5 arc min per 15 minutes (about X-axis)
Pointing Accuracy:	1 arc sec per 15 minutes
Pointing Knowledge:	1 arc sec
Science Telemetry:	200 kbps (continuous for 2 months), 40 kbps (16 hours per day for 10 months per year), 200 kbps (8 hours per day for 10 months per year, real time contact)

SOHO Instruments

1) Charge, Element and Isotope Analysis (CELIAS)

D. Hovestadt, PI

The CELIAS experiment is designed to measure the mass, ionic charge and energy of the low and high speed solar wind, of suprathermal ions, and of low-energy flare particles. CELIAS includes three mass and charge discriminating sensors based on the time-of-flight technique: CTOF for the elemental, charge, and velocity distribution of the solar wind; MTOF for the elemental and isotopic composition of the solar wind; and STOF for the mass, charge, and energy distribution of suprathermal ions.

2) Coronal Diagnostic Spectrometer (CDS)

R. Harrison, PI

The prime objective of CDS is to obtain intensity ratios of selected extreme ultraviolet (EUV) line pairs, with spatial and temporal scales appropriate to the fine scale features of the solar atmosphere. The wavelength band chosen will allow coverage of a large portion of the atmosphere, with characteristic temperatures between 2×10^4 – 3×10^6 K. The CDS will also have a modest capability for the detection of flows of ~ 30 km s⁻¹ and above. For the CDS optics scheme, the spatial resolution of the full-revolution Wolter II telescope will be 3 arc seconds within a 4 arc minute field of view. The CDS will use a grazing incidence spectrometer of 15–80 nm with a spectral resolution of 1,000 - 10,000 and angular resolution of 3".

3) Comprehensive Suprathermal and Energetic Particle Analyzer (COSTEP)

H. Kunow, PI

The COSTEP consortium of instruments will investigate steady state processes in the solar atmosphere, energy release and particle acceleration in the solar atmosphere, and samples of solar atmospheric material. Two sensors furnished by COSTEP include LION and EPHIN. The LION detector consists of three ion implanted silicon detectors arranged in a unique 2-in-1 telescope configuration. LION will measure energy spectra of ions and electrons in the range of 40 keV to 5 MeV for protons and 40 keV to 300 KeV for electrons, with nominal sampling times ranging from 4 to 16 seconds. The instrument has a total power requirement of 1.9 W and a mass of 2.6 kg. The EPHIN is a multi-element array of solid state detectors capable of measuring energy spectra of electrons in the range 150 keV to 5 MeV and hydrogen and helium isotopes from 4 MeV/n to 53 MeV/n.

4) Energetic Particle Analyzer (ERNE)

J. Torsti, PI

The ERNE experiment will investigate the solar atmosphere and outer heliosphere by detecting particles produced in various kinds of solar energy release processes. The ERNE instrument is designed to measure solar particles from about 1 MeV/n upwards. Two sensor designs are included: the Low-Energy Detector (LED) and High-Energy Detector (HED). LED will measure the differential energy spectra of nuclei from hydrogen to iron starting from 1.4 MeV/n for protons. HED will enable spectral and abundance measurements of nuclei in the charge range $Z=1-30$ over the energy range from 11–40 MeV/n up to 107–540 MeV/n depending on Z . HED will also measure electron spectra in the range of 5 to 60 MeV.

5) Extreme Ultraviolet Imaging Telescope (EIT)

J.P. Delaboudinière, PI

The EIT will provide full disk images in emission lines formed at temperatures that map solar structures ranging from the chromospheric network to the hot magnetically confined plasma in the corona. Images in four narrow bandpasses will be obtained using normal incidence multilayered optics deposited on quadrants of a Ritchey-Chretien telescope. A rotating mask will allow the image from each single multilayer to reach alternatively the CCD detector in order to sharply image distinct solar structures that normally coexist in the temperature range from 6×10^4 to 3×10^6 K. The EIT will be capable of providing a uniform 5 arc second resolution (2.5" pixel size) over its entire 50 x 50 arc min field of view. The telescope will have an equivalent focal length of 1.65 m and a collecting aperture diameter of 10.5 cm.

6) Global Oscillations at Low Frequencies (GOLF)

A. Gabriel, PI

The GOLF experiment studies the internal structure of the Sun by measuring the spectrum of free global oscillations—both p and g mode oscillations—with the emphasis on the low-order long-period waves. The instrument will measure the mean disk line-of-sight velocity over a range of frequencies from 10^{-7} to 6×10^{-3} Hz, with a sensitivity of 1 mm/s. A sodium vapor resonance scattering spectrometer is used in a longitudinal magnetic field to sample the two wings of the solar absorption line. The use of a modulating magnetic field provides a continuous internal calibration of the sensitivity. By adding an additional rotating polarizer, experimenters are able to make measurements of the average solar magnetic field.

7) Large Angle and Spectrometric Coronagraph (LASCO)

G. Brueckner, PI

The LASCO coronagraph will provide electron column densities from just above the Sun's limb, at 1.1 R_e , out into deep heliospheric space, at 30 R_e . The corona will be analyzed spectroscopically by a high-resolution scanning imaging interferometer. The spectral profiles of three emission lines and one Fraunhofer line will be measured for each picture point, giving temperatures, velocities, turbulent motions, and volume densities. The technique used by LASCO includes one internal and two externally occulted coronagraphs with a Fabry-Perot interferometer.

8) Michelson Doppler Imager (MDI)

P.H. Scherrer, PI

The MDI will organize SOHO observations into four types of observing programs: structure (at all times), dynamics (2 months/year), campaign (8 hours/day, 10 months/year), and magnetic fields (few minutes/day). The MDI will measure line-of-sight velocity by Doppler shift, transverse velocity by local correlation tracking, line and continuum intensity, and line-of-sight magnetic fields with both 4 and 1.4 arc second resolution (2 and 0.7 arc sec pixels respectively).

9) Solar Ultraviolet Measurements of Emitted Radiation (SUMER)

K. Wilhelm, PI

The SUMER instrument will study flows, turbulent motions, waves, temperatures, and densities of the plasma in the Sun's upper atmosphere. SUMER will take images of the Sun in EUV light with high resolution in space, wavelength, and time. It will provide a spatial resolution of 1.5 arc

sec. Spectral shifts can be determined with sub-pixel accuracy. The wavelength range will extend from 500 to 1,600 Å; the integration time can be as short as 1 second. Information will be obtained on line profiles, shifts, and broadenings, as well as on ratios of temperature and density sensitive EUV emission lines that are formed at temperatures between 10^4 and 2×10^6 K.

10) Solar Wind Anisotropies (SWAN)
J.L. Bertaux, PI

The SWAN instrument consists of two identical sensor units placed on opposite sides of SOHO driven by one single common electronic box. Each sensor has a two-mirror scanning system, a light baffle, a hydrogen cell with tungsten filament, and the detector with a power supply. The objective of SWAN is to obtain a map of the Lyman-alpha light distribution in the sky approximately once per one or two days, with a resolution of 1 degree. The SWAN overall field of view is about 2π sr for each sensor, with a photometric sensitivity of 0.6 counts per second per Rayleigh. The spectral resolution of the hydrogen cell is better than 1.1% for 45 seconds counting time on IP signal.

11) Ultraviolet Coronagraph Spectrometer (UVCS)
J.L. Kohl, PI

The UVCS will provide ultraviolet spectroscopic observations of the solar corona out to 10 solar radii from Sun-center. The basic design of the UVCS consists of an occulted telescope and a high-resolution spectrometer assembly. The spectrometer assembly consists of three sections. The first section is optimized for line profile measurements; the second section is optimized for line intensity measurements; and the third section is used to measure the polarized radiance of the visible light corona.

12) Variability of Solar Irradiance (VIRGO)
C. Frohlich, PMOD/WRC, PI

The VIRGO experiment contains two types of active cavity radiometers for monitoring of the solar constant; two three-channel Sunphotometers (SPM) for the measurement of spectral irradiance at 402, 500, and 862 nm; and a low-resolution imager (LOI) with 12 pixels. VIRGO's main objective is to probe the solar interior by helioseismology with p and g mode solar oscillations determined from spectral irradiance (SPM) and radiance (LOI) variations on time scales of minutes to the mission time. VIRGO will determine the frequencies, amplitudes, and phases for oscillation modes in the frequency range of 1 μ Hz to 10 mHz.

SOHO Instruments Summary

	<i>Investigation</i>	<i>Range</i>
CELIAS	Charge, Element and Isotope Analysis	0.1–1000 keV/e
CDS	Coronal Diagnostic Spectrometer	150–800 Å
COSTEP	Comprehensive Suprathermal and Energetic Particle Analyzer	p, He: 0.04 - 53 MeV/n e: 0.04 - 5 MeV
ERNE	Energetic Particle Analyzer	p-Ni: 1.4–540 MeV/n e: 5 - 60 MeV/n
EIT	Extreme Ultraviolet Imaging Telescope	304–170Å
GOLF	Global Oscillations at Low Frequencies	0.1μHz–6mHz
LASCO	Large Angle and Spectrometric Coronagraph	1.1–30 R _O
MDI	Michelson Doppler Imager	0.2, 0.1 Å
SUMER	Solar Ultraviolet Measurements of Emitted Radiation	500–1600 Å
SWAN	Solar Wind Anisotropies	
UVCS	Ultraviolet Coronagraph Spectrometer	1145–1287Å 944–1070Å
VIRGO	Variability of Solar Irradiance and Gravity Oscillations	3402, 500, 862 nm

Project Scientist (ESA): Vicente Domingo, ESTEC, 31-1719-83583

Project Scientist (USA): Art Poland, GSFC, (301) 286-7076

Program Scientist (ESA): Martin Hubner, ESTAC, 31-1719-83552

Program Scientist (USA): Bill Wagner, NASA/HQ, (202) 358-0911

The Solar, Anomalous, and Magnetospheric Particle Explorer (SAMPEX) Mission and Payload

The zenith-pointing SAMPEX satellite, in near-polar orbit, will carry out studies of outstanding questions in the field of space plasma physics, solar physics, heliospheric physics, cosmic ray physics, and middle atmosphere physics. The instruments can measure the electron and ion composition of energetic particle populations from 0.4 MeV/nucleon using a coordinated set of detectors of excellent charge and mass resolution, and with higher sensitivity than any flown before.

While over the magnetic poles, SAMPEX will detect solar energetic particles, interplanetary particles, and galactic cosmic rays. The changing geomagnetic cutoff encountered by the spacecraft at differing latitudes will allow studies of the ionization state of these particles at energies much higher than can be studied from interplanetary space. The instruments will also observe precipitating magnetospheric electrons, which undergo interactions with the middle atmosphere.

The primary objectives of the SAMPEX mission are as follows:

- Determine the charge-state Q of anomalous cosmic rays and thereby verify whether or not they are indeed singly charged and thus represent a sample of neutral interstellar medium
- Search for evidence of galactic evolution effects on the isotopic composition of local galactic material accelerated in the heliosphere
- Provide significantly improved determinations of the solar elemental and isotopic composition based on direct sampling of solar material
- Probe the acceleration mechanisms in impulsive ^3He -rich flares by improved composition and charge state measurements
- Separate the Q/M dependence of the coronal shock acceleration process by measuring ion spectra over an extremely broad energy range
- Determine the average charge-state of energetic solar particles, thereby characterizing the temperature of the acceleration site
- Characterize precipitating electrons during periods of declining solar activity
- Determine whether or not odd nitrogen and odd hydrogen molecules are produced by precipitating electrons in the middle atmosphere at a sufficient rate to affect O_3 depletion
- Extend the search for isotopic differences between galactic and solar cosmic material to several additional key elements

- Determine the dominant nucleosynthesis processes contributing to cosmic ray source material

Key SAMPEX Mission Statistics

Launch Date:	3 July 1992
Launch Vehicle:	Scout G-1
Launch Site:	VAFB
Mission Duration:	4 years
Orbit Apogee:	450 km
Perigee:	850 km
Inclination:	82°
S/C Mass:	162 kg
Stabilization:	3-axis, zenith pointing
Pointing Accuracy:	1°
Pointing Knowledge:	0.1°
Power:	115 watts
Science Telemetry:	4, 16, and 900 kb/s
Data Storage:	16 Mbytes

SAMPEX Instruments

SAMPEX PI is Glen Mason

1) Low-Energy Ion Composition Analyzer (LEICA)

LEICA point of contact is G. Mason

The LEICA instrument is a mass spectrometer that identifies incident mass and energy by simultaneously measuring the time of flight and residual kinetic energy of particles that enter the telescope and stop in one of four Si solid state detectors. The instrument will detect: H (0.75–8 MeV/nucleon), He (0.41–8 MeV/nucleon), C 0.35–12 MeV/nucleon), Si (0.26–18 MeV/nucleon), Fe (0.16–25 MeV/nucleon).

2) Heavy Ion Large Telescope (HILT)

HILT point of contact is B. Klecker

The HILT sensor is a large geometry factor (65 cm² sr) instrument that will measure galactic cosmic rays and solar energetic particles in the region of the Earth's magnetic poles. In addition, the instrument will determine the energy and elemental composition of anomalous cosmic rays at energies where they are most abundant. HILT will measure the direction, energy, and charge of: He (3.9–9 MeV/nucleon), C (7.2–160 MeV/nucleon), Si (9.6–117 MeV/nucleon), Fe (11–90 MeV/nucleon).

3) Mass Spectrometer Telescope (MAST)

MAST point of contact is D. Meweldt

This instrument determines the direction, energy, element, and isotope of all elements up to nickel entering the instrument with velocities between 12 percent and 75 percent of the speed of

light. It detects H (1–15 MeV/nucleon), He (7–91 MeV/nucleon), C (12–210 MeV/nucleon), Si (19–345 MeV/nucleon), Fe (24–470 MeV/nucleon).

4) Proton/Electron Telescope (PET)

PET point of contact is D. Meweldt

The PET instrument was designed to complement the MAST experiment by measuring the energy of electrons, protons, and helium nuclei coming from the Earth's radiation belts, the Sun, interplanetary space, and interstellar space. The electrons will be moving very close to the speed of light and could have a significant effect on the destruction of ozone high in the Earth's atmosphere. The instrument will detect: Electrons (1–30 MeV), H (18–250 MeV/nucleon), He (18–350 MeV/nucleon), Si (54–195 MeV/nucleon), C (34–120 MeV/nucleon), Fe (70–270 MeV/nucleon).

SAMPEX Instruments Summary

	<i>Investigation</i>	<i>Range</i>	<i>Type</i>
LEICA	Low-Energy Ion Composition	0.16 to 25 MeV	TOF mass spectrometer
HILT	Heavy Ion Large Telescope	3.9 to 177 MeV	Ion drift chamber
MAST	Mass Spectrometer Telescope	1 to 470 MeV	Mass spectrometer
PET	Proton/Electron Telescope	1 to 350 MeV	Solid state

Project Scientist: Dan Baker, GSFC, (301) 286-8112
Program Scientist: Vernon Jones, NASA/HQ, (202) 358-0885

The Spartan Missions and Payload

The Spartan 201 experiment objectives include the following:

- To provide important electron temperature data not obtainable from previous rocket (electron density, outflow velocities) or ground (electron density) experiments in order to enhance understanding of the heating and acceleration of the solar wind
- To serve as a prototype for important aspects of UVCS and LASCO experiments on SOHO
- To represent the only source of data for a pre-mission focus of the coronal science from SOHO by the international consortium
- To influence the onboard SOHO science software and observing programs
- To supply Ulysses with supporting data during its 1994 and 1995 polar passes

The Spartan 201 experiment will provide critical information for developing science software and observing programs for the Ultraviolet Coronagraph Spectrometer (UVCS) and the Large-Field Spectrographic Coronagraph (LASCO) on the Solar and Heliospheric Observatory (SOHO) mission. At present, only 15 minutes of sounding rocket data from an ultraviolet coronagraph spectrometer exist. Nearly all of those data measure the resonantly scattered Lyman alpha, including upper limits to O_{VI} intensities but not electron scattered Lyman alpha data.

The Spartan 200 series of experiments employs a free-flying platform that is deployed and retrieved as a payload on the Space Shuttle. The Spartan 200 common service module contains the attitude control system (ACS) electronics, battery boxes, thermal louvers, data handling electronics, cold plate, and wiring bay. The science instrumentation and the ACS pneumatics are customized for each Spartan mission. The Spartan 200 pointing timeline program requires release from the orbiter's remote manipulator system at a specific attitude and time. One of several stored pointing timelines is selected by the crew prior to deployment. Several Sun trackers are available, measuring down to ± 30 arc-seconds null stability. Power is supplied by silver-zinc primary cells. Typically, 3 KWH are available to the experiment. This suffices for 40–50 hours of mission time.

Key Spartan Mission Statistics

Launch Dates:	April 8, 1993 (STS-56); 1994 (STS-63); 1995, (STS-73)
Launch Vehicle:	STS
Launch Site:	KSC
Mission Duration:	40 hours
Operational Orbit:	160 nmi x 160 nmi, 57 degree inclination
S/C Mass:	5,000–5,500 lbs Spartan/REM/MPSS; 3,000 lbs Spartan deployed
Propulsion ΔV :	Stored impulse (2 bottles) sufficient for 500 maneuvers (1°/sec) plus 48-hour limit cycle
Stabilization:	± 1 arc-min for alignment
Pointing Accuracy:	± 3 arc-min; gyro drift < 0.1° per hour; jitter < 10 arc-sec peak to peak
Pointing Knowledge:	1 arc-min
Power:	28 VDC nominal; 3 KWH available (silver-zinc primary cells)

Science Telemetry: no RF link
Data Storage: 6×10^9 bits for data storage on tape recorder PCM encoder @ 6.25–50 kbps

1) Ultraviolet Coronagraph Spectrometer (UVCS)
J. Kohl, PI

The UVCS will use ultraviolet emissions from neutral hydrogen and ions in the corona to determine the velocities of the coronal plasma within the solar wind source region, and the temperature and density distributions of protons. The primary targets for the UVCS will be helmet streamers and the boundary regions between streamers and coronal regions of exceptionally low density and temperature (called coronal holes). Temperature, density and velocity models for these regions will be determined using measurements of the atomic (neutral) hydrogen Lyman-alpha line profiles and the intensities of the ionized oxygen lines. They will provide information on solar wind source regions and acceleration processes, while also mapping the sources of solar-wind streams detected by distant *in situ* measurements with the Ulysses spacecraft.

The line-of-sight random velocity distribution of the atomic hydrogen can be determined from the spectral profile of the resonantly-scattered Lyman-alpha line. These measurements will determine the coronal atomic hydrogen and proton kinetic temperature from 1.5 to 3.5 solar radii. Doppler dimming of the hydrogen line profile will additionally establish proton outflow velocities in the 100 to 300 kilometer per second range. Observation of the ionized oxygen lines will determine bulk outflow velocities of ionized oxygen in the 30 to 250 kilometer per second range.

2) White Light Coronagraph (WLC)
R. Fisher, PI

The WLC will investigate the distribution of mass in the corona, while providing context information for the UVCS in its determination of bulk flows in the corona. The WLC will use polarized radiance measurements to determine the electron densities in large-scale closed and open magnetic structures, such as helmet streamers and coronal holes from 1.8 to 3.0 solar radii.

The WLC is an externally occulted coronagraph with a CCD detector and built-in polarimeter capable of detecting the linear Stokes parameters. It can therefore be used to separate the dust-scattered light of the corona (F-corona, unpolarized) from the electron-scattered light of the corona (K-corona, polarized). From these observations it is possible to determine the distribution of the brightness (K+F coroneae), polarized brightness, and degree of polarization of the electron-scattered corona and thus make a model-dependent estimate of the 3-D distribution of the electron mass in the corona.

Temporal changes in the white light corona will also be investigated over the period of the mission among the range of coronal structures available. The rate of coronal mass ejection transient activity is anticipated to be greater than one event per day, so there is a better than 50% chance that the WLC will observe such an ejection as it observes one half of the solar limb during the 40-hour mission.

Spartan Instruments Summary

	<i>Investigation</i>	<i>Range</i>	<i>Type</i>
UVCS	Ultraviolet Coronagraph Spectrometer	1.3–10 R_{\odot}	Liner array telescopeG3
WLC	White Light Coronagraph	1.1–30 R_{\odot}	CCD camera

Project Scientist (USA): Dick Fisher, GSFC, (301) 286-8811
Program Scientist (USA): Bill Wagner, NASA/HQ, (202) 358-0911

The Ulysses Mission and Payload

Ulysses is a joint NASA and ESA mission to explore the heliosphere over the full range of solar latitudes and provide an accurate assessment of the total solar environment. The spacecraft was launched on October 6, 1990, by the shuttle *Discovery* (STS-41), and a PAM/TUS placed the spacecraft into an ecliptic transfer orbit to Jupiter. At the time of escape, Ulysses was the fastest man-made object in the solar system, with an escape velocity over 15 km/s.

Ulysses arrived at Jupiter in February 1992, 16 months after departing from Earth and after traveling nearly 1 billion kilometers in the ecliptic plane. On 2 February, almost a week before closest approach, Ulysses crossed the Jovian bow shock at a distance of 113 Jovian radii from the planet. Closest approach to Jupiter occurred at 12:02 UT on 8 February, when Ulysses was 450,000 km from the center of the planet at a latitude of 40° North. The primary aim of the flyby was to obtain a gravity assist from Jupiter that would generate the energy necessary to place the spacecraft in its final heliocentric out-of-ecliptic orbit, with minimum risk to the onboard systems and scientific payload. Scientific observations at Jupiter were therefore a secondary objective of the mission.

The most intense scientific activity will commence when Ulysses reaches 70 degrees south solar latitude in May 1994 and begins its pass over the Sun's south pole. The spacecraft will spend about four months south of latitude 70° at a distance of about 330 million km (2 AU) from the Sun. Nine scientific instruments will collect data, as a function of solar latitude, about the solar corona, the solar wind, the heliospheric magnetic field, cosmic radiation from outside the solar system, and other solar and interstellar particles and fields. Ulysses will then cross the Sun's equator in February 1995, at a distance of about 1 AU, followed by a four-month pass of the Sun's northern polar region that begins in May 1995. By September 1995 Ulysses will have explored the heliosphere at nearly all latitudes, measured phenomena over both of the Sun's poles, and investigated interplanetary particles and fields. As the spacecraft leaves the region of the Sun's north pole the baseline mission will end, and Ulysses will remain in a heliocentric orbit of perihelion 1.3 AU and aphelion 5.4 AU. An extended mission to provide polar passes during the next solar maximum is being considered.

The primary scientific objectives of the Ulysses mission are to investigate, as a function of solar latitude, the properties of the solar corona; the solar wind; the structure of the Sun-wind interaction; the heliospheric magnetic field; solar and non-solar cosmic rays; solar radio bursts and plasma waves; solar x rays; and the interstellar/interplanetary neutral gas and dust. For the first time ever, *in situ* measurements will be made far out of the plane of the ecliptic and over the solar poles.

Specifically, the space physics goals of Ulysses are as follows:

- To gain knowledge of the interplanetary medium at high solar latitudes due to solar chromospheric and photospheric conditions, sunspots, solar flares, prominences, and coronal holes
- To characterize various particles from the ecliptic to the Sun's poles, including the solar wind, galactic cosmic rays, interplanetary dust, and solar energetic particles

- To analyze the heliospheric medium from the ecliptic to the poles, including plasma waves, solar radio waves, and heliospheric magnetic fields

Secondary science objectives include interplanetary physics during the ecliptic cruise phase; measurements of the Jovian magnetosphere during the Jupiter fly-by phase; and a search for gravitational waves from cataclysmic cosmic events.

Key Ulysses Mission Statistics

Launch Date:	6 October 1990
Launch Vehicle:	STS/TUS/PAM-S
Launch Site:	KSC
Mission Duration:	5 years (baseline)
Orbit Type:	Heliocentric
Aphelion:	1.3 AU
Perihelion:	5.4 AU
Inclination:	79° to the ecliptic
S/C Mass:	366.59 kg
Stabilization:	Spin stabilized, 5 rpm
Pointing Accuracy:	1°
Pointing Knowledge:	0.1°
Power:	1 RTG, 282 watts at launch, 244 watts at end of mission
Science Telemetry:	1.0 kb/s maximum real-time
Data Storage:	Two 45 MB recorders

Ulysses Instruments

1) Magnetic Fields (VHM/FGM) A. Balogh, PI

This experiment consists of a triaxial vector helium magnetometer (VHM) and a fluxgate magnetometer (FGM) attached to a 5 m radial boom. The VHM is located at the end of the boom, while the fluxgate magnetometer is 1.2 m inboard from the VHM. The VHM is a two-range instrument operating over the ranges ± 8.19 nT and ± 65.52 nT, corresponding to scale factors of 1.6 nT/V and 12.8 nT/V respectively. The FGM measures the magnetic field vector in four ranges; ± 8 nT, ± 64 nT, ± 2048 nT, and 44,000 nT full scales. The first two ranges are for use in interplanetary space during all mission phases; the third range was used during Jupiter encounter below 30 R_J; and the last range is to facilitate testing.

2 Solar-Wind Plasma (SWOOPS) J. Phillips, PI

The Solar-Wind Plasma Experiment will accurately characterize the bulk flow and internal state conditions of the interplanetary plasma in three dimensions at all heliocentric distances and heliographic latitudes. Electron and ion measurements are made simultaneously and independently with two separate instruments, which provides a measure of redundancy. Each instrument uses a curved-plate electrostatic analyzer with a spherical section geometry that is cut off in the form of a sector, equipped with multiple continuous Channel Electron Multipliers (CEM's). Electrons with energies between 1 eV and 900 eV will be detected at seven polar

angles and various combinations of azimuth angle. Ions will be detected between 257 eV/Q and 35 keV/Q using appropriate subsets of 16 CEM's.

3) Solar Wind Ion Composition (SWICS)
J. Geiss and G. Gloeckler, Co-PI's

The Solar Wind Ion Composition Spectrometer will determine uniquely the elemental and ionic charge compositions and the temperatures and mean speeds of all major solar wind ions, from H through Fe, at solar wind speeds ranging from 145 km/s (protons) to 1352 km/s (Fe⁺⁸). The instrument, which covers an energy per charge range from 110 eV/Q to 66.7 keV/Q in 13 mins, combines an electrostatic analyzer with post-acceleration, followed by a time-of-flight and energy measurement.

4) Low-Energy Ions and Electrons (HI-SCALE)
L. Lanzerotti, PI

This instrument is designed to obtain measurements of interplanetary ions and electrons, and make significant advances toward understanding the physical processes involved in the solar control of low-energy particles in the heliosphere. The ions ($E_i > 50$ keV) and electrons ($E_e > 30$ keV) are detected by five separate solid state detector telescopes oriented to give essentially complete pitch-angle coverage from the spinning spacecraft. Ion elemental abundances are determined by a ΔE vs E telescope using a thin (5 μm) front detector element in a three-element telescope.

5) Energetic Particle Composition and Interstellar Neutral Gas (EPAC/GAS)
E. Keppler, PI

The EPAC/GAS instrument consists of two independent systems: an energetic particle composition experiment to measure the intensities, anisotropies, and energy spectra of low-to-medium energetic interplanetary ions and resolve their masses; and a gas experiment to observe directly the interstellar neutral helium penetrating into the heliosphere. The energetic particle instrument consists of four telescopes, each comprising two Si-surface barrier detectors. It measures the composition of energetic ions from H to Fe, in the energy range 80 keV to 15 MeV. The gas experiment consists of two nearly identical detector channels, each consisting of a mechanical collimator, conversion plates of lead glass coated with LiF, and channel electron multipliers (CEM's).

6) Cosmic Rays and Solar Particles (COSPIN)
J. A. Simpson, PI

The Cosmic Rays and Solar Particles investigation will, for the first time, make direct measurements in regions of the heliosphere far from the ecliptic plane. Measurements will be made of intensities, spectra, anisotropies, and the chemical and isotopic composition of nuclei from hydrogen through iron in various energy ranges from 0.3 to 600 MeV/nucleon, and of electrons between 1 and 300 MeV. A set of five telescope subsystems are combined to cover the charged particle flux over a wide energy range. The high-energy telescope (HET) will make spectral and chemical-abundance measurements of all elements from H to Ni over an energy range of 14 to 600 MeV/nucleon. The low-energy telescope (LET) will provide spectral and chemical-abundance measurements over the charge range $Z = 1$ to 26, to carry the chemical

composition downward in energy to 1.8 MeV for protons and 3 MeV/nucleon for particles with $Z > 5$. The twin anisotropy telescopes (AT) will measure the three-dimensional anisotropies of protons and alpha particles in the energy range 0.8 to 6 MeV/nucleon. The high-flux telescope (HFT) will provide measurements of protons and heavier particles with high immunity to electron contamination under high flux conditions and with high azimuthal resolution. The electron telescope (KET) is designed to measure electron fluxes between 4 and 2,000 MeV and to determine energy spectra in the range 12 to 300 MeV.

7) Unified Radio and Plasma Waves (URAP)

R. G. Stone, PI

The scientific objectives of the Ulysses Unified Radio and Plasma wave (URAP) experiment are twofold: 1) the determination of the direction, angular size, and polarization of radio sources for remote sensing of the heliosphere and the Jovian magnetosphere and 2) the detailed study of local wave phenomena, which determine the transport coefficients of the ambient plasma. The tracking of solar radio bursts, for example, can provide three dimensional "snapshots" of the large scale magnetic field configuration along which the solar exciter particles propagate. The study of observed wave-particle interactions will improve our understanding of the processes that occur in the solar wind and of radio wave generation. The URAP sensors consist of a 72.5 m electric field antenna in the spin plane, a 7.5-m electric field monopole along the spin axis and a pair of orthogonal search coil magnetic antennas. The various receivers, designed to encompass specific needs of the investigation, cover the frequency range from DC to 1 MHz. A relaxation sounder provides very accurate electron density measurements. As of February 1994, the experiment continues to function nominally.

8) Solar-Flare X-Rays and Cosmic Gamma-Ray Bursts (GBS)

K. Hurley and M. Sommer, Co-PI's

The HUS experiment is designed to detect and record the intensity and the spectral characteristics of solar x-ray emissions and cosmic gamma-ray bursts as a function of time. In addition, the instrument will serve a solar-flare patrol function. The soft x-ray sensor consists of two Si surface barrier detectors, each 500 μm thick, which detect x rays in the energy range 5–15 keV. The gamma-ray sensor consists of two hemispherical CsI scintillation crystals, each 2 mm thick and optically coupled to a hemispherical photocathode photomultiplier tube. It measures x rays and gamma rays in the energy range 15–150 keV.

9) Cosmic Dust (DUST)

E. Grun, PI

The dust experiment provides direct observations of particulate matter with masses between 10^{-19} and 10^{-10} kg in the solar system, investigates its physical and dynamic properties as a function of ecliptic latitude and heliocentric distance, and studies its interaction with solar radiation, the solar wind, and the interplanetary magnetic field. The investigation uses a 0.1 m^2 multicoincidence impact plasma detector and electron multiplier to measure the mass, speed, flight direction, and electric charge of individual dust particles.

10) Coronal Sounding (SCE)

M.K. Bird, PI

This investigation will determine the density, turbulence spectrum, and velocity of the coronal plasma in the acceleration regime of the solar wind by conducting dual frequency ranging,

doppler measurements, and spectral measurements during times of superior conjunction. The accuracy of the combined spacecraft/ground ranging system is about $\pm 3 \times 10^{17}$ el/m², while the differential doppler precision is in the range $\pm 2 \times 10^{14}$ el/m².

11) Gravitational Waves (GWE)
B. Bertotti, PI

The objective of the gravitational wave investigation is to search for low frequency gravitational waves crossing the solar system using the spacecraft doppler detection method. The method is most sensitive to wave periods between approximately 100 sec and 8000 sec. The experiment was performed during two periods of solar opposition (December 1990 and February 1992).

Ulysses Instruments Summary

<i>Investigation</i>	<i>Range</i>	<i>Type</i>
VMS/FGM Magnetic Fields	± 0.01 nt to $\pm 44,000$ nt	Triaxial VHVM and fluxgate
SWOOPS Solar Wind Plasma	1 eV to 35 keV	CEM's
SWICS Solar Wind Ion Composition	145 to 1,352 km/s	Electrostatic
HI-SCALE Low-Energy Ions and Electrons	30 keV to 5 MeV	Solid state
EPAC/GAS Energetic Particle Composition and Interstellar Gas	80 keV to 15 MeV	CEM's
COSPIN Cosmic Rays and Solar Particles	0.3 to 2,000 MeV	Solid state
URAP Unified Radio and Plasma Waves	0 to 940 Hz	Dipole, monopole, loop
GRB Solar X-rays and Cosmic Gamma Ray Bursts	5 to 150 keV	Si solid state CsI scintillators
DUST Cosmic Dust	10^{-7} to 10^{-16} g	Channeltron
SCE Coronal Sounding		Doppler
GWE Gravitational Waves		Doppler

Project Scientist (USA): Ed Smith, JPL, (818) 354-2248
 Project Scientist (ESA) Richard Marsden, ESTEC, 31-1719-83583
 Program Scientist (USA): Vernon Jones, NASA/HQ, (202) 358-0885
 Project Manager (ESA): K.-Peter Wenzel, ESTEC, 31-1719-83573

The Upper Atmosphere Research Satellite (UARS) Mission and Payload

NASA's Upper Atmosphere Research Satellite (UARS) is carrying out the first systematic, comprehensive study of the stratosphere and furnishes important new data on the mesosphere and thermosphere. The UARS will measure the global energy radiated by the atmosphere, the energy absorbed or scattered from sunlight passing through the atmosphere and then provide the detailed information on chemical constituents, temperature, winds, and the effect of energy inputs from sunlight and the solar wind. UARS will help to reveal the mechanisms that control the structure and variability of the upper atmosphere, to improve the predictability of ozone depletion, and to define the role of the upper atmosphere in the Earth's climate system.

The UARS program builds upon decades of research with rockets, balloons, aircraft, and satellites. The primary UARS mission objectives are to provide an increased understanding of:

- Energy input into the upper atmosphere
- Global photochemistry of the upper atmosphere
- Dynamics of the upper atmosphere
- The coupling among these processes
- The coupling between the upper and lower atmosphere

Deployed by the Space Shuttle in late 1991, UARS operates 600 km above the Earth in an orbit inclined 57 degree to the Equator so that the UARS sensors can provide essentially global coverage of the stratosphere and mesosphere, and make measurements over the full range of local times at all geographic locations every 36 days. The UARS observatory includes the nine instruments in the three types of measurements: (1) composition and temperature, (2) wind, and (3) energy inputs. Four UARS instruments are devoted to measurements of the first kind; they spectroscopically determine the concentrations of many different chemical species and derive the variation of atmospheric temperature with altitude by observing infrared emissions from carbon dioxide. Two instruments, utilizing high-resolution interferometer, will study upper atmosphere wind by sensing the Doppler shift in light absorbed by or emitted from atmospheric molecules. An additional three investigations will obtain estimates of the energy incident on the atmosphere by measuring solar ultraviolet radiation and the flux of charged particles from the Earth's mesosphere.

Key Wind Mission Statistics

Launch Date:	October 1991
Launch Vehicle:	Space Shuttle
Mission Duration:	Three years
Operational Orbit:	600 km circular with period of 97 minutes
Inclination:	57°
Latitude coverage:	80° N to 80° S
S/C Mass:	6800 kg
Stabilization:	Three-axis to less than 0.1 degree
Power:	1.6 kW

Telemetry rate: 32 kbps
Data Storage: Two tape recorders and tape playback at 512 kbps
Data relay: Tracking and Data Relay Satellite System (10 min/orbit)

UARS instruments

1) Cryogenic Limb Array Etalon Spectrometer (CLAES) A. E. Roche, PI

The CLAES will determine concentration of members of the nitrogen and chlorine families, as well as ozone, water vapor, methane, and carbon dioxide, through observations of infrared thermal emissions at wavelengths from 3.5 to 12.7 microns. To obtain a vertical profile of species concentration, CLAES utilizes a telescope, a spectrometer, and a linear array of 20 detectors to make simultaneous measurements at 20 altitudes ranging from 10 to 60 km.

Because the detectors and optics generate their own thermal emissions, they must be cooled to temperatures which suppress this emission to below that of the gases under observation. The CLAES cryogenic system consists of two components: a block of solid neon at -260°C , which cools the detectors to minimize detector noise, and a surrounding block of solid carbon dioxide at -150°C to reduce background emission. The cryogenics limits the useful observing lifetime of the instrument, but it is the only practical way of achieving the very low temperatures required for the CLAES detectors.

2) Improved Stratospheric and Mesospheric Sounder (ISAMS) F. W. Taylor, PI

The ISAMS, an improved version of one that operated aboard Nimbus-7, is a filter radiometer of 8 detectors to observe infrared molecular emissions by means of a movable off-axis reflecting telescope. In addition to scanning the atmosphere vertically, the telescope can also be commanded to view regions to either side of the UARS observatory, thus providing increased geographic coverage. The ISAMS instrument utilizes a Stirling-cycle refrigerator to cool its 8 detectors to -195°C , an approach that yields a potentially long operating lifetime.

One of the interesting features of ISAMS is that it carries samples of some of the gases to be measured in cells within the instruments. Atmospheric radiation collected by the telescope will pass through these cells on its way to the detectors. This design allows ISAMS to match the full spectra of the gases in the cells with the spectra observed in the atmosphere. In addition, ISAMS employs broadband filters to isolate portions of the spectrum, thus permitting measurements of those gases which, because of their chemical activity, cannot be confirmed in cells.

The ISAMS experiment will measure the concentrations of nitrogen chemical species, as well as ozone, water vapor, methane, and carbon monoxide, through observation in the infrared spectral region from 4.6 to 16.6 microns.

3) Microwave Limb Sounder (MLS) J. W. Waters, PI

The MLS will measure emissions of chlorine monoxide, hydrogen peroxide, water vapor, and ozone in the microwave spectral region at frequencies of 63, 183, and 205 GHz (i.e. wavelengths

of 4.8, 16.4, and 1.46 mm). The observations of chlorine monoxide are of particular importance, since this gas is a key reactant in the chlorine chemical cycle that destroys ozone; microwave measurements are essential for observations of this species, and MLS is unique among the UARS instruments in providing microwave sensitivity. The MLS observations will provide, for the first time, a global data set on chlorine monoxide in the upper atmosphere. MLS will also determine the altitudes of atmospheric pressure levels. Because MLS is a microwave instrument, it employs an antenna rather than optical devices to gather radiation.

4) Halogen Occultation Experiment (HALOE)

J. M. Russell, PI

Through measurements of atmospheric infrared absorption at wavelengths from 2.43 to 10.25 microns, the HALOE will determine the vertical distributions of hydrofluoric and hydrochloric acids as well as those of methane, carbon dioxide, ozone, water vapor, and members of the nitrogen family. Both of the halogen acids are reservoir species, and HALOE will be especially effective in measuring their concentrations.

The HALOE experiment uses samples of several of the gases to be observed as absorbing filters in front of the detectors to obtain high degree of spectral resolution. The instrument also utilizes broadband filters to detect gases for which such high spectral resolution is not required.

During every UARS orbit, at times of spacecraft sunrise and sunset, HALOE will be pointed toward the Sun and measure the absorption of energy along this line of sight. There are 28 solar occultation opportunities per day, providing data for 14 different longitudes in each of the Northern and Southern Hemispheres.

5) High Resolution Doppler Imager (HRDI)

P. B. Hays

At altitudes below about 45 km, the HRDI will observe the Doppler shifts of spectral lines within the atmospheric band system of molecular oxygen to determine the wind field. There are no sharp emission lines in the radiance of the Earth's limb at such altitudes, but the oxygen bands contain many lines that appear as deep absorption features in the brilliant spectrum of scattered sunlight. A triple-etalon Fabry-Perot interferometer, serving as a high-resolution spectral filter, will ensure efficient rejection of the intense emission continuum outside the absorption lines. HRDI will exploit these daytime absorption features to provide wind data for the stratosphere and upper troposphere to an accuracy of 5 m/s or better.

At altitudes above about 60 km, HRDI will observe emission lines of neutral and ionized atomic oxygen in the visible and near-infrared spectral regions by the same interferometric technique. Unlike the molecular absorption lines, however, the emission lines are observable both day and night. These measurements will furnish the wind field in the mesosphere and thermosphere to an accuracy of 15 m/s or better.

The HRDI instrument incorporates a baffled, off-axis telescope on a two-axis gimballed structure, whose motion is controlled by a microprocessor. An altitude scan is typically executed first in the direction forward of the spacecraft velocity. The telescope is then rotated backward for a second altitude scan, which yields measurements of the same atmospheric region some 7 minutes

after the first scan; this interval is short compared to characteristic timescales for changes in the wind field. The HRDI field of view allows a vertical resolution of 4 km at the Earth's limb.

6) Wind Imaging Interferometer (WINDII)
G. G. Shepherd, PI

The WINDII utilizes emission lines for the basic Doppler-shift measurements. In addition to lines of neutral and ionized atomic oxygen, these include two lines of the OH molecule and a molecular-oxygen line. WINDII will obtain measurements both day and night at altitudes above 80 km.

The WINDII spectral filter is a high-resolution Michelson interferometer. The instrument consists of a telescope, the interferometer, and a detector array. The telescope views 45° and 135° from the spacecraft velocity vector simultaneously. In normal operation, the detector provides a vertical resolution of about 4 km and a horizontal resolution of some 20 km. Wind velocity accuracy within 10 m/s is expected in the altitude range between 80 and 300 km.

7) Solar Ultraviolet Spectral Irradiance Monitor (SUSIM)
G. E. Brueckner, PI

The SUSIM mounted on the UARS solar/stellar positioning platform, will measure solar ultraviolet radiation in the wavelength range from 120 to 400 nm with a resolution down to 0.1 nm. The instrument is designed to provide its own long-term, absolute calibration light sources to track any change in instrument response during spaceflight.

SUSIM incorporates two spectrometers, seven detectors, and a set of four deuterium ultraviolet calibration lamps. One spectrometer will observe the Sun and measure the variation in solar ultraviolet flux as a function of time, while the second will monitor the calibration lamps. One of the four deuterium lamps within the instrument will serve as a calibration source. Once each day, this ultraviolet lamp will be turned on and positioned sequentially in front of each spectrometer. Stability in the output of this primary deuterium calibration lamp will be verified against the other three lamps, which will be utilized weekly, monthly, and annually for additional confidence in the calibration.

8) Solar/Stellar Irradiance Comparison Experiment (SOLSTICE)
G. J. Rottman, PI

Also mounted on the solar/stellar positioning platform, the SOLSTICE will measure solar ultraviolet radiation in the wavelength range from 115 to 430 nm with a resolution of 0.12 nm. This instrument has the unique ability to compare the solar ultraviolet output with the ultraviolet radiation of stable bright blue star, using the same optics. These stars thus constitute the standards against which the solar irradiance is measured. In the future, instruments similar to SOLSTICE can be placed in orbit to continue measurements of the solar output relative to these stellar calibration standards, thus creating a record of the long-term variation of the solar ultraviolet spectrum.

The experiment consists of a spectrometer with three spectral channels, each with a separate grating and photomultiplier tube. SOLSTICE will be pointed toward the Sun during the daylight portion of each orbit, and toward one of the calibration stars during most of the nighttime portion

of the orbit. To accommodate the large difference in signal strength between the solar and stellar measurements, SOLSTICE can vary the duration of the measurement from 1 second to 17 minutes, the spectral bandpass from 0.1 to 5.0 nm, and the area of the entrance slit by a factor of 10,000.

9) Particle Environment Monitor (PEM)

J. D. Winningham, PI

The PEM instrument will determine the type, amount, energy, and distribution of charged particles injected into the Earth's thermosphere, mesosphere, and stratosphere. PEM will utilize three separate boom-mounted sensors to measure electrons with energies from 1 eV to 5 MeV, protons with energies from 1 eV to 150 MeV, and the strength of the Earth's magnetic field—all in the vicinity of the spacecraft.

To complement these in situ particle measurements, PEM includes a 16-element array of X-ray detectors to provide wide spatial coverage of the energy injected into the upper atmosphere by high-energy electrons. As these electrons are slowed in their passage through the atmosphere, X-rays are emitted and scattered in all directions. PEM will provide X-ray images in the energy range from 2 to 50 keV, leading to the reconstruction of the global, three-dimensional energy input spectrum of electrons up to 1 MeV in energy.

UARS Instrument Summary

	<i>Investigation</i>	<i>Range</i>	<i>Type</i>
CLAES	Cryogenic Limb Array Etalon Spectrometer	Infrared emission of 3.5-12.7 microns	Telescope, spectrometer
ISAMS	Improved Stratospheric and Mesospheric Sounder	Infrared emission of 4.6-16.6 microns	Filter radiometer, off-axis reflecting telescope
MLS	Microwave Limb Sounder	Microwave emission at 63, 183, and 205 GHz	Radiometer
HALOE	Halogen Occultation Experiment	Infrared absorption 2.43-10.25 microns	Radiometer
HRDI	High Resolution Doppler Imager	Visible and near-infrared emissions and absorptions	Fabry-Perot Interferometer
WINDII	Wind Imaging Interferometer	Visible and near-infrared emissions	Michelson interferometer
SUSIM	Solar Ultraviolet Spectral Irradiance Monitor	Solar ultraviolet radiation from 120 to 400 nm	Full disk solar ultraviolet irradiance spectrometer
SOLSTICE	Solar/Stellar Irradiance Comparison Experiment	Solar ultraviolet radiation from 115 to 430 nm	Full disk solar ultraviolet irradiance spectrometer
PEM	Particle Environment Monitor	electron (1eV-5 MeV), proton (1eV-150 MeV) X-ray (2-50keV)	Spectrometer

Project Scientist: Carl A. Reber, GSFC, (301) 286-6534
 Program Scientist: Robert J. McNeal, NASA/HQ, (202) 358-0239

The Voyager Missions and Payloads

The planetary phase of the dual-spacecraft Voyager mission to Jupiter, Saturn, Uranus, Neptune, and their moons was completed in August 1989, when Voyager 2 passed approximately 4,850 km above Neptune's north pole. The Voyager spacecraft officially began the Voyager Interstellar Mission (VIM) phase of this epic journey on January 1, 1990. The Voyagers are 3-axis-stabilized craft based on previous Mariner and Viking Orbiter designs, with modifications to satisfy the specific Voyager mission requirements of long-range communications, precision navigation, solar-independent power, and science instrumentation support. A 3.7 m diameter high-gain antenna provides S and X band communications, while biasable Sun sensors in conjunction with the Canopus tracker provide the celestial reference for 3 axis stabilized attitude control. The Sun sensor may reach its design limitations at a distance of about 80 AU, which will be reached in the year 2001 for Voyager 1 and 2006 for Voyager 2. However, there is a good chance that the sensor will continue to function well beyond 80 AU. Thereafter, declining hydrazine reserves and/or power will probably cause the spacecraft to cease functioning in about 2015, when Voyagers 1 and 2 will be at heliocentric distances of 130 AU and 110 AU respectively. Communications will be maintained as long as the spacecraft continue to operate.

In August 1992 both Voyager spacecraft began detecting intense low-frequency radio emissions, which reached a peak in December before gradually fading out. It is believed that these 2-to-3 kHz emissions provide the first physical evidence of the heliopause. They are thought to be caused by powerful gusts of solar wind impacting the interstellar wind of cold gases. Calculations made with the Voyager data place the heliopause somewhere between 82 and 130 AU from the Sun.

As presently envisioned, only the four fields and particle experiments and the UV spectrometer

The scientific objectives for VIM are as follows:

- To characterize the evolution of the solar wind with distance from the Sun
- To observe and characterize the periodic reversal of the Sun's magnetic field
- To search for and observe the inner heliospheric shock front and the heliopause, the boundary zone where the influence of the solar wind terminates
- To explore the nature of particle acceleration mechanisms in the interplanetary medium
- To search for evidence of interstellar hydrogen and helium and an interstellar wind
- To search for low-energy cosmic rays
- To search for radio emissions from the Sun in an environment well removed from planetary sources
- To search for and characterize galactic sources of EUV emissions

Key Voyager Mission Statistics

Basic Data

<i>Launch Data</i>	<i>Voyager 1</i>	<i>Voyager 2</i>
Launch Date:	5 September 1977	20 August 1977
Launch Vehicle:	Titan 3E/Centaur	Titan 3E/Centaur
Launch Site:	CCAFS	CCAFS
Mission Duration:	To RTG expiration	To RTG expiration

Asymptotic Trajectory Parameters for Voyagers 1 and 2 and the Direction and Speed of the Solar System Relative to the Local Interstellar Medium in Heliocentric Ecliptic Coordinates with an Equinox of 1950.

<i>Asymptotic Trajectory</i>	<i>Voyager 1</i>	<i>Voyager 2</i>	<i>Solar System</i>
Longitude	261°	294°	252 ± 3°
Latitude	+36°	-48°	3° ± 3°
Speed (AU/yr)	3.50	3.13	26 ± 1 km/s

Mission Statistics

S/C Mass:	825 kg
Stabilization:	3-axis, Sun and star trackers or gyros, 16 hydrazine thrusters
Pointing Accuracy:	±0.1°
Pointing Knowledge:	±0.05°
Power:	3 RTG's, 475W (total power at launch), 230W (at expiration ~2015)
Science Telemetry:	0.6 kb/s nominal, 7.2 kb/s maximum
Data Storage:	Digital tape recorder, 500 Mb

Voyager Instruments

All but four of the science instruments are mounted on the scan platform or its supporting boom, and of those four the Magnetometer uses its own boom; the Planetary Radio Astronomy experiment shares an antenna with the Plasma Wave Subsystem; and the Radio Science Subsystem uses the radio beams of the high-gain antenna.

1) Ultraviolet Spectrometer (UVS) A.L. Broadfoot, PI

The UVS is a grating spectrometer that detects ultraviolet radiation in the range 400–1600 Å with 10 Å resolution. The instrument is designed to operate in two modes: airglow (1° x 0.1° FOV) and occultation (1° x 0.3° FOV). The UVS identifies elements, compounds, and processes within planetary atmospheres, and is also making fundamental contributions to ultraviolet astronomy.

2) Plasma Subsystem (PLS)

J.W. Belcher, PI

The PLS subsystem studies the properties of the very hot ionized gases that exist in interplanetary space, employing two orthogonal sensors that detect low-energy particles. Ions are measured in the energy range 10 eV–6 keV and electrons in the energy range 4 eV–6 keV.

3) Low Energy Charged Particle experiment (LECP)

S.M. Krimigis, PI

LECP consists of two solid-state detector systems mounted on a rotating platform. The two subsystems are the Low-Energy Particle Telescope (LEPT) and the Low-Energy Magnetospheric Particle Analyzer (LEMPA). Electrons are detected in the energy range 10 keV–10 MeV and nucleon ions in the range 10 keV–150 MeV.

4) Cosmic Ray Subsystem (CRS)

E.C. Stone, PI

The cosmic ray subsystem's multiple solid-state detectors measure the energy spectra and three-dimensional anisotropies of electrons and cosmic ray nuclei using three independent systems: a High-Energy Telescope (HET), a Low Energy Telescope (LET), and an Electron Telescope (TET).

5) Magnetometer (MAG)

N.F. Ness, PI.

The magnetic fields experiment consists of four magnetometers: two are low-field instruments (10^{-6} –0.5 G) mounted on a 13-m boom away from the field of the spacecraft, while the other two are high-field (5×10^{-4} –20 G) magnetometers mounted on the body of the spacecraft. All four operate in the 0–16.7 Hz range.

6) Plasma Wave Subsystem (PWS)

D.A. Gurnett, PI

The PWS covers a frequency range of 10 Hz to 56.2 kHz, either scanning over sixteen channels sequentially or sampling the entire band, and samples the behavior of plasmas in planetary magnetospheres by measuring the radio waves generated by those plasmas. It can also detect the presence of planetary lightning. The PWS incorporates a 150 Hz to 10 kHz waveform analyzer, and shares a pair of 10 m long-wire monopole antennas with the PRA instrument.

Voyager 1 & 2 Instruments Summary

	<i>Investigation</i>	<i>Range</i>	<i>Type</i>
UVS	Ultraviolet Spectrometer	500–1,700 Å	Grating
PLS	Plasma Subsystem	4 eV–6 keV	
LECP	Low-Energy Charged Particle	10–150,000 keV	Solid state
CRS	Cosmic Ray Subsystem	1–500 MeV	Solid state
MAG	Magnetometers	10 ⁻⁶ –20 G	4 instruments
PWS	Plasma Wave Subsystem	10 Hz–56.2 kHz	Scanning receiver

Project Scientist: Ed Stone, JPL, (818) 354-3407
Program Scientist: Vernon Jones, NASA/HQ, (202) 358-0885

The Wind Mission and Payload

The Wind spacecraft is scheduled at present for a 1994 launch using a Delta II expendable launch vehicle from the Eastern Space and Missile Center. The spacecraft will be placed into a 185-km circular parking orbit having an inclination of 28.7 degrees. The upper stage will be ignited at a predetermined location to boost the spacecraft into its initial orbit. The Wind spacecraft will utilize lunar swingby orbit adjustments to maintain apogee on the Earth's dayside so as to survey the upstream region to distances of 250 Earth radii during the first year to two years after launch. In this orbit, the line of apsides is held close to the Earth-Sun line throughout the year by means of lunar swingby maneuvers. Wind may then be placed in a small (160,000 km) halo orbit at the L1 libration point. In this position, it will provide optimum interplanetary measurements on a continuous basis. Wind mission trajectory goals include the following:

- Maximize dwell time in the forward extension of the geomagnetic tail
- Provide multiple passes through the bow shock region
- Minimize the total fuel expenditures
- Minimize eclipse times

To fulfill the Wind science objectives, the Wind satellite will specifically measure magnetic fields, radio and plasma waves, hot plasma composition, energetic particles, solar wind plasma, and cosmic gamma rays. The objectives of the Wind mission are as follows:

- Provide complete plasma, energetic particle and magnetic field input for magnetospheric and ionospheric studies
- Determine the magnetospheric output to interplanetary space in the upstream region
- Investigate basic plasma processes occurring in the near-Earth solar wind
- Provide baseline ecliptic plane observations to be used in heliospheric latitudes by ULYSSES

Key Wind Mission Statistics

Launch Date:	April 1994
Launch Vehicle:	Delta II 7925
Launch Site:	ETR
Mission Duration:	Three years
Operational Orbit:	Years 1-2, Double lunar swingby at 250 Earth radii Year 3, 160,000 km halo orbit at the L1 libration point
L1 Orbital Period:	6 months L1 halo
S/C Mass:	1155 kg
Stabilization:	Spin stabilized open loop control
Pointing Accuracy:	Spin axis normal to the ecliptic $\pm 1^\circ$
Pointing Knowledge:	$\pm 0.05^\circ$ to 0.25°

Power: 324 W (maximum load)
Science Telemetry: 5.56 kbps (tracking mode, real-time), 64 kbps (playback)
Data Storage: Two tape recorders for 1×10^9 bit/unit

Wind Instruments

1) Three-Dimensional Plasma Analyzer (PLASMA) R. Lin, PI

The PLASMA instrument will explore the interplanetary suprathermal particle population, identify particle input and output from the magnetosphere. The instrument will also study particle acceleration at the Sun and the transport of particles in the interplanetary medium. The PLASMA instrument contains three sensors mounted on deployed "boomlets," each with high voltage and microprocessor. The PLASMA instrument consists of three detector systems: the semiconductor detector telescopes (SST), the electron electrostatic analyzers (EESA), and the ion electrostatic analyzers (PESA). The SST measures electron and ion fluxes above ~ 20 keV. The EESA-L and -H and PESA-L and -H detectors are pairs of electrostatic analyzers with widely different geometric factors to cover the wide range of particle fluxes from ~ 3 eV to 30 keV and provide significant measurements even at the lowest flux levels likely to be encountered. In addition there is a fast particle correlator (FPC) for the measurement of the perturbation to the electron distribution function on fast time scales in wave particle interactions upstream of the Earth's bow shock, and in the interplanetary medium.

2) Energetic Particles Acceleration Composition Transport (EPACT) T. Von Roseninge, PI

The EPACT instrument will study the acceleration, elemental and isotopic composition, and transport of a wide variety of energetic particle populations, including solar flare and interplanetary shock events, anomalous and galactic cosmic rays. The high-sensitivity EPACT will measure abundances, spectra, and angular distribution of electrons from 0.2 to 10 MeV and ions from 20 KeV to 360 MeV/nucleon, and potentially make the first observations of ultra-heavy ions up to $Z = 90$ in solar flare events. EPACT contains a three-sensor subsystem in a body-mounted configuration, each with high voltage and microprocessor. The three-sensor subsystem includes the Low Energy Matrix Telescope (LEMT), two Alpha-Proton-Electron Telescopes (APE), a Supra-Thermal Energetic Particle Telescope (STEP) system, an Isotope Telescope (IT).

3) Russian Gamma Ray Spectrometer (Konus) E. Mazets, PI

The Konus instrument will perform high-resolution gamma-ray burst studies in the energy range of 10 keV–10 MeV, as well as burst with energy > 10 MeV. Konus contains dual sensors to provide full sky coverage and limited directional resolution. The dual sensors will be in a body-mounted configuration each with high voltage. Konus contains two sensors, S1 and S2, four amplitude analyzers for pulse height analysis, four time history analyzers, two high-resolution time history analyzers and a background measurement system (BM) in the Konus instruments. The two sensors are identical and interchangeable NaI scintillation crystal detectors of 200 cm^2 area and shielded by Pb-Sn. The two sensors ensure practically isotropic angular sensitivity. Konus will provide burst data to the Transient Gamma Ray Spectrometer (TGRS).

4) Magnetic Field Investigation (MFI)

R. Lepping, PI

The MFI experiment will investigate the large scale and fluctuation characteristics of the interplanetary magnetic field. The MFI detectors, with microprocessor, are mounted on a lanyard boom at 8 and 12 meters. MFI will be capable of special data analysis, compression modes, and high-time-resolution modes. MFI will also supply magnetic field information to other Wind instruments. The basic configuration of MFI consists of dual, wide range (± 0.004 nT to $\pm 65,536$ nT) triaxial fluxgate magnetometers and a microprocessor controlled data processing and control unit. Total RMS noise level of the MFI fluxgate sensors over the 0–10 Hz band does not exceed 0.006 nT, which is several orders of magnitude below the lowest recorded levels of IMF fluctuations at 1 AU and is more than adequate properly to detect and identify all magnetic field phenomena of interest to MFI. The MFI will provide near-real-time data at three measurement rates: nominally one vector per 92 seconds for key parameter data, 10.8 vectors/second for rapid data for standard analysis, and 44 vectors/second for snapshot memory data and Fast Fourier Transform data.

5) Solar Wind and Suprathermal Ion Composition Experiment (SMS)

G. Gloeckler, PI

The SMS instrument will provide the characteristics of matter entering the Earth's magnetosphere by measuring the mass, charge state, and energy distribution of solar wind suprathermal ions. It will also study physical processes going on in the Sun's atmosphere by measuring the elemental, isotopic and ionic-charge composition of solar wind ions. SMS will also study interplanetary shock acceleration and interstellar ion pickup processes by measuring the three-dimensional distribution function of H, He, C, O, Si, and Fe. The SMS instrument will measure uniquely the elemental, isotopic and ionic-charge composition of solar wind ions over the range of 0.3 to 2 keV per charge. It will also measure the differential energy spectra (and thus the densities, bulk speeds and kinetic temperatures) of all major solar wind ions, from H to Fe at solar wind speeds range from 130 km/s (Fe^{10+}) to 2400 km/s (protons), and the composition, charge state, and 3-dimensional distribution functions of suprathermal ions of energies between 0.1 to 230 keV per charge. The SMS contains three separate sensor subsystems, mounted on both appendages and the spacecraft body, each with high voltage and microprocessor. The three sensor subsystems include: the solar wind ion composition spectrometer (SWICS), the supra-thermal ion composition spectrometer (STICS), and the high-resolution solar wind ion mass spectrometer (MASS).

6) Solar Wind Experiment (SWE)

K. Ogilvie, PI

The SWE instrument is a comprehensive integrated set of sensors that will provide the high-sensitivity ion and electron thermal distribution function observations required to investigate most of the outstanding problems in the magnetosheath, bow shock, and solar wind. The instrument comprises of two Vector Electron and Ion Spectrometer (VEIS) subsystems, two Faraday cup subsystems, and a single Strahl sensor. The VEIS will measure the 3-D distribution of ions and electrons from 10 eV to 22 keV for plasma having mach numbers less than 1 by using 6 cylindrical electrostatic analyzers, which are in sets of 3 with each pair directed orthogonally. The Faraday cup will measure the bulk properties of the proton population from 100 eV to 8 keV

in the solar wind. The Strahl sensor, a single wide angle toroidal electrostatic analyzer with a multi-anode channel plate sensor, will make electron velocity distribution and pitch angle measurements from 5 eV to 5 keV as the $\pm 30^\circ$ solid angle passes through the magnetic field.

7) Transient Gamma Ray Spectrometer (TGRS)
B. Teegarden, PI

The TGRS instrument will conduct high-resolution observations of transient gamma ray burst and make the first high-resolution spectroscopic survey of cosmic gamma-ray transients with fine time resolution and a wide field of view for energies from 15 keV to 10 MeV. The TGRS will also be used to study solar flares and solar coronal processes and to search for a diffuse 511 keV positron-electron annihilation radiation background. The TGRS will use an occulter to modulate the signal. The TGRS components will use a body-mounted configuration, each with high voltage and microprocessor. Periodic decontamination for the 2-stage passive cooler may be required. The inner stage operating temperature will be on the order of 85°K.

8) Radio and Plasma Wave Experiment (WAVES)
J.-L. Bougeret, PI

The WAVES experiment will provide comprehensive measurements of radio and plasma waves in the solar wind upstream of Earth and in several magnetospheric regions over a wide frequency range of DC to 14 MHz. Data from WAVES in coordination with other instruments on Wind and other ISTP spacecraft will be used to study kinetic process in the solar wind, understand the interactions between interplanetary plasma and solar transient phenomena, study the heat flux and anisotropies at plasma boundaries and monitor the electron density and temperature of the solar wind near the Earth, as well as upstream waves. The WAVES instrument includes five major subsystems: a fast Fourier transform receiver (FFT: DC to 10 kHz), a broadband multichannel analyzer (TNR) principally devoted to the study of thermal electron noise (4 kHz to 256 kHz), two dual radio receivers covering the 20 kHz to 16 MHz band (RAD1 and RAD2), and a time-domain waveform sampler (TDS) (sampling to 120,000 samples/s).

Wind Instruments Summary

	<i>Investigation</i>	<i>Range</i>	<i>Type</i>
PLASMA	Three-Dimensional Plasma Analyzer	3 eV–30 keV	EESA, PESA, SST
EPACT	Energetic Particles Acceleration, Composition, and Transport	20 keV– 360 MeV/nucleon	LEMT APE IT
Konus	Gamma Ray Spectrometer	10 keV–10 MeV	NaI scintillation crystal detectors
MFI	Magnetic Fields Investigation	0.08–65,536 nT	fluxgate magnetometer
SMS	Solar Wind and Suprathermal Ion Composition	0.5–30 keV/Q 0.5–11.6 keV/Q 8–226 keV/Q	SWICS MASS STICS
SWE	Solar Wind Experiment	5 eV–5 keV 10 eV–22 keV 100 eV–8 keV	Strahl detector VEIS Faraday cup
TGRS	Transient Gamma Ray Spectrometer	15 keV–8.2 MeV	N-type germanium crystal detector
WAVES	Radio/Plasma Wave Experiment	DC–14 MHz	TDS, FFT, TNR, RAD1/2

Project Scientist: Keith Ogilvie, GSFC, (301) 286-5904
 Program Scientist: Elden Whipple, NASA/HQ, (202) 358-0888

The Yohkoh Mission and Payload

The Yohkoh mission is a Japanese program designed to answer the many questions in solar flare physics that were raised by the highly successful Hinotori and SMM missions. The mission includes the United States and the United Kingdom as cooperating partners. The Japanese Institute of Space and Astronautical Science (ISAS) provides overall program management, the launch vehicle, the spacecraft, and two science instruments—a Hard X-Ray Telescope (one of two primary mission instruments) and a Wide Band Spectrometer. NASA, in collaboration with ISAS, provides the other primary mission instrument, the Soft X-Ray Telescope, as well as tracking support by the Deep Space Network (DSN). The U.K., with Japan, provides a Bragg Crystal Spectrometer.

No previous solar mission has flown such a potent combination of hard and soft x-ray imaging and spectroscopic instruments, operating over such a wide energy band, and with adequate dynamic range and time resolution to study even the brightest flares. Together, these instruments allow studies of the pre-flare coronal structures immediately prior to energetic flares, the physical processes that are responsible for energy release, the nature of the particle acceleration processes that occur during the flare impulsive phase, and the means by which energy is transported away from the primary release site to other parts of the solar atmosphere.

The primary science objectives of the Yohkoh mission are as follows:

- To obtain, for the first time, simultaneous images of solar flares with high resolution in space and time in both hard and soft x rays, in order to observe the full morphology of the flare precisely enough to reveal the underlying physical processes
- To image the solar corona in soft x rays, with high resolution in space and time, to reveal properties of the global coronal magnetic fields and inner solar wind
- To measure variations in photospheric brightness, with modest spatial resolution, for studies of solar irradiance and global oscillations

Key Yohkoh Mission Statistics:

Launch Date:	30 August 1991
Launch Vehicle:	M-3SII-6
Launch Site:	Kagoshima Space Center
Orbit Apogee:	770 km
Perigee:	520 km
Inclination:	31°
Period:	97 mins
S/C Mass:	390 kg
Power:	6 solar panels, 560 watts max.; two 19 ampere-hour NiCd cells
Stabilization:	3-axis; control moment gyro with momentum wheel
Pointing Accuracy:	3 arc minutes (P-P)
Pointing Knowledge:	1 arc second (P-P)
Science Telemetry:	1, 4, 32, or 262 kb/s
Data Storage:	Bubble memory, 80 Mb

Yohkoh Instruments

1) Soft X-ray Telescope (SXT)

T. Hirayama, Principal Investigator (PI)
L. Acton, PI

The SXT uses grazing incidence optics to form direct images of the Sun on a CCD detector. The telescope's Nariai-Werner design differs from the more commonly used Wolter Type 1 in that both mirror segments have been made hyperbolic in order to gain better off-axis performance at the expense of a slight loss of on-axis resolution. The optical system includes an entrance aperture filter, the x-ray mirror, a filter wheel assembly, a rotating shutter, and the CCD camera. A coaxially mounted objective lens assembly for aspect determination allows images to be made in visible light on the same CCD detector that is used to form the soft x-ray images. The CCD is cooled to -20°C in order to reduce the effect of dark spikes. Angular resolution is better than 4 arc sec, and time resolution is 0.5 seconds.

2) Hard X-ray Telescope (HXT)

K. Makishima, PI

The HXT imager consists of 64 photomultiplier tubes, each with its own thallium-doped sodium iodide (NaI(Tl)) scintillation crystal, using 64 independent collimators in a "push-pull" Fourier transform system which yields a set of 32 visibility functions. Angular resolution is 5 arc sec, and time resolution is 0.5 seconds.

3) Wide-Band Spectrometer (WBS)

J. Nishimura, PI

The WBS consists of four subsystems: a soft x-ray spectrometer (SXS), a hard x-ray spectrometer (HXS), a gamma ray spectrometer (GRS), and a radiation belt monitor (RBM). The SXS, HXS, and GRS are used to observe solar flares, while the RBM serves as an alarm for the South Atlantic Anomaly passage. Time resolution is less than 1 second.

4) Bragg Crystal Spectrometer (BCS)

E. Hiei, PI
J. Culhane, PI

The primary function of the BCS is to study plasma heating and dynamics during the impulsive phase of solar flares. The wavelength range is determined by bending the crystal. There are no moving parts; the crystals are set before launch. BCS uses four crystals to cover x-ray line groups of diagnostic importance, indicating the progressive heating of plasma before and during the impulsive phase and certain transient effects. The groups are near the resonance lines S XV (5.0160–5.1143), Ca XIX (3.1613–3.1912), Fe XXV (1.8298–1.8942), and Fe XXVI (1.7636–1.8044). Spectral resolution is 1/3,000–1/7,000; time resolution is 0.125 seconds.

Yohkoh Instruments Summary

	<i>Investigation</i>	<i>Range</i>	<i>Type</i>
SXT	Soft X-Ray Telescope	0.4-4 keV	CCD
HXT	Hard X-Ray Telescope	10-100 keV	Scintillation counters
WBS	Wide-Band Spectrometer	2-10 ⁵ keV	Scintillation counters and Proportional counters
BCS	Bragg Crystal Spectrometer	2.5-6.9 keV	Bent crystal detector

Project Scientist (USA): John Davis, MSFC, (205) 544-7600
Project Scientist (Japan): Yutaka Uchida, TAO, 81-3-5800-6885
Program Scientist (USA): Bill Wagner, NASA/HQ, (202) 358-0911
Program Manager (Japan): Yoshiaki Ogawara, ISAS, 81-427-51-3951

**Principal Investigators
Listed Alphabetically**

PI	Institute	E-mail address	Mission	Instrument
Acton, L.	Montana State U., USA	SAG::ACTON	Yohkoh	SXT
Afonin, V.	IKI AN, Russia		APEX	KM-10
Afonin, V.	IKI, Russia		Mars-94	MARIPROB
Afonin, V.É	IKI, Russia		Interball	KM-7
Amata, E.	CNR, IFSI, Italy	amata@hp.ifs.i.fra.cnr.it	Interball	OPERA
Anderson, J. D.	U. of Iowa, USA		Galileo	RS-CM
Arshinkov, I.	SDS Lab, Bulgaria		Interball	IMAP-3
Arshinkov, I.	SDS Lab, Bulgaria		Interball	IMAP-2
Balogh, A.	ICST, UK	postmaster@uk.ac.ic.ph.spva	Cluster	FGM
Balogh, A.	ICST, UK	postmaster@uk.ac.ic.ph.spva	Ulysses	VHM/FGM
Barnes, A.	Ames Research Center, USA	barnes@windec.arc.nasa.gov	Pioneer	PA
Belcher, J. W.	MIT, USA	MITCCD::JWB	Voyager	PLS
Belian, R.	LANL, USA	BSSDP1::BELIAN	MPA/SOPA	SOPA
Belikova, A.	IKI, Russia		Interball	IFPE
Belikova, A.É	IKI, Russia		Interball	ADS
Belton, M. J. S.	NOAO, USA		Galileo	SSI
Bertaux, J. L.	SA, Varières-le-Buisson, France		SOHO	SWAN
Berthelier, J. J.	CRP L'Environ./CNET, France	CRPEIS::BERTHELIER	Interball	HYPER-BOLOID
Berthelier, J. J.	CRP L'Environ./CNET, France	CRPEIS::BERTHELIER	Mars-94	DIMIO
Bezrukhikh, V.	IKI, Russia		Interball	ALFA-3
Bezrukhikh, V.	IKI, Russia		Interball	ALPHA-3
Bird, M. K.	U. of Bonn, Germany	MBIRD@ASTRO.UNI-BONN.DE	Ulysses	SCE
Blake, B.	Aerospace Corporation, USA	5418::BLAKE	Polar	CEPPAD
Borodkova, N.	IKI, Russia		Interball	ELECTRON
Bougeret, J.	Observatoire de Paris-Meudon, France	MEUDON::BOUGERET	Wind	WAVES
Broadfoot, A. L.	U. of Arizona, USA	broadfoot@looney.lpl.arizona.edu	Voyager	UVS
Brueckner, G.	NRL, USA	11343::BRUECKNER	SOHO	LASCO
Brueckner, G. E.	NRL, USA	11343::BRUECKNER	UARS	SUSIM
Buechner, J.	Max Planck Institut, Germany	jb@mpe.fta-berlin.de	Interball	IFPE
Carlson, C.	UC, Berkeley, USA	UCBSP::MARSHA	FAST	EESA
Carlson, C.	UC, Berkeley, USA	UCBSP::MARSHA	FAST	EFPE
Carlson, C.	UC, Berkeley, USA	UCBSP::MARSHA	FAST	MAG
Carlson, C.	UC, Berkeley, USA	UCBSP::MARSHA	FAST	TEAMS
Carlson, R. W.	CalTech, USA		Galileo	NIMS
Charikov, Yu	LFTI, Leningrad, Russia		Coronas	IRIS
Chmirev, V.	IZMIRAN, Russia		APEX	DEP-2E
Chmirev, V.	IZMIRAN, Russia		APEX	DEP-2R
Chmirev, V.	IZMIRAN, Russia		APEX	SGR-5
Chmirev, V.	IZMIRAN, Russia		APEX	MNCH
Chmyrev, V.	IZMIRAN, Russia		Interball	IESP-2
Chobanu, M	IKI, Romania		APEX	SGR-7
Cogger, L. L.	U. of Calgary, Canada	cogger@phys.ucalgary.ca	Interball	UVAI
Cornilleau-Wehrlin, N.	CRP L'Environ./CNET, France	RPEVZB::CORNILLEAU	Cluster	STAFF
Culhane, J.	U. College London, UK	JLC@a.mssl.ucl.ac.uk	Yohkoh	BGS
Dachev, Tc.	IKI BAN, Bulgaria		APEX	DANI
Dachev, Tc.	IKI BAN, Bulgaria		APEX	DAN-S
Decreau, P. M. E.	LPCE/CNRS, France	pdecreau@cnsr-orleans.fr	Cluster	WHISPER
Delaboudinière, J. P.	LAS, France		SOHO	EIT
Doke, T.	Waseda U., Japan	AMES::"tdoke@jpnwasod.BITNET"	Geotail	HEP
Dokukin, V.	IZMIRAN, Russia		APEX	UEM-2
Dokukin, V.	IZMIRAN, Russia		APEX	UPM
Dokvicia, V	IZMIRAN, Russia		APEX	DANI
Farnik, F.	Anstronomy Inst., Czechoslovakia		Interball	RF-15-I
Fedorov, A.	IKI, Russia		Interball	MONITOR-3
Fedorov, A.	IKI, Russia		Interball	VDP
Fillus, R. W.	U. Southern California, USA	walker%cass.span@Sdsc.edu	Pioneer	TRF
Fischer, H. M.	Universität Kiel, Germany		Galileo	EPI
Fisher, L.	Astronomy Inst., Czechislovakia		Interball	AKR-X
Fisher, R.	GSFC, USA	SOLAR::RFISHER	Spartan	WLC
Fisher, S.	Anstronomy Inst, Czechoslovakia		Interball	SKA-2

Fisher, S.	Praha Univ., Czechia		APEX	PEAS
Fisher, S.	Praha Univ., Czechia		APEX	MPS
Fisher, S.	Praha Univ., Czechia		APEX	SEA
Fornichev, V.			Coronas	SORS
Frank, L.	U. of Iowa, USA	IOWASP::FRANK	Geotail	CPI
Frank, L.	U. of Iowa, USA	IOWASP::FRANK	Polar	VIS
Frank, L. A.	U. of Iowa, USA	IOWASP::FRANK	Galileo	PLS
Frank, L. A.	U. of Iowa, USA	IOWASP::FRANK	IMP-8	IOE
Fritz, T.	Boston U., USA	ESSDP2::FRITZ	Polar	CAMMICE
Frohlich, C.	PMOD-WRC, Switzerland	cfrohlich@ezrz1.vmsmail.ethz.ch	SOHO	VIRGO
Fukunishi, H.	Tohoku U, Japan		Akebono	MGF
Gabriel, A.	LAS, France		SOHO	GOLF
Galperin, Yu. I.	IKI, Russia		Interball	RON
Galperin, Yu. I.	IKI, Russia		Interball	UVAI
Garcia, H.	SEL/NOAA, USA		GOES	SEM/XRS
Garrard, T. L.	CalTech, USA	TLG@CITSRL.srl.CALTECH.EDU	Galileo	HIC
Geiss, J.	U. of Bern, Germany	U21G@CBEEDA3T.BITNET	Ulysses	SWICS
Gloeckler, G.	U. of Maryland, USA	UMDSP::GLOECKLER	Ulysses	SWICS
Gloeckler, G.	U. of Maryland, USA	UMDSP::GLOECKLER	Wind	SMS
Goljavin, A.	IZMIRAN, Russia		Interball	NVK-ONCH
Gosling, J.	LANL, USA	ESSDP1::073500	IMP-8	LAP
Gosling, S.	LANL, USA	ESSDP1::073500	ISEE-3	BAH
Greenstadt, G.	TRW, USA		ISEE-3	SCH
Grigorjeva, V.	Astronomy Inst. of Moscow, Russia		Interball	AKR-X
Gringauz, K.	IKI AN, Russia		APEX	PEAS
GrŸn, E	Max-Planck-Institut, Germany		Galileo	DDS
Grun, E.	MPI, Heidelberg, Germany		Ulysses	DUST
Gumett, D.	U. of Iowa, USA	gumett@iowave.physics.uiowa.edu	Polar	PWI
Gumett, D. A.	U. of Iowa, USA	gumett@iowave.physics.uiowa.edu	Cluster	WBD
Gumett, D. A.	U. of Iowa, USA	gumett@iowave.physics.uiowa.edu	Galileo	PWS
Gumett, D. A.	U. of Iowa, USA	gumett@iowave.physics.uiowa.edu	Voyager	PWS
Gustafsson, G.	SISP, Sweden	SISP	Cluster	EFW
Hanash, J.	SRC, Poland		Interball	POLRAD
Harrison, R.	RAL, UK	19592::RAH	SOHO	CDS
Hayakawa, H.	ISAS, Japan	HAYAKAWA@GTL.ISAS.AC.JP	Akebono	EFD
Hays, P. B.	U. of Michigan, USA	hays@sprlj.sprl.umich.edu	UARS	HRDI
Hiei, E.	Meisei U.	HIEI@SPOT.MTK.NAO.AC.JP	Yohkoh	BCS
Hirayama, T.			Yohkoh	SXT
Hord, C. W.	LASP, U. Colorado, USA		Galileo	UVS
Hovestadt, D.	Max Planck Institut, Germany		ISEE-3	HOH
Hovestadt, D.	MPE, Garching, Germany		SOHO	CELIAS
Howard, H. T.	Stanford U., USA		Galileo	RS-RP
Hurley, K.	U. of California, Berkeley, USA	UCBSP::KHURLEY	Ulysses	GBS
Hynds, R.			ISEE-3	DFH
Imhof, W.	Lockheed, USA	IMHOF@LOCKHD.dnet.nasa.gov	Polar	PIXIE
Ipevich, F.	U. of Maryland, USA	IPAVICH@ampte.dnet.nasa.gov	IMP-8	MAE
Istomin, V.	IKI AN, Russia		APEX	NAM-5
Jimenez, R.	Cuba		Interball	CORALL
Johnstone, A.	MSSL, UK	adj@mssl.dnet.nasa.gov	Mars-94	FONEMA
Johnstone, A. D.	MSSL, UK	adj@mssl.dnet.nasa.gov	Cluster	PEACE
Juchnievicz, J.	Polish Academy of Sci.s, Poland	romanw@camk.edu.pl	Interball	ADS
Judge, D. L.	U. Southern California, USA	djudge@lism.usc.edu	Pioneer	UV
Kazachevskaya, T.	IPG, Moscow, Russia		Coronas	SUVR0
Kepler, E.	Max Planck Institut, Germany	ECD1::LINMPI::KEPPLER@brunet.span.nasa.gov	Ulysses	EPAC/GAS
Kimura, I.	Kyoto U, Japan	KIMURA@KUEE.KYOTO-U.AC.JP	Akebono	VLF
Kivelson, M. G.	UCLA, USA	mkivelson@igpp.ucla.edu	Galileo	MAG
Klimov, S.	IKI, Russia		Interball	ASPI
Klimov, S.	IKI, Russia		Mars-94	ELISMA
Kloss, Z.	CKI PAN, Poland		APEX	VCH-VK
Kohl, J.	SAO, USA	KOHL@CFA4.bitnet	Spartan	UVCS
Kohl, J. L.	SAO, USA	KOHL@CFA4.bitnet	SOHO	UVCS

Kokubun, S.	Nagoya U., Japan	41920::KOKUBUN	Geotail	MGF
Koleva, R.	STIL, Bulgaria		Interball	AMEI-2
Kovrazhkin, R. È	Space Research Inst., Russia	rkovrazh@esoc1.BITNET	Interball	SKA-3
Kovrazhkin, R. A.	Space Research Inst., Russia	rkovrazh@esoc1.BITNET	Interball	ION
Krimigia, S. M.	APL, USA	APLSP::KRIMIGIS	IMP-8	APP
Krimigia, S. M.	APL, USA	APLSP::KRIMIGIS	Voyager	LECP
Kudela, K.	IBP, Czechoslovakia		Interball	DOK-2A
Kudela, K.	IBP, Czechoslovakia		Interball	DOK-2X
Kudela, K.	GFT CAN, Czechiya		APEX	DOK-A-S
Kunow, H.	Universitaet Kiel, Germany	HKUNOW@SOLAR.bitnet	SOHO	COSTEP
Kuzmin, A.	IKI, Russia		Interball	SKA-3
Kuzmin, A.	IKI, Russia		Interball	UPSIPS
Kuznetzov, V.			Coronas	SCR
Lanzerotti, L. J.	Bell Laboratories, USA	ljl@physics.att.com	Galileo	LRD
Lanzerotti, L.	Bell Laboratories, USA	ljl@physics.att.com	Ulysses	HI-SCALE
Lazarus, A.	MIT, USA	ajl@space.mit.edu	IMP-8	MAP
Lefeuve, F.	LPCE, France	CNESTA::LEFEUVRE	Interball	MEMO
Lepping, R.	GSFC, USA	U5RPL@LEPVAX.dnet.nasa.gov	IMP-8	GNF
Lepping, R.	GSFC, USA	U5RPL@LEPVAX.dnet.nasa.gov	Wind	MFI
Likin, O.	IKI, Russia		Interball	RF-15-I
Lin, R.	U. of California, Berkeley, USA	UCBSP::LIN	Wind	PLASMA
Lishin, I.	IRE, Russia		Interball	POLRAD
Lomovsky, A.	IPG, Moscow, Russia		Coronas	VUSS
Lundin, R.	SISP, Sweden	LUNDIN@plafys.dnet.nasa.gov	Mars-94	ASPERA-S
Lutsenko, V. È	IKI, Russia		Interball	DOK-2A
Lutsenko, V. È	IKI, Russia		Interball	DOK-2X
MacKenna-Lawlor, S.	St. Patrick College, Ireland		Mars-94	SLED-2
Makishima, K.			Yohkoh	HXT
Mason, G.	U. of Maryland, USA	UMDSP::MASON	SAMPEX	HILT
Mason, G.	U. of Maryland, USA	UMDSP::MASON	SAMPEX	LEICA
Mason, G.	U. of Maryland, USA	UMDSP::MASON	SAMPEX	MAST
Mason, G.	U. of Maryland, USA	UMDSP::MASON	SAMPEX	PET
Matsumoto, H.	Kyoto U., Japan	matsumoto@kurasc.kyoto-u.ac.jp	Geotail	PWI
Mazets, E.	LETI, Leningrad, Russia		Coronas	HELIKON
Mazets, E.			Wind	Konus
McComas, D.	LANL, USA	ESSDP1::MCCOMAS	MPA/SOPA	MPA
McDonald, F. B.	U. of Maryland, USA	sm27@umail.umd.edu	Pioneer	CRT
McGuire, R.	GSFC, USA	NCF::MCGUIRE	IMP-8	GME
Meyer, P.	U. of Chicago, USA	meyer@odysseus.uchicago.edu	ISEE-3	MEH
Milchailov, Yu.	IZMIRAN, Russia		APEX	NVK-ONCH
Mogilevsky, M.	IKI, Russia		Interball	POLRAD
Mogilevsky, M. È	IKI, Russia		Interball	MEMO
Molchanov, O.	Inst. of Earth Physics, Russia		Interball	NVK-ONCH
Moore, T.	MSFC, USA	SSL::MOORET	Polar	TIDE
Morozova, E. È	IKI, Russia		Interball	SKA-2
Mozer, F.	U. of California, Berkeley, USA	MARSHA%UCBSSL@BERKELEY.EDU	Polar	EFI
Mukai, T.	ISAS, Japan	mukai@gtl.isas.ac.jp	Akebono	LEP
Mukai, T.	ISAS, Japan	mukai@gtl.isas.ac.jp	Geotail	LEP
Muliarchik, T.	IKI, Russia		Interball	HYPER-BOLOID
Nemechek, Z.	Karlov U., Czechoslovakia		Interball	MONITOR-3
Nemechek, Z.	Karlov U., Czechoslovakia		Interball	VDP
Ness, N. F.	U. of Delaware, USA	BARTOL::NFNESS	Voyager	MAG
Niemann, H. B.	GSFC, USA	HNIEMANN@gsfcmail.nasa.gov	Galileo	GPMS
Nishimura, J.			Yohkoh	WBS
Nozdrachev, M.	IKI, Russia		Interball	MIF-M
Nozdrachev, M. È	IKI, Russia		Interball	OPERA
Ogilvie, K.	GSFC, USA	LEPVAX::U2KWO	ISEE-3	OGH
Ogilvie, K.	GSFC, USA	LEPVAX::U2KWO	Wind	SWE
Oguti, T.	Nagoya U, Japan		Akebono	ATV
Oya, H.	Tohoku U, Japan	41759::OYA	Akebono	PWS
Oyama, K.	ISAS, Japan		Akebono	TED

Palazov, K.	IKI BAN, Bulgaria		Interball	UFSIPS
Parks, G.	U. of Washington, USA	parka@geophys.washington.edu	Polar	UVI
Paschmann, G.	Max Planck Institut, Germany	28821::GEP	Cluster	EDI
Petkov, N.	IKI BAN, Russia		APEX	FS
Petkov, N.	IKI BAN, Bulgaria		APEX	FDS
Phillips, J.	LANL, USA	ESSDP1::102657	Ulysses	SWOOPS
Pissarenko, N.É	IKI, Russia		Interball	PROMICS-3
Pissarenko, N.É	IKI, Russia		Interball	PROMICS-3
Pulinets, S.	IZMIRAN, Moscow, Russia		Coronas	SORS
Pulinets, S.	IZMIRAN, Russia		APEX	VCH-VK
Ragent, B.	GSFC, USA		Galileo	NEP
Reidler, W.	Space Research Inst., Austria		Mars-94	MAREMF
Reine, H.	CESR, France	REME@CNESTA.dnet.nasa.gov	Cluster	CIS
Riedler, W.	Inst. of Weltraumforschung, Austria		Cluster	ASPOC
Riedler, W.	Space Research Inst., Austria		Interball	RON
Roche, A. E.	Lockheed, USA		UARS	CLAES
Romanov, S.	IKI, Russia		Interball	MIF-M
Romanov, S.	IKI, Russia		Interball	PRAM
Romanov, S.	IKI, Russia		Interball	ASPI
Rothkachtl, H.	CKI PAN, Poland		APEX	PRS-2-C
Rottman, G. J.	NCAR, USA	rottman@hao.ucar.edu	UARS	SOLSTICE
Russell, C.	UCLA, USA	crussell@igpp.ucla.edu	Polar	MFE
Russell, E. E.	Santa Barbara Res. Ctr, USA		Galileo	PPR
Russell, J. M.	Langley Research Center, USA	JMRUSSELL@NASAMAIL.NASA.gov	UARS	HALOE
Ruzhin, Yu.	IZMIRAN, Russia		APEX	UF-3K
Rybyeva, N.	IKI, Russia		Interball	PRAM
Sandahl, I.	SISP, Sweden	ingrid@ifr.se	Interball	PROMICS-3
Sandahl, I.	SISP, Sweden	ingrid@ifr.se	Interball	PROMICS-3
Sauer, H.	SEL/NOAA, USA		GOES	SEM/EPS
Sauer, K.	Zentr. Inst. Astrophis., Germany		APEX	ZL-A-S
Sauvaud, J. A.	CESR, France	SAUVAUD@CNESTA.span.nasa.gov	Interball	ELECTRON
Sauvaud, J. A.	CESR, France	SAUVAUD@CNESTA.span.nasa.gov	Interball	ION
Savin, S.	IKI, Russia		Interball	OPERA
Scherrer, P. H.	Stanford U., USA	pscherrer@solar.stanford.edu	SOHO	MDI
Schmidt, R.	ESA/ESTEC, Netherland	RSCHMIDT@ESTCS1.span.nasa.gov	Interball	RON
Scudder, J.	U. of Iowa, USA	U2JDS@LEPVAX.span.nasa.gov	Polar	HYDRA
Seiff, A.	San Jose State U., USA		Galileo	ASI
Shafrankova, Ya.	Karlov U., Czechoslovakia		Interball	MONITOR-3
Shelley, E.	Lockheed, USA	shelley@lockhd.span.nasa.gov	Polar	TIMAS
Shepherd, G. G.	York U., Canada	gordon@windic.yorku.ca	UARS	WINDII
Shmilauer, Ja.	GFI CAN, Czechiya		APEX	KM-10
Shmilauer, Ja.	GFI CAN, Czechiya		APEX	NAM-5
Shmilauer, Ja.	GFI CAN, Czechiya		APEX	KM-12
Shutte, N. M.	IKI AN, Russia		APEX	PEAS
Silvester, J.É	Space Research Center, Poland		Interball	RF-15-1
Simpson, J. A.	U. of Chicago, USA	simpson@odysseus.uchicago.edu	IMP-8	CHE
Simpson, J. A.	U. of Chicago, USA	simpson@odysseus.uchicago.edu	Pioneer	CPI
Simpson, J. A.	U. of Chicago, USA	simpson@odysseus.uchicago.edu	Ulysses	COSPIN
Singer, H.	SEL/NOAA, USA	hsinger@selvax.sel.bldrdoc.gov	GOES	SEM/MAG
Skalsky, A.É	IKI, Russia		Interball	IFPE
Skalsky, A.	IKI, Russia		Interball	ADS
Smilauer, J.	Astronomy Inst., Czechoslovakia		Interball	KM-7
Smirnov, V.	IKI, Russia		Interball	AMEI-2
Smirnov, V.	IKI, Russia		Interball	SKA-1
Smith, E. J.	Jet Propulsion Laboratory, USA	ESMITH@JPLSP.span.nasa.gov	ISEE-3	SMH
Smith, E. J.	Jet Propulsion Laboratory, USA	ESMITH@JPLSP.span.nasa.gov	Pioneer	HVM
Sobelman, I.	FIAN, Moscow, Russia		Coronas	RES-C
Sobelman, I.	FIAN, Moscow, Russia		Coronas	TEREK
Sommer, M.	Max-Planck-Institut, Germany		Ulysses	GBS
Sromovsky, L. A.	U. Wisconsin-Madison, USA		Galileo	NFR
Stanev, G.	CLKI, Bulgaria		Interball	IESP-2
Stanev, G.	IKI BAN, Russia		APEX	DEP-2E
Stanev, G.	IKI BAN, Russia		APEX	DEP-2R

Steinberg, J.	MIT, USA	jts@space.mit.edu	ISEE-3	SBH
Stiazhkin, V.	IZMIRAN, Russia		Interball	IMAP-2
Stiazhkin, V.	IZMIRAN, Russia		Interball	IMAP-3
Stone, E.	CalTech, USA	ecs@citsrl.srl.caltech.edu	ACE	CRIS
Stone, E.	CalTech, USA	ecs@citsrl.srl.caltech.edu	ACE	EPAM
Stone, E.	CalTech, USA	ecs@citsrl.srl.caltech.edu	ACE	MAG
Stone, E.	CalTech, USA	ecs@citsrl.srl.caltech.edu	ACE	SEPICA
Stone, E.	CalTech, USA	ecs@citsrl.srl.caltech.edu	ACE	SIS
Stone, E.	CalTech, USA	ecs@citsrl.srl.caltech.edu	ACE	SWEPAM
Stone, E.	CalTech, USA	ecs@citsrl.srl.caltech.edu	ACE	SWICS
Stone, E.	CalTech, USA	ecs@citsrl.srl.caltech.edu	ACE	SWIMS
Stone, E.	CalTech, USA	ecs@citsrl.srl.caltech.edu	ACE	ULEIS
Stone, E. C.	CalTech, USA	ecs@citsrl.srl.caltech.edu	IMP-8	CAI
Stone, E. C.	CalTech, USA	ecs@citsrl.srl.caltech.edu	Voyager	CRS
Stone, R. G.	GSFC, USA	U2RGS@LEPVAX.span.nasa.gov	Ulysses	COSPIN
Sylwester, J.	AI, Prague, CBK, Wroclaw		Coronas	DIOGENES
Taylor, F. W.	Oxford U., UK		UARS	ISAMS
Teegarden, B.	GSFC, USA	TEEGARDEN@LHEAVX.span.nasa.gov	ISEE-3	STH
Teegarden, B.	GSFC, USA	TEEGARDEN@LHEAVX.span.nasa.gov	Wind	TGRS
Teltcov, M.	NIJAF MGU, Russia		APEX	PEAS
Torsti, J.	U. of Turku, Finland	21905::KONTU::TORSTI@brunet.span.nasa.gov	SOHO	ERNE
Triska, P.	GFI CAN, Czechiya		APEX	KEM-1
Triska, P.	Geophysics Inst., Czechoslovakia		Interball	C2-A
Triska, P.	Geophysics Inst., Czechoslovakia		Interball	C2-X
Tsuruda, K.	ISAS, Japan	BTSURUTANI@JPLSP.span.nasa.gov	Geotail	EFD
Vaisberg, O.	IKI, Russia		Interball	SKA-1
Vaisberg, O.É	IKI, Russia		Interball	ELECTRON
Van Allen, J. A.	U. of Iowa, USA	VANALLEN@IOWASP.span.nasa.gov	Pioneer	GTT
Voita, Ya.	Geophysics Inst., Czechoslovakia		Interball	C2-A
Voita, Ya.	Geophysics Inst., Czechoslovakia		Interball	C2-X
von Rosenvinge, T.	GSFC, USA	VONROSEN@NSSDCA.span.nasa.gov	ISEE-3	TYH
von Rosenvinge, T.	GSFC, USA	VONROSEN@NSSDCA.span.nasa.gov	Wind	EPACT
von Zahn, U.	U. of Bonn, Germany		Galileo	HAD
Waters, J. W.	Jet Propulsion Lab, USA		UARS	MLS
Whalen, B.	NRC, Canada	WAM@HIASMS.span.nasa.gov	Akebono	SMS
Wilhelm, K.	MPAE, Germany	NSP::WILHELM@LINMPI.span.nasa.gov	SOHO	SUMER
Wilken, B.	Max Planck Institut, Germany	ECD1::LINMPI::WILKEN@brunet.span.nasa.gov	Cluster	RAPID
Williams, D.	APL, USA	APLSP::WILLIAMS	Geotail	EPIC
Williams, D. J.	APL, USA	APLSP::WILLIAMS	Galileo	EPD
Williams, D. J.	APL, USA	APLSP::WILLIAMS	IMP-8	GWP
Winningham, J. D.	Southwest Research Inst., USA	david@dews1.space.swri.edu	UARS	PEM
Woolliscroft, L. J. C.	U. of Sheffield, UK	LJCW@RLVK.span.nasa.gov	Cluster	DWP
Yermolaev, Yu.	Space Research Inst., Russia	LZELENYI@ESOC1.bitnet	Interball	CORALL
Zastenker, G.	IKI, Russia		Interball	VDP
Zhitnik, I.	FIAN, Moscow, Russia		Coronas	RES-C
Zhitnik, I.	FIAN, Moscow, Russia		Coronas	TEREK
Zhugzhda, Y.	IZMIRAN, Moscow, Russia		Coronas	DIFOS



**Principal Investigators
Listed by Mission**



Mission	Instrument	PI	Institute	E-mail address
ACE	CRIS	Stone, E	CalTech, USA	ecs@citsrl.srl.caltech.edu
ACE	EPAM	Stone, E	CalTech, USA	ecs@citsrl.srl.caltech.edu
ACE	MAG	Stone, E	CalTech, USA	ecs@citsrl.srl.caltech.edu
ACE	SEPICA	Stone, E	CalTech, USA	ecs@citsrl.srl.caltech.edu
ACE	SIS	Stone, E	CalTech, USA	ecs@citsrl.srl.caltech.edu
ACE	SWEPAM	Stone, E	CalTech, USA	ecs@citsrl.srl.caltech.edu
ACE	SWICS	Stone, E	CalTech, USA	ecs@citsrl.srl.caltech.edu
ACE	SWIMS	Stone, E	CalTech, USA	ecs@citsrl.srl.caltech.edu
ACE	ULEIS	Stone, E	CalTech, USA	ecs@citsrl.srl.caltech.edu
Akebono	ATV	Oguti, T.	Nagoya U, Japan	
Akebono	EFD	Hayakawa, H.	ISAS, Japan	HAYAKAWA@GTL.ISAS.AC.JP
Akebono	LEP	Mukai, T.	ISAS, Japan	mukai@gtl.isas.ac.jp
Akebono	MGF	Fukunishi, H.	Tohoku U, Japan	
Akebono	PWS	Oya, H.	Tohoku U, Japan	41759::OYA
Akebono	SMS	Whalen, B.	NRC, Canada	WAM@HIASMS.span.nasa.gov
Akebono	TED	Oyama, K.	ISAS, Japan	
Akebono	VLF	Kimura, I.	Kyoto U, Japan	KIMURA@KUEE.KYOTO-U.AC.JP
APEX	UEM-2	Dokukin, V.	IZMIRAN, Russia	
APEX	UPM	Dokukin, V.	IZMIRAN, Russia	
APEX	PEAS	Gringauz, K.	IKI AN, Russia	
APEX	PEAS	Shutte, N. M.	IKI AN, Russia	
APEX	PEAS	Teltcov, M.	NIJAF MGU, Russia	
APEX	PEAS	Fisher, S.	Praha Univ., Czechiya	
APEX	DEP-2E	Chmirev, V.	IZMIRAN, Russia	
APEX	DEP-2E	Stanev, G.	IKI BAN, Russia	
APEX	DEP-2R	Chmirev, V.	IZMIRAN, Russia	
APEX	DEP-2R	Stanev, G.	IKI BAN, Russia	
APEX	DANI	Dachev, Tc.	IKI BAN, Russia	
APEX	DANI	Dokvicia, V	IZMIRAN, Russia	
APEX	KM-10	Afonin, V.	IKI AN, Russia	
APEX	KM-10	Shmilauer, Ja.	GFI CAN, Czechiya	
APEX	NVK-ONCH	Milchailov, Yu.	IZMIRAN, Russia	
APEX	UF-3K	Ruzhin, Yu.	IZMIRAN, Russia	
APEX	FS	Petkov, N.	IKI BAN, Russia	
APEX	SGR-5	Chmirev, V.	IZMIRAN, Russia	
APEX	MNCH	Chmirev, V.	IZMIRAN, Russia	
APEX	NAM-5	Istomin, V.	IKI AN, Russia	
APEX	NAM-5	Shmilauer, Ja.	GFI CAN, Czechiya	
APEX	VCH-VK	Pulinets, S.	IZMIRAN, Russia	
APEX	VCH-VK	Kloss, Z.	CKI PAN, Poland	
APEX	SGR-7	Chobanu, M	IKI, Romania	
APEX	KEM-1	Triska, P.	GFI CAN, Czechiya	
APEX	KM-12	Shmilauer, Ja.	GFI CAN, Czechiya	
APEX	ZL-A-S	Sauer, K.	Zentr. Inst. Astrophis., Germany	
APEX	PRS-2-C	Rothkachl, H.	CKI PAN, Poland	
APEX	DAN-S	Dachev, Tc.	IKI BAN, Bulgaria	
APEX	DOK-A-S	Kudela, K.	GFI CAN, Czechiya	
APEX	MPS	Fisher, S.	Praha Univ., Czechiya	
APEX	SEA	Fisher, S.	Praha Univ., Czechiya	
APEX	FDS	Petkov, N.	IKI BAN, Bulgaria	
Cluster	ASPOC	Riedler, W.	Inst. of Weltraumforschung, Austria	
Cluster	CIS	Reme, H.	CESR, France	REME@CNESTA.dnet.nasa.gov
Cluster	DWP	Woolliscroft, L. J. C.	U. of Sheffield, UK	LJCW@RLVK.span.nasa.gov
Cluster	EDI	Paschmann, G.	Max Planck Institut, Germany	28821::GEP
Cluster	EFW	Gustafsson, G.	SISP, Sweden	SISP
Cluster	FGM	Balogh, A.	ICST, UK	postmaster@uk.ac.ic.ph.spva
Cluster	PEACE	Johnstone, A. D.	MSSL, UK	adj@mssl.dnet.nasa.gov
Cluster	RAPID	Wilken, B.	Max Planck Institut, Germany	ECD1::LINMPI::WILKEN@brunet.span.nasa.gov
Cluster	STAFF	Cornilleau-Wehrin, N.	CRP L'Environ./CNET, France	RPEVZB::CORNILLEAU
Cluster	WBD	Gurnett, D. A.	U. of Iowa, USA	gurnett@iowave.physics.uiowa.edu
Cluster	WHISPER	Decreau, P. M. E.	LPCE/CNRS, France	pdecreau@cnsr-orleans.fr

Coronas	DIFOS	Zhugzhda, Y.	IZMIRAN, Moscow, Russia	
Coronas	DIOGENES	Sylwester, J.	AI, Prague, CBK, Wroclaw	
Coronas	HELIKON	Mazets, E.	LETI, Leningrad, Russia	
Coronas	IRIS	Charikov, Yu	LFTI, Leningrad, Russia	
Coronas	RES-C	Sobelm, I.	FIAN, Moscow, Russia	
Coronas	RES-C	Zhitnik, I.	FIAN, Moscow, Russia	
Coronas	SCR	Kuznetzov, V.		
Coronas	SORS	Fomichev, V.		
Coronas	SORS	Pulinets, S.	IZMIRAN, Moscow, Russia	
Coronas	SUVRO	Kazachevskaya, T.	IPG, Moscow, Russia	
Coronas	TEREK	Zhitnik, I.	FIAN, Moscow, Russia	
Coronas	TEREK	Sobelm, I.	FIAN, Moscow, Russia	
Coronas	VUSS	Lomovsky, A.	IPG, Moscow, Russia	
FAST	EESA	Carlson, C.	UC, Berkeley, USA	UCBSP::MARSHA
FAST	EFPE	Carlson, C.	UC, Berkeley, USA	UCBSP::MARSHA
FAST	MAG	Carlson, C.	UC, Berkeley, USA	UCBSP::MARSHA
FAST	TEAMS	Carlson, C.	UC, Berkeley, USA	UCBSP::MARSHA
Galileo	ASI	Seiff, A.	San Jose State U., USA	
Galileo	DDS	GrYn, E	Max-Planck-Institut, Germany	
Galileo	EPD	Williams, D. J.	APL, USA	APLSP::WILLIAMS
Galileo	EPI	Fischer, H. M.	Universität Kiel, Germany	
Galileo	GPMS	Niemann, H. B.	GSFC, USA	HNIEMANN@gsfcmail.nasa.gov
Galileo	HAD	von Zahn, U.	U. of Bonn, Germany	
Galileo	HIC	Garrard, T. L.	CalTech, USA	TLG@CITSRL.srl.CALTECH.EDU
Galileo	LRD	Lanzerotti, L. J.	Bell Laboratories, USA	ljl@physics.att.com
Galileo	MAG	Kivelson, M. G.	UCLA, USA	mkivelson@igpp.ucla.edu
Galileo	NEP	Ragent, B.	GSFC, USA	
Galileo	NFR	Sromovsky, L. A.	U. Wisconsin-Madison, USA	
Galileo	NIMS	Carlson, R. W.	CalTech, USA	
Galileo	PLS	Frank, L. A.	U. of Iowa, USA	IOWASP::FRANK
Galileo	PFR	Russell, E. E.	Santa Barbara Res. Ctr, USA	
Galileo	PWS	Gurnett, D. A.	U. of Iowa, USA	gurnett@iowave.physics.uiowa.edu
Galileo	RS-CM	Anderson, J. D.	CalTech, USA	
Galileo	RS-RP	Howard, H. T.	Stanford U., USA	
Galileo	SSI	Belton, M. J. S.	NOAO, USA	
Galileo	UVS	Hord, C. W.	LASP, U. Colorado, USA	
Geotail	CPI	Frank, L.	U. of Iowa, USA	IOWASP::FRANK
Geotail	EFD	Tsuruda, K.	ISAS, Japan	BTSURUTANI@JPLSP.span.nasa.gov
Geotail	EPIC	Williams, D.	APL, USA	APLSP::WILLIAMS
Geotail	HEP	Doke, T.	Waseda U., Japan	AMES::"tdoke@jpnwasod.BITNET"
Geotail	LEP	Mukai, T.	ISAS, Japan	mukai@gtl.isas.ac.jp
Geotail	MGF	Kokubun, S.	Nagoya U., Japan	41920::KOKUBUN
Geotail	PWI	Matsumoto, H.	Kyoto U., Japan	matsumoto@kurasc.kyoto-u.ac.jp
GOES	SEM/EPS	Sauer, H.	SEL/NOAA, USA	
GOES	SEM/MAG	Singer, H.	SEL/NOAA, USA	hsinger@selvax.sel.bldrdoc.gov
GOES	SEM/XRS	Garcia, H.	SEL/NOAA, USA	
IMP-8	APP	Krimigis, S. M.	APL, USA	APLSP::KRIMIGIS
IMP-8	CAI	Stone, E. C.	CalTech, USA	ecs@citsrl.srl.caltech.edu
IMP-8	CHE	Simpson, J. A.	U. of Chicago, USA	simpson@odysseus.uchicago.edu
IMP-8	GME	McGuire, R.	GSFC, USA	NCF::MCGUIRE
IMP-8	GNF	Lepping, R.	GSFC, USA	USRPL@LEPVAX.dnet.nasa.gov
IMP-8	GWP	Williams, D. J.	APL, USA	APLSP::WILLIAMS
IMP-8	IOE	Frank, L. A.	U. of Iowa, USA	IOWASP::FRANK
IMP-8	LAP	Gosling, J.	LANL, USA	ESSDP1::073500
IMP-8	MAE	Ipevich, F.	U. of Maryland, USA	IPAVICH@ampte.dnet.nasa.gov
IMP-8	MAP	Lazarus, A.	MIT, USA	ajl@space.mit.edu
Interball	ADS	Belikova, A.Ê	IKI, Russia	
Interball	ADS	Juchniewicz, J.	Polish Academy of Sci.s, Poland	romanw@camk.edu.pl
Interball	ADS	Skalski, A.	IKI, Russia	

Interball	AKR-X	Fisher, L.	Astronomy Inst., Czechoslovakia	
Interball	AKR-X	Grigorjeva, V.	Astronomy Inst. of Moscow, Russia	
Interball	ALFA-3	Bezrukikh, V.	IKI, Russia	
Interball	ALPHA-3	Bezrukikh, V.	IKI, Russia	
Interball	AMEI-2	Koleva, R.	STIL, Bulgaria	
Interball	AMEI-2	Smimov, V.	IKI, Russia	
Interball	ASPI	Klimov, S.	IKI, Russia	
Interball	ASPI	Romanov, S.	IKI, Russia	
Interball	C2-A	Triska, P.	Geophysics Inst., Czechoslovakia	
Interball	C2-A	Voita, Ya.	Geophysics Inst., Czechoslovakia	
Interball	C2-X	Triska, P.	Geophysics Inst., Czechoslovakia	
Interball	C2-X	Voita, Ya.	Geophysics Inst., Czechoslovakia	
Interball	CORALL	Jimenez, R.	Cuba	
Interball	CORALL	Yermolaev, Yu.	Space Research Inst., Russia	LZELENYI@ESOC1.binnet
Interball	DOK-2A	Kudela, K.	IEP, Czechoslovakia	
Interball	DOK-2A	Lutsenko, V.É	IKI, Russia	
Interball	DOK-2X	Kudela, K.	IEP, Czechoslovakia	
Interball	DOK-2X	Lutsenko, V.É	IKI, Russia	
Interball	ELECTRON	Borodkova, N.	IKI, Russia	
Interball	ELECTRON	Sauvaud, J. A.	CESR, France	SAUVAUD@CNESTA.span.nasa.gov
Interball	ELECTRON	Vaisberg, O.É	IKI, Russia	
Interball	HYPER-BOLOID	Bertheliet, J. J.	CRP L'Environ./CNET, France	CRPEIS::BERTHELIER
Interball	HYPER-BOLOID	Muliarchik, T.	IKI, Russia	
Interball	IESP-2	Chmyrev, V.	IZMIRAN, Russia	
Interball	IESP-2	Stanev, G.	CLKI, Bulgaria	
Interball	IFPE	Belikova, A.	IKI, Russia	
Interball	IFPE	Buechner, J.	Max Planck Institut, Germany	jib@mpe.fta-berlin.de
Interball	IFPE	Skalsky, A.É	IKI, Russia	
Interball	IMAP-2	Arshinkov, I.	SDS Lab, Bulgaria	
Interball	IMAP-2	Stiazhkin, V.	IZMIRAN, Russia	
Interball	IMAP-3	Arshinkov, I.	SDS Lab, Bulgaria	
Interball	IMAP-3	Stiazhkin, V.	IZMIRAN, Russia	
Interball	ION	Kovrazhkin, R. A.	Space Research Inst., Russia	rkovrazh@esoc1.BITNET
Interball	ION	Sauvaud, J. A.	CESR, France	SAUVAUD@CNESTA.span.nasa.gov
Interball	KM-7	Afonin, V.É	IKI, Russia	
Interball	KM-7	Smilauer, J.	Astronomy Inst., Czechoslovakia	
Interball	MEMO	Lefevvre, F.	LPCE, France	CNESTA::LEFEUVRE
Interball	MEMO	Mogilevsky, M.É	IKI, Russia	
Interball	MIF-M	Nozdrachev, M.	IKI, Russia	
Interball	MIF-M	Romanov, S.	IKI, Russia	
Interball	MONITOR-3	Fedorov, A.	IKI, Russia	
Interball	MONITOR-3	Nemechek, Z.	Karlov U., Czechoslovakia	
Interball	MONITOR-3	Shafrankova, Ya.	Karlov U., Czechoslovakia	
Interball	NVK-ONCH	Goljavin, A.	IZMIRAN, Russia	
Interball	NVK-ONCH	Molchanov, O.	Inst. of Earth Physics, Russia	
Interball	OPERA	Amata, E.	CNR, IFSI, Italy	amata@hp.ifs1.fra.cnr.it
Interball	OPERA	Nozdrachev, M.É	IKI, Russia	
Interball	OPERA	Savin, S.	IKI, Russia	
Interball	POLRAD	Hanash, J.	SRC, Poland	
Interball	POLRAD	Lishin, I.	IRE, Russia	
Interball	POLRAD	Mogilevsky, M.	IKI, Russia	
Interball	PRAM	Romanov, S.	IKI, Russia	
Interball	PRAM	Rybyeva, N.	IKI, Russia	
Interball	PROMICS-3	Pissarenko, N.É	IKI, Russia	
Interball	PROMICS-3	Pissarenko, N.É	IKI, Russia	
Interball	PROMICS-3	Sandahl, I.	SISP, Sweden	ingrid@ifr.se
Interball	PROMICS-3	Sandahl, I.	SISP, Sweden	ingrid@ifr.se
Interball	RF-15-I	Famik, F.	Anstronomy Inst., Czechoslovakia	
Interball	RF-15-I	Likin, O.	IKI, Russia	
Interball	RF-15-I	Silvester, J.É	Space Research Center, Poland	
Interball	RON	Galperin, Yu. I.	IKI, Russia	
Interball	RON	Riedler, W.	Space Research Inst., Austria	
Interball	RON	Schmidt, R.	ESA/ESTEC, Netherland	RSCHMIDT@ESTCS1.span.nasa.gov
Interball	SKA-1	Smimov, V.	IKI, Russia	
Interball	SKA-1	Vaisberg, O.	IKI, Russia	
Interball	SKA-2	Fisher, S.	Anstronomy Inst, Czechoslovakia	

Interball	SKA-2	Morozova, E.É	IKI, Russia	
Interball	SKA-3	Kovrazhkin, R.É	Space Research Inst., Russia	rkovrazh@esoc1.BITNET
Interball	SKA-3	Kuzmin, A.	IKI, Russia	
Interball	UFSIPS	Kuzmin, A.	IKI, Russia	
Interball	UFSIPS	Palazov, K.	IKI BAN, Bulgaria	
Interball	UVAI	Cogger, L. L.	U. of Calgary, Canada	cogger@phys.ucalgary.ca
Interball	UVAI	Galperin, Yu. I.	IKI, Russia	
Interball	VDP	Fedorov, A.	IKI, Russia	
Interball	VDP	Nemechek, Z.	Karlovy U., Czechoslovakia	
Interball	VDP	Zastenker, G.	IKI, Russia	
ISEE-3	BAH	Gosling, S.	LANL, USA	ESSDP1::073500
ISEE-3	DFH	Hynds, R.		
ISEE-3	HOH	Hovestadt, D.	Max Planck Institut, Germany	
ISEE-3	MEH	Meyer, P.	U. of Chicago, USA	meyer@odysseus.uchicago.edu
ISEE-3	OGH	Ogilvie, K.	GSFC, USA	LEPVAX::U2KWO
ISEE-3	SBH	Steinberg, J.	MIT, USA	jts@space.mit.edu
ISEE-3	SCH	Greenstadt, G.	TRW, USA	
ISEE-3	SMH	Smith, E. J.	Jet Propulsion Laboratory, USA	ESMITH@JPLSP.span.nasa.gov
ISEE-3	STH	Teegarden, B.	GSFC, USA	TEEGARDEN@LHEAVX.span.nasa.gov
ISEE-3	TYH	von Rosenvinge, T.	GSFC, USA	VONROSEN@NSSDCA.span.nasa.gov
Mars-94	ASPERA-S	Lundin, R.	SISP, Sweden	LUNDIN@plafys.dnet.nasa.gov
Mars-94	DIMIO	Berthelier, J. J.	CRP L'Environ./CNET, France	CRPEIS::BERTHELIER
Mars-94	ELISMA	Klimov, S.	IKI, Russia	
Mars-94	FONEMA	Johnstone, A.	MSCL, UK	adj@mssl.dnet.nasa.gov
Mars-94	MAREMF	Reidler, W.	Space Research Inst., Austria	
Mars-94	MARIPROB	Afonin, V.	IKI, Russia	
Mars-94	SLED-2	MacKenna-Lawlor, S.	St. Patrick College, Ireland	
MPA/SOPA	MPA	McComas, D.	LANL, USA	ESSDP1::MCCOMAS
MPA/SOPA	SOPA	Belian, R.	LANL, USA	ESSDP1::BELIAN
Pioneer	CPI	Simpson, J. A.	U. of Chicago, USA	simpson@odysseus.uchicago.edu
Pioneer	CRT	McDonald, F. B.	U. of Maryland, USA	sm27@umail.umd.edu
Pioneer	GTT	Van Allen, J. A.	U. of Iowa, USA	VANALLEN@IOWASP.span.nasa.gov
Pioneer	HVM	Smith, E. J.	Jet Propulsion Laboratory, USA	ESMITH@JPLSP.span.nasa.gov
Pioneer	PA	Barnes, A.	Ames Research Center, USA	barnes@windee.arc.nasa.gov
Pioneer	TRF	Fillus, R. W.	U. Southern California, USA	walker@cass.span@Sdsc.edu
Pioneer	UV	Judge, D. L.	U. Southern California, USA	djudge@lism.usc.edu
Polar	CAMMICE	Fritz, T.	Boston U., USA	ESSDP2::FRITZ
Polar	CEPPAD	Blake, B.	Aerospace Corporation, USA	5418::BLAKE
Polar	EFI	Mozer, F.	U. of California, Berkeley, USA	MARSHA%UCBSSL@BERKELEY.EDU
Polar	HYDRA	Scudder, J.	U. of Iowa, USA	U2JDS@LEPVAX.span.nasa.gov
Polar	MFE	Russell, C.	UCLA, USA	ctrussell@igpp.ucla.edu
Polar	PIXIE	Imhof, W.	Lockheed, USA	IMHOF@LOCKHD.dnet.nasa.gov
Polar	PWI	Gurnett, D.	U. of Iowa, USA	gumett@iowave.physics.uiowa.edu
Polar	TIDE	Moore, T.	MSFC, USA	SSL::MOORET
Polar	TIMAS	Shelley, E.	Lockheed, USA	shelley@lockhd.span.nasa.gov
Polar	UVI	Parks, G.	U. of Washington, USA	parks@geophys.washington.edu
Polar	VIS	Frank, L.	U. of Iowa, USA	IOWASP::FRANK
SAMPEX	HILT	Mason, G.	U. of Maryland, USA	UMDSP::MASON
SAMPEX	LEICA	Mason, G.	U. of Maryland, USA	UMDSP::MASON
SAMPEX	MAST	Mason, G.	U. of Maryland, USA	UMDSP::MASON
SAMPEX	PET	Mason, G.	U. of Maryland, USA	UMDSP::MASON
SOHO	CDS	Harrison, R.	RAL, UK	19592::RAH
SOHO	CELIAS	Hovestadt, D.	MPE, Garching, Germany	
SOHO	COSTEP	Kunow, H.	Universitaet Kiel, Germany	HKUNOW@SOLAR.bitnet
SOHO	EIT	Delaboudinière, J. P.	LAS France	
SOHO	ERNE	Torsti, J.	U. of Turku, Finland	21905::KONTU::TORSTI@brunet.span.nasa.gov
SOHO	GOLF	Gabriel, A.	LAS France	
SOHO	LASCO	Brueckner, G.	NRL, USA	11343::BRUECKNER
SOHO	MDI	Scherrer, P. H.	Stanford U., USA	psherrer@solar.stanford.edu

SOHO	SUMER	Wilhelm, K.	MPAE, Germany	NSP::WILHELM@LINMPI.span.nasa.gov
SOHO	SWAN	Bertaux, J. L.	SA, Varrières-le-Buisson, France	
SOHO	UVCS	Kohl, J. L.	SAO, USA	KOHL@CFA4.bitnet
SOHO	VIRGO	Frohlich, C.	PMOD-WRC, Switzerland	cfrohlich@ezrz1.vmsmail.ethz.ch
Spartan	UVCS	Kohl, J.	SAO, USA	KOHL@CFA4.bitnet
Spartan	WLC	Fisher, R.	GSFC, USA	SOLAR::RFISHER
UARS	CLAES	Roche, A. E.	Lockheed, USA	
UARS	HALOE	Russell, J. M.	Langley Research Center, USA	JMRUSSELL@NASAMAIL.NASA.gov
UARS	HRDI	Hays, P. B.	U. of Michigan, USA	hays@sprlj.sprlj.umich.edu
UARS	ISAMS	Taylor, F. W.	Oxford U., UK	
UARS	MLS	Waters, J. W.	Jet Propulsion Lab, USA	
UARS	PEM	Winningham, J. D.	Southwest Research Inst., USA	david@dews1.space.swri.edu
UARS	SOLSTICE	Rottman, G. J.	NCAR, USA	rottman@hao.ucar.edu
UARS	SUSIM	Brueckner, G. E.	NRL, USA	11343::BRUECKNER
UARS	WINDII	Shepherd, G. G.	York U., Canada	gordon@windic.yorku.ca
Ulysses	COSPIN	Simpson, J. A.	U. of Chicago, USA	simpson@odysseus.uchicago.edu
Ulysses	COSPIN	Stone, R. G.	GSFC, USA	U2RGS@LEPVAX.span.nasa.gov
Ulysses	DUST	Grun, E.	MPI, Heidelberg, Germany	
Ulysses	EPAC/GAS	Keppeler, E.	Max Planck Institut, Germany	ECD1::LINMPI::KEPPLER@brunet.span.nasa.gov
Ulysses	GBS	Hurley, K.	U. of California, Berkeley, USA	UCBSP::KHURLEY
Ulysses	GBS	Sommer, M.	Max-Planck-Institut, Germany	
Ulysses	HI-SCALE	Lanzerotti, L.	Bell Laboratories, USA	ljl@physics.att.com
Ulysses	SCE	Bird, M. K.	U. of Bonn, Germany	MBIRD@ASTRO.UNI-BONN.DE
Ulysses	SWICS	Geiss, J.	U. of Bern, Germany	U21G@CBEEDA3T.BITNET
Ulysses	SWICS	Gloeckler, G.	U. of Maryland, USA	UMDSP::GLOECKLER
Ulysses	SWOOPS	Phillips, J.	LANL, USA	ESSDP1::102657
Ulysses	VHM/FGM	Balogh, A.	ICST, UK	postmaster@uk.ac.ic.ph.spva
Voyager	CRS	Stone, E. C.	CalTech, USA	ecs@citsrl.srl.caltech.edu
Voyager	LECP	Krimigis, S. M.	APL, USA	APLSP::KRIMIGIS
Voyager	MAG	Ness, N. F.	U. of Delaware, USA	BARTOL::NFNESS
Voyager	PLS	Belcher, J. W.	MIT, USA	MITCCD::JWB
Voyager	PWS	Gurnett, D. A.	U. of Iowa, USA	gurnett@iowave.physics.uiowa.edu
Voyager	UVS	Broadfoot, A. L.	U. of Arizona, USA	broadfoot@looney.lpl.arizona.edu
Wind	EPACT	von Rosenvinge, T.	GSFC, USA	VONROSEN@NSSDCA.span.nasa.gov
Wind	Konus	Mazets, E.		
Wind	MFI	Lepping, R.	GSFC, USA	U5RPL@LEPVAX.dnet.nasa.gov
Wind	PLASMA	Lin, R.	U. of California, Berkeley, USA	UCBSP::LIN
Wind	SMS	Gloeckler, G.	U. of Maryland, USA	UMDSP::GLOECKLER
Wind	SWE	Ogilvie, K.	GSFC, USA	LEPVAX::U2KWO
Wind	TGRS	Teegarden, B.	GSFC, USA	TEEGARDEN@LHEAVX.span.nasa.gov
Wind	WAVES	Bougeret, J.	Observatoire de Paris-Meudon, France	MEUDON::BOUGERET
Yohkoh	BCS	Culhane, J.	U. College London, UK	JLC@a.mssl.ucl.ac.uk
Yohkoh	BCS	Hiei, E.	Meisei U.	HIEI@SPOT.MTK.NAO.ACJP
Yohkoh	HXT	Makishima, K.		
Yohkoh	SXT	Acton, L.	Montana State U., USA	SAG::ACTON
Yohkoh	SXT	Hirayama, T.		
Yohkoh	WBS	Nishimura, J.		

